

Routing and Disaster Awareness in Optical Networks

Muhammad Iqbal, Muhammad Al Farabi

DOI

[10.4233/uuid:64cd0a44-acc7-49bc-905a-017c4855511a](https://doi.org/10.4233/uuid:64cd0a44-acc7-49bc-905a-017c4855511a)

Publication date

2016

Document Version

Final published version

Citation (APA)

Muhammad Iqbal, M. A. F. (2016). *Routing and Disaster Awareness in Optical Networks*. [Dissertation (TU Delft), Delft University of Technology]. <https://doi.org/10.4233/uuid:64cd0a44-acc7-49bc-905a-017c4855511a>

Important note

To cite this publication, please use the final published version (if applicable).
Please check the document version above.

Copyright

Other than for strictly personal use, it is not permitted to download, forward or distribute the text or part of it, without the consent of the author(s) and/or copyright holder(s), unless the work is under an open content license such as Creative Commons.

Takedown policy

Please contact us and provide details if you believe this document breaches copyrights.
We will remove access to the work immediately and investigate your claim.

**ROUTING AND DISASTER AWARENESS
IN OPTICAL NETWORKS**

ROUTING AND DISASTER AWARENESS IN OPTICAL NETWORKS

Proefschrift

ter verkrijging van de graad van doctor
aan de Technische Universiteit Delft,
op gezag van de Rector Magnificus prof. ir. K.C.A.M. Luyben,
voorzitter van het College voor Promoties,
in het openbaar te verdedigen op woensdag 7 september 2016 om 15:00 uur

door

Muhammad Al Farabi bin MUHAMMAD IQBAL

Master of Engineering (Electrical - Electronics and Telecommunications),
Universiti Teknologi Malaysia, Johor, Malaysia,
geboren te Ohio, United States of America.

Dit proefschrift is goedgekeurd door de

promotor: Prof. dr. ir. P.E.A. Van Mieghem

copromotor: Dr. ir. F.A. Kuipers

Samenstelling promotiecommissie:

Rector Magnificus,	voorzitter
Prof. dr. ir. P.E.A. Van Mieghem	Technische Universiteit Delft
Dr. ir. F.A. Kuipers	Technische Universiteit Delft

Onafhankelijke leden:

Prof. dr. ir. M. Pickavet	Universiteit Gent, Belgium
Prof. dr. -ing. P.E. Heegaard	Norwegian University of Science and Technology, Norway
Prof. dr. C. Witteveen	Technische Universiteit Delft
Prof. dr. ir. P.J.M. van Oosterom	Technische Universiteit Delft

Overige leden:

Dr. ir. R.C.J. Smets SURFnet BV

ISBN 978-94-6186-704-9

This research was supported by the Malaysian Ministry of Higher Education.

Keywords: Impairment-Aware Routing, Risk-Averse Routing, Spatially-Close Links, Spatiotemporal Disasters, Technology-Aware Routing, Technology Incompatibilities, Transmission Impairments.

Copyright © 2016 by Muhammad Al Farabi bin Muhammad Iqbal

An electronic version of the thesis is available at
<http://repository.tudelft.nl/>.

Printed in The Netherlands.

To my children.

CONTENTS

Summary	xi
Samenvatting	xiii
1 Introduction	1
1.1 Routing	2
1.1.1 Shortest Paths.	3
1.1.2 (Maximally) Disjoint Paths.	5
1.2 Disaster Awareness.	9
1.2.1 Proactive Failure Prevention	12
1.2.2 Reactive Failure Compensation	13
1.3 Motivations and Contributions	14
1.4 Thesis Outline	16
2 Technology-Aware Routing	19
2.1 Introduction	20
2.2 Related Work	24
2.3 Network Model	27
2.4 Problem Formulation	31
2.5 Routing Algorithms	32
2.5.1 Pseudocodes	33
2.5.2 Illustrative Example	36
2.5.3 Time Complexity	39
2.5.4 Correctness Proof.	39
2.6 Simulations	40
2.7 Chapter Conclusion	44
3 Impairment-Aware Routing	45
3.1 Introduction	46
3.2 Link Structure.	47
3.2.1 Power Level	48
3.2.2 Dispersion.	49

3.2.3	Figure-of-Merit (FoM)	49
3.2.4	Figure-of-Impact (FoI)	49
3.2.5	Computation Example	50
3.3	The Figure-of-Impact (FoI)	52
3.4	Application	55
3.4.1	Phase 1	55
3.4.2	Phase 2	56
3.4.3	Simulation and Analysis	59
3.5	Chapter Conclusion	61
4	Spatiotemporal Disaster Risks	63
4.1	Introduction	64
4.2	Grid-Based Model	65
4.2.1	Availability of Grid Rectangles	65
4.2.2	Availability of Links and Paths	68
4.3	Detection of Vulnerable Connections.	69
4.3.1	Problem Definition	69
4.3.2	Our Approach.	70
4.3.3	Analysis	71
4.4	Spatiotemporal Risk-Averse Routing	76
4.4.1	Problem Definition	77
4.4.2	Our Approach.	79
4.4.3	Analysis	79
4.5	Related Work	80
4.6	Chapter Conclusion	81
5	Spatially-Close Fibers	83
5.1	Introduction	84
5.2	Detection of Spatially-Close Fiber Segments.	86
5.2.1	Fiber Structure	86
5.2.2	Problem Definition.	86
5.2.3	Our Approach.	87
5.2.4	Proof-of-Concept.	89
5.3	Intervals of Spatially-Close Fibers.	91
5.3.1	Intervals of a Pair of Spatially-Close Fiber Segments.	92
5.3.2	Problem Definition.	93
5.3.3	Our Approach.	94
5.3.4	Proof-of-Concept.	95

5.4	Grouping of Spatially-Close Fibers	96
5.4.1	Problem Definition	97
5.4.2	Our Approach	98
5.4.3	Proof-of-Concept	99
5.5	Related Work	99
5.6	Chapter Conclusion	101
6	Conclusion	103
6.1	Thesis Contributions	104
6.2	Directions for Future Work	106
	References	107
	Abbreviations	125
	Notations	129
	Acknowledgements	133
	Curriculum Vitæ	135
	List of Publications	137

SUMMARY

Optical networks facilitate the configurations of high-speed network connections with tremendous bandwidth between the optical switches. Optical switches are interconnected by optical fibers that act as the mediums in which data are transferred using lightpaths. Due to the importance of optical networks to many societal needs, e.g., the Internet and banking services, network connections must be configured as efficient and reliable as possible. This thesis focus on two important research topics related to the management and survivability of network connections, namely routing and disaster awareness. Routing enables the assignment of the optimal end-to-end path to each network connection, while disaster awareness increases the preparedness of network operators in ensuring that network connections are protected against the adverse impacts of disasters.

The first part of the thesis, namely Chapters 2, 3 and 4 relate to the topic of routing, specifically on technology-aware routing, impairment-aware routing and risk-averse routing. Technology-aware routing is required for establishing network connections across multi-domain networks with technology incompatibilities, impairment-aware routing enables network operators to establish network connections in the presence of transmission impairments, and risk-averse routing enables connections to be assigned with the safest paths (against failing due to disasters). The second part of the thesis, namely Chapters 4 and 5 relate to the topic of disaster awareness, by proposing approaches for ensuring the survivability of network connections in the risk of disasters, such as modeling of (spatiotemporal) disasters, identifying vulnerable connections, detecting spatially-close fiber segments, computing spatially-close intervals of spatially-close fibers, and grouping spatially-close fibers efficiently. Though the thesis emphasizes on optical network use cases, the provided insights and contributions in each chapter are general enough to be extended for application in other network types as well.

SAMENVATTING

Optische netwerken faciliteren hogesnelheids netwerkverbindingen met enorme bandbreedte tussen optische switches. De optische switches zijn onderling verbonden met glasvezelkabels die optreden als de mediums waarover data verzonden wordt door het gebruik van lichtpaden. Door het belang van optische netwerken voor maatschappelijke behoeften, zoals het Internet en financiële diensten, moeten netwerken zo efficiënt en betrouwbaar als mogelijk geconfigureerd zijn. Deze thesis focust op twee belangrijke onderzoeksthema's gerelateerd tot het beheer en overlevingsvermogen van netwerk verbindingen, namelijk routing en rampbewustzijn. Routing voorziet in de aanwijzing van de meest optimale paden tussen elke netwerk verbinding, terwijl rampbewustzijn de paraatheid van netwerk beheerders verhoogt door te verzekeren dat netwerkverbindingen beveiligd zijn tegen de schadelijke gevolgen van rampen.

De eerste deel van deze thesis, namelijk hoofdstukken 2, 3 en 4, betreffen het onderwerp routing, met name specifiek technologiebewust routeren, signaalverstoringsbewust routeren en risicomijdend routeren. Technologiebewuste routing is noodzakelijk bij het opzetten van netwerkverbindingen over multidomein netwerken met incompatibele technologieën, signaalverstoringsbewuste routing stelt netwerk operators in staat om netwerkverbindingen op te zetten in het geval van verstoringen in de signaaloverdracht en risicomijdende routing stelt verbindingen in staat om aan paden toegewezen te worden die het veiligst (tegen storingen door rampen) zijn. De tweede deel van de thesis, namelijk hoofdstukken 4 en 5, betreffen het onderwerp van rampbewustzijn en stelt methoden voor om het overlevingsvermogen van netwerkverbindingen te verzekeren bij het gevaar van rampen, zoals het modelleren van (ruimtelijk-temporele) rampen, het identificeren van kwetsbare verbindingen, het detecteren van ruimtelijk nabije kabelsegmenten, het berekenen van ruimtelijk nabije intervallen van ruimtelijk nabije kabels en het efficiënt groeperen van ruimtelijk nabije kabels. Hoewel de thesis de nadruk legt op de toepassing van optische netwerken, zijn de verschaftte inzichten en bijdragen in elk hoofdstuk tevens voldoende algemeen om uitgebreid te worden voor toepassing in andere soorten netwerken.

1

INTRODUCTION

Networks are prevalent in our daily lives. Our power grid networks consist of networks of generating stations interconnected by high-voltage transmission lines, our transportation networks consist of networks of cities interconnected by highways, and the backbone of our telecommunication networks, namely the optical networks consist of networks of optical switches interconnected by high-speed optical fibers. Without these networks, society (nowadays) might cease to function. Due to the importance of networks, this thesis focuses on two research topics regarding the management and survivability of network services, namely routing and disaster awareness. This chapter provides the necessary background on the topics of routing and disaster awareness, while discussing several notable existing works in both research topics. The chapter continues with the motivations and contributions of the thesis, while providing corresponding research questions that are at the focus of the thesis. The chapter ends with an outline of the thesis.

Parts of this chapter have been published in Wiley Encyclopedia of Electrical and Electronics Engineering, June 2015 [1].

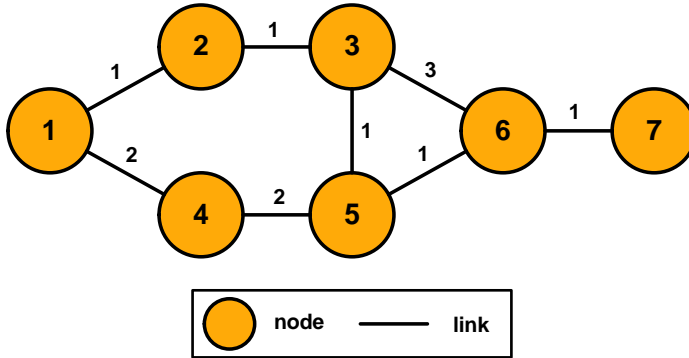


Figure 1.1: An example of a network represented by nodes and links.

1.1. ROUTING

In graph theory [2], networks can be represented by an interconnection of nodes by links. Network nodes represent the points-of-interest of the network, while network links represent the connectors that bind points-of-interest together. Figure 1.1 shows an example of a network that is modeled by a graph of seven nodes and eight undirected links. Links can also be assigned with link weights (usually written on the links as shown in Figure 1.1) that represent specific link properties. Numerous link properties can be represented using link weights, e.g., link delay, link energy consumption, link length, link availability, link throughput and many more. Similarly, nodes can also be assigned with node weights that represent specific node properties, e.g., node energy consumption, node availability, node throughput and many more. However, attention is often given to link weights since weighted nodes can trivially be transformed into two corresponding unweighted nodes that are connected by a weighted link, using a graph transformation approach such as mentioned in [1].

Routing is the process of finding path(s) in a network. A path is a sequence of network link(s) between two specific network nodes. The path can be either directed or undirected, depending on whether the network links are directed or undirected. One of the most studied routing problems is the shortest path problem, which is the problem of finding a path from a network node to another network node such that the sum of the weights of the network links constituting the path is minimized. In a formal definition, given a network $G = (N, L)$ of a set N of $|N|$ network nodes and a set L of $|L|$ weighted network links, a source node $x \in N$, and a destination node $y \in N$, the objective is to find the shortest path P

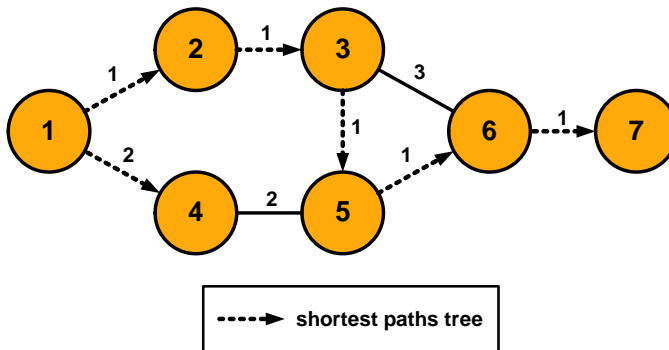


Figure 1.2: The shortest paths tree rooted at node 1.

from node x to node y , such that the sum of the weights of the links constituting the path P is minimized. Using the shortest path, freights can be sent with minimal fuel cost between two ports in a maritime network, cars can commute between cities faster, and data can be transferred with minimal transmission delay between two optical switches in an optical network.

Using different link property as the link weight leads to different optimality criteria of the shortest path, such that the routing objective varies accordingly, e.g., minimizing the path delay, minimizing the path energy consumption or minimizing the path length, maximizing the path availability or maximizing the path throughput. There have been extensive researches on the topic of routing, such that many prominent routing algorithms have been proposed throughout the past years. We will discuss a few basic routing problem and corresponding notable algorithms for the problems, as to introduce the topic of routing.

1.1.1.1. SHORTEST PATHS

The Breadth-First Search (BFS) algorithm [3, 4] is one of the earliest proposed algorithms for finding the shortest paths tree that is rooted at a single source node. The shortest paths tree is a directed graph in which the root node is connected to all other nodes by shortest paths. Each network link that is not part of any shortest paths from the source node to any other nodes will not be part of the shortest paths tree. For instance, Figure 1.2 shows the shortest paths tree rooted at node 1 for the network shown in Figure 1.1. BFS begins its search procedure at the source node and explores the immediate neighbor nodes of the source node first, before exploring the next level neighbors. The worst-case time complexity of BFS is $O(|N| + |L|)$, since each node and link is processed exactly once

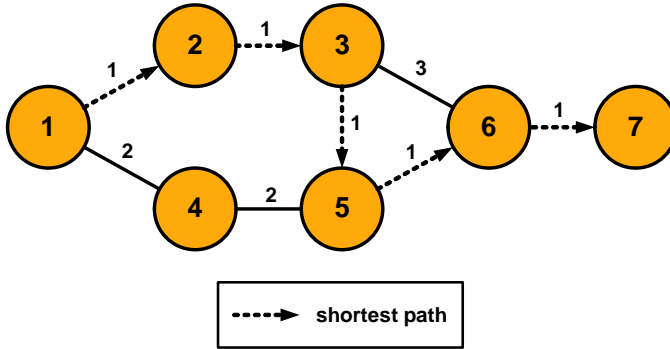


Figure 1.3: The shortest path from node 1 to node 7.

by BFS. The Dijkstra's algorithm [5] was later proposed for finding the shortest paths tree with lower worst-case time complexity. In contrast to BFS, Dijkstra's algorithm employs a greedy approach for finding the shortest paths tree that is rooted at a single source node, by enumerating nodes with lower shortest path distance from the source node before nodes with higher shortest path distance, in $O(|N| \log |N| + |L|)$ time with the use of a Fibonacci heap [6].

Unlike Dijkstra's algorithm, which only works in graphs with positive link weights, the Bellman-Ford algorithm [7, 8] is able to find the shortest paths tree that is rooted at a single source node in graphs with positive and negative link weights, provided that there are no negative cycles in the graph. A negative cycle is a sequence of nodes starting and ending at the same node, whose interconnecting link weights sum to a negative value. Bellman-Ford algorithm utilizes dynamic programming for relaxing the path weights under a fixed number of iterations. The worst-case time-complexity of Bellman-Ford algorithm is $O(|N||L|)$. The Johnson's algorithm [9] also finds the shortest paths tree that is rooted at a single source node in graphs with both positive and negative link weights, provided that there are no negative cycles in the graph. Johnson's algorithm uses a graph transformation preprocessing that transform all negative weights into corresponding positive link weights, before utilizing conventional shortest path algorithm on the transformed graph. The worst-case time complexity of Johnson's algorithm is $O(|N|^2 \log |N| + |N||L|)$, when using Dijkstra's algorithm as the shortest path algorithm. It is also possible to modify Dijkstra's algorithm to handle negative weight links directly [10, 11], but the running time of the modified Dijkstra's algorithm may then become exponential [12], since a node may be processed more than once.

If only the shortest path from a single source node to a single destination node is required, Dijkstra's algorithm can also be terminated earlier once the corresponding shortest path has been acquired, instead of continuing on finding the shortest paths tree from the source node to all other nodes. For instance, Figure 1.3 shows the shortest path from node 1 to node 7 for the network shown in Figure 1.1. Faster termination can also be acquired by running two simultaneous search processes from both the source node and the destination node via the bidirectional search algorithm [13]. The Floyd-Warshall algorithm [14, 15] can also be used to find the shortest paths between all possible node pairs in a weighted graph within $O(|N|^3)$ worst-case time complexity. Dreyfus [16] provided a good overview on a number of other older shortest path algorithms. When more than a single shortest path is required between the source node and the destination node, the Yen's algorithm [17] can be used for finding the k shortest simple paths between the nodes. A simple path is a sequence of network links with no repeating nodes.

1.1.2. (MAXIMALLY) DISJOINT PATHS

It might also be of interest to find several paths that do not share any common links (or nodes) between the network nodes. Node-disjoint paths do not share any common network nodes, except at the source and destination nodes, ensuring that at least one path remains available from the source node to the destination node in case of a node or link failure. On the other hand, link-disjoint paths share no common network links, ensuring that at least one path remains available from the source node to the destination node in case of a link failure. Finding node-disjoint paths is more restrictive than finding link-disjoint paths, since if two paths are node-disjoint, they are also link-disjoint. Link-disjoint paths algorithms can be used to find node-disjoint paths, using the node-splitting technique of [18]. Providing disjoint paths to network traffic would increase the reliability of network connections, and correspondingly the network survivability. Network survivability is the network's capability to provide continuous service in the presence of node or link failures [19]. By sending the traffic concurrently on multiple disjoint paths (e.g., in telecommunication networks), the failure of one of the path would not affect the performance of other paths, and the traffic would still reach its destination when at least a single path remains operational. Traffic can also use one of the paths as its initial primary path, and switch (in a very short time) to another backup path in case of the failure of the primary path. Though we only discuss on providing resiliency via the use of disjoint paths in this sec-

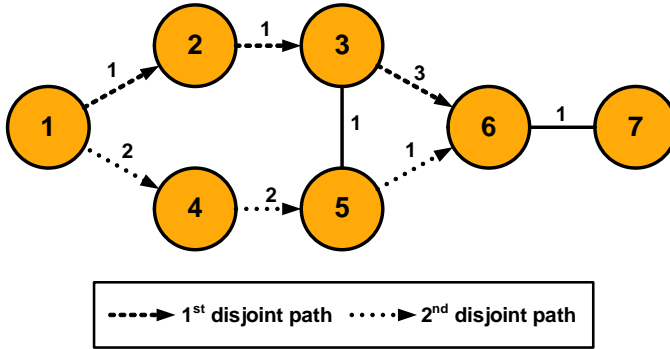


Figure 1.4: Two min-sum disjoint path from node 1 to node 6.

tion, there exist varieties of other resiliency approaches such as post-failure traffic restoration, link-based protection [20], or by transporting data multiple times using a single path and using a referee to select on the basis of majority outcome.

Disjoint paths, as depicted in Figure 1.4, are often used to assign alternative paths for network connections. A simple but naive approach for finding such disjoint paths from a single source node to a single destination node, is by using Dijkstra's algorithm iteratively (e.g., in [21]). At each iteration, all of the links constituting the earlier $\{i\}_{1 \leq i < k}$ disjoint paths are removed from the network (temporarily) before Dijkstra's algorithm is used for finding the k -th disjoint path. However, this iterative approach is but a heuristic and cannot always return the optimal solution even when it exists. For instance, in the presence of trap topology [21], where the temporary removal of the earlier $\{i\}_{1 \leq i < k}$ disjoint paths prevents the next $\{i+1\}_{1 \leq i+1 \leq k}$ disjoint path from being found, the iterative approach would fail to return a solution. Since path 1-2-3-5-6 is the shortest path from node 1 to node 6 in Figure 1.3, the iterative approach will fail to find another disjoint path in the network from node 1 to node 6, although it can exist if path 1-2-3-6 is chosen as the primary path instead of the shortest path, as shown in Figure 1.4.

Example of routing algorithms that are capable of finding k min-sum (the sum of the weights of all the constituent links of the k paths is minimized) disjoint paths from a single source node to a single destination node, even in the presence of trap topology, are the Suurballe's algorithm [22] and the Bhandari's algorithm [11]. Figure 1.4 shows the two min-sum disjoint paths from node 1 to node 6 of the network shown in Figure 1.1. Suurballe proposes an iterative scheme for finding k one-to-one disjoint paths. At each iteration, the network

is (temporarily) transformed into a canonic equivalent network (similar the concept used in Johnson's algorithm) such that the network has non-negative link weights and zero-weight links on the links of the shortest path tree rooted at the source node. Dijkstra's algorithm can then be applied for finding the k -th disjoint path from the knowledge of the earlier $\{i\}_{1 \leq i < k}$ disjoint paths, since the network contains no negative link weights. The worst-case time complexity of Suurballe's algorithm is $k(|N| \log |N| + E)$, since Dijkstra's algorithm is run k number of times to find the k disjoint paths. Bhandari later proposed a simplification of Suurballe's algorithm, also by an iterative scheme for finding the k -th one-to-one disjoint path from the optimal solution of the $\{i\}_{1 \leq i < k}$ disjoint paths. At each iteration, the direction and algebraic sign of the link weight are reversed for each link of the $\{i\}_{1 \leq i < k}$ disjoint paths. The network can thus contain negative link weights. The modified Dijkstra's algorithm [10, 11] or Bellman-Ford algorithm, both usable in networks with negative link weights, can then be applied for finding the k -th disjoint path. The worst-case time complexity of Bhandari's algorithm depends on the number of needed k disjoint paths, and whether modified Dijkstra's algorithm or Bellman-Ford algorithm are used. Instead of the min-sum condition, other conditions can be imposed on the disjoint paths, such as:

Min-sum disjoint paths problem - the sum of the weights of all the constituent links of the k paths is minimized.

Min-max condition - the sum of the weights of all the constituent links of the path with the largest path weight is minimized.

Min-min condition - the sum of the weights of all the constituent links of the path with the smallest path weight is minimized.

Bounded condition - the sum of the weights of all the constituent links of each path should each be less than a given constraint.

Li et al. [23] proved that the min-max condition is strongly NP-complete, except in directed acyclic graphs (DAGs) [24], where it is (weakly) NP-complete. The min-max condition is useful when all the k paths are used simultaneously to send the traffic (e.g., in telecommunication networks). The min-min condition is NP-hard to solve [25], and to be approximated within a factor of ϵ for any constant $\epsilon > 1$ [26]. The min-min condition is useful when only one path is active and used by traffic, while the other $k - 1$ paths remain idle as backups. Only when an active path fails will one of the backup paths be activated to substitute the active

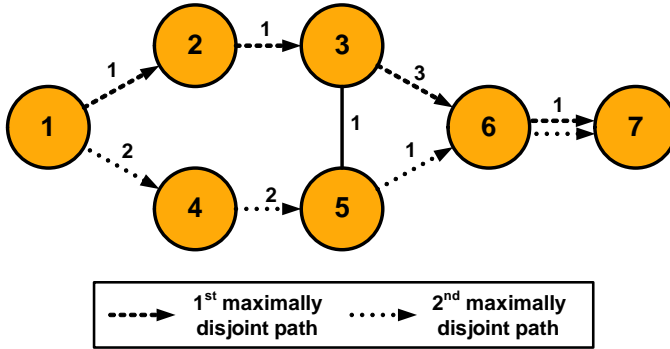


Figure 1.5: Two maximally disjoint path from node 1 to node 7.

path. Hence, the active path should have as minimal weight as possible, since the active path is used more frequently than the backup paths. The bounded condition is NP-hard [27] and APX-hard [28]. The bounded condition is helpful when each of the path weights needs to be constrained. The k paths may or may not have similar path weight constraint. Although the min-sum condition can be solved efficiently, the presence of secondary conditions (e.g., min-max, min-min or bounded conditions) for resolving a tie of solutions, the variant of the min-sum condition will then become NP-hard [29].

Both Suurballe's algorithm and Bhandari's algorithm need to be repeated $|N|$ times for finding k disjoint paths from a single source node to all other possible destination nodes, since both algorithms return only the one-to-one directed min-sum disjoint paths between two given nodes. The Suurballe-Tarjan algorithm [30] has reduced worst-case time complexity for finding $k = 2$ disjoint paths from a single source node to other reachable destination nodes, albeit with limitation of $k = 2$. Suurballe-Tarjan algorithm also uses the canonic equivalent network transformation of Suurballe's algorithm to ensure that the network contains no negative link weights in each run of Dijkstra's algorithm. Since only two iteration of Dijkstra's algorithm is needed (k is limited to 2), the worst-case time complexity of Suurballe-Tarjan algorithm is thus equal Dijkstra's algorithm.

Fully disjoint paths may or may not exist in a sparse network. For a network to have k disjoint paths between network nodes x and y , both network nodes x and y must have at least k node degree (i.e., k neighbors). There must also exist enough network nodes and links such that having k disjoint paths are possible. Maximally disjoint paths are useful if fully disjoint paths do not exist. A pair of paths is maximally disjoint if the number of network (nodes) links com-

mon to both paths is minimum. The MADSWIP algorithm [31] is an extension of Suurballe-Tarjan algorithm that returns a pair (i.e., $k = 2$) of maximally disjoint paths from a single source node to a single destination node. For instance, Figure 1.5 shows two min-sum maximally disjoint paths from node 1 to node 7 for the network shown in Figure 1.1. The worst-case time complexity of MADSWIP algorithm is equal to Suurballe-Tarjan algorithm.

1.2. DISASTER AWARENESS

Modern telecommunication networks deliver a multitude of high-speed network services through large-scale connection-oriented (or packet-oriented) virtual networks running on top of optical networks as the backbone physical networks. Due to the high socio-economic importance of network services, network survivability is becoming ever more important nowadays. As society heavily depends on modern telecommunication networks, much has been done to prevent network failure, e.g., by improving the equipment environment and physical aspects of the material. However, the past century of telecommunications has shown that nodes and links still fail regularly [32]. The survivability of network services is highly dependent on the survivability of the nodes and links. For instance, optical fibers carry a huge amount of important data, such that even a single fiber failure can already be disastrous to the network operation (e.g., connection failures, data losses [33], and service outages). It was estimated in [34] that losses due to service downtime can range between \$25000 to \$150000 per hour.

Regardless of the preventive protection measures taken, network nodes and links will eventually malfunction and cease to function, especially in the event of disasters. Physical telecommunication links such as (submarine) optical fibers are known to be vulnerable to failure due to the occurrences of small-scale or large-scale disasters [35] (i.e., also referred to as external aggressions or challenges [36]), be it natural disasters (e.g., animal bites, earthquakes, fires, floods, hurricanes, or tsunamis) or anthropogenic disasters [37] (adverse events due to human actions, negligence or errors, e.g., anchor drags/drops, anti-corporate attacks, blackouts, cyber-attacks, electromagnetic pulse attacks, nuclear explosion, sabotages, terrorist attacks, or vandalism). Link failures can also be simultaneous or cascading [38]. Different disaster types and sizes may also have different impact to the network [39]. Natural disasters are particularly known to have a high destructive power that can cause a significant number of simultaneous link failures over their vast disaster area-of-effect. However, link failures often occur more due to anthropogenic disasters rather than natural disasters. For instance,

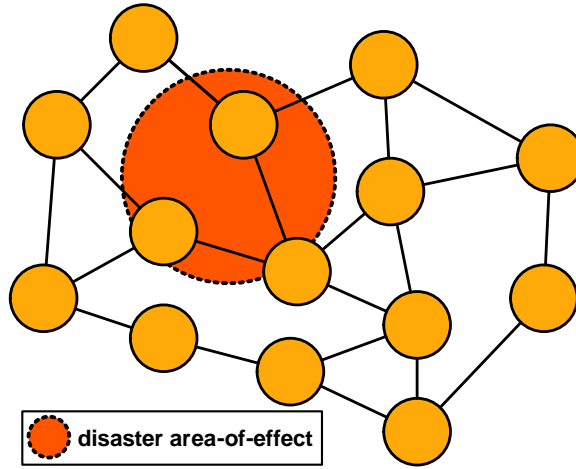


Figure 1.6: Example of a disaster with circular area-of-effect.

most of the terrestrial optical fiber failures are due to fiber cuts by construction companies and excavators, while most of the submarine optical fiber failures are due to shipping, fishing activities and anchorage [40].

In studying the impact of disasters to networks, disasters can be considered to have either deterministic [41–44] or probabilistic [33, 40, 45–47] impacts. A deterministic disaster model considers that all of the nodes and links within the area-of-effect of a disaster will cease to function upon the occurrences of the disaster, while all the network nodes or links outside of the area-of-effect of the disaster will continue to function normally. On the other hand, a probabilistic disaster model considers that the failure of nodes and links to be probabilistic, such that the failure probability of nodes and links within the area-of-effect of the disaster depends on either a fixed probability [47], a random probability [45], or the distance from the epicenter of the disaster [33, 40, 46]. Similar to the deterministic disaster model, all the nodes and links outside of the area-of-effect of the disaster will continue to function normally. The area-of-effect of a disaster (often referred to as a region [48]) is often modeled as a line cut [41, 43, 44], a circular disk [40, 42, 45–47, 49], an ellipse disk [42], a general polygon [42], a half-plane [50], or follow a specific disaster hazard map [51].

Disasters may also have area-of-effect that expands over time [45, 49, 53], move on a trajectory [53] (as shown in Figure 1.7), or favor specific geographic area. For instance, floods often occur in areas close to the sea or rivers, the West

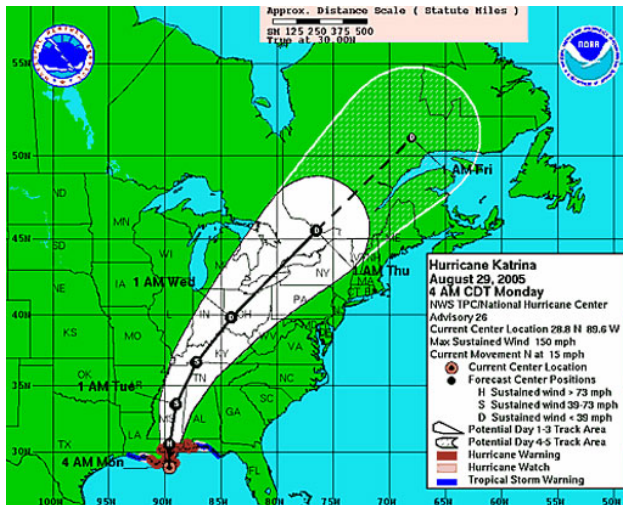


Figure 1.7: The predicted trajectory of Hurricane Katrina [52].

Coast of the United States is more vulnerable to earthquakes while the East Coast of the United States is more vulnerable to hurricanes [54], and ninety percent of the world's earthquakes occur along the Pacific Ring of Fire [55]. Certain parts of the area within the disaster risk area, are also likely to have higher measure of disaster protections, depending on the importance of the area. For instance, the Dutch has adopted this protection principle into practice in protecting the Netherlands against the threat of floods by considering the cost of flood protection and the benefit of protection [55]. We refer readers to the survey of [54] for further reading in the topic of disaster awareness in optical networks.

Network operator needs to protect network services from the risk of failing in the event of disasters, and recover disrupted network services upon the occurrences of disasters. Misjudging the adverse effect that disasters could bring to networks can prove to be a costly decision once the disasters manifest. Hence, it is crucial for network operators to proactively prepare and respond appropriately in protecting the network against the risk of disasters, such that the network services are protected against the risk of failing in the occurrences of disasters. Network operators must also take reactive measure to compensate the effect of disasters in ensuring that network services can still be satisfied upon the occurrences of disasters.

1.2.1. PROACTIVE FAILURE PREVENTION

Network operators can increase their preparedness for the adverse impact that disasters could bring to their network by identifying and finding the vulnerable parts of their network. The most vulnerable network area is the network area that will lead to the most disruptive effect if confronted by a disaster, with disaster impact computed as a measure of network disconnectivity [33, 41–43, 50, 56], the expected number of failed network nodes or total expected data loss [33]. There have been a number of works that aim to find the most vulnerable network area of a predefined size, under specific disaster models, e.g., under line disasters [43], circular disasters [33, 41–43, 47], elliptical disasters [42], or general polygon disasters [42]. [50, 56] also evaluate the probability of disconnecting two nodes under probabilistic disaster occurrences, while [41] considers the problem of finding the minimum number of circular disasters needed to disconnect a pair of network nodes. By identifying the vulnerable parts of their network, network operators can thus allocate higher level of disaster protection measures at corresponding network areas.

Another approach of ensuring the network survivability against the occurrences of disasters is by designing a network that is as robust as possible. Ill-planned network design may lead to highly vulnerable network nodes and links that are doomed to fail often or simultaneously. [40] proposed a disaster-aware optical fiber deployment that aims to place a single submarine optical fiber span using an elliptic cable shape between two terrestrial network nodes such that the monetary loss incurred by the network operator for fixing the deployed span if the span fails is reduced. [46] proposes a non-straight disaster-aware deployment of submarine optical fiber span to minimize the span failure probability and later generalizes it to a network design problem. Several rules of thumb for designing networks that are robust against large-scale disasters are also discussed in [56, 57]. Although proactive disaster-aware network design can ensure the network survivability against disasters, green-field network planning is not a luxury that many network operators have (since many optical networks are upgraded from existing older copper-based networks). The disaster-aware network design may also lead to higher network deployment costs when too many failure-leading scenarios are considered.

Instead of relying on a green-field network design approach to ensure the survivability of network services, there have been a number of works that focus on preventive disaster-aware routing. [58, 59] proposed an Integer Linear Program (ILP) and a heuristic for disaster-aware routing that minimizes the mon-

etary loss to network operator should the established network connections fail in the event of a disaster. [42] proposed algorithms for finding a pair of minimum region-disjoint paths such that both paths cannot fail simultaneously due to occurrences of a disaster with a predefined diameter. However, disaster-aware routing comes with a trade-off of assigning network connections with possibly longer [60] (but safer) paths, which in the long run can lead to inefficient network resource usage. Hence, network connections can also be routed regularly using the shortest paths, and assuming that disasters can be predicted, vulnerable network connections can be rerouted prior to the disaster events through safer parts of the network based on the network centrality metric [49] or based on the failure probability of the vulnerable paths [45].

1.2.2. REACTIVE FAILURE COMPENSATION

Regardless of the preventive measures taken to ensure the survivability of network services, network services are bound to fail eventually, especially in the event of large-scale disasters. While nodes and links can often be repaired once they have failed, the repair process may incur very high time consumption and expenses, e.g., recovering datacenter failures may take months [61]. Fixing optical fibers requires the network operator to first localize the broken or damaged part of the fiber spans, since the spans are often very long. Although failure localization can be done very fast, the actual repair duration can be lengthy due to the traveling time of the repair workers, the needs for specialized repair equipment, repair location may not be easily accessible, weather conditions may not be permitting, and many more factors. Repairing broken submarine optical fibers often took longer than repairing broken terrestrial optical fiber spans.

Considering that the repair process needs to be conducted as efficiently as possible due to the limitation of repair resources and varying importance of nodes and links, there have been a number of works such as [61] that aims to determine the most optimal sequence of nodes (or links) to be recovered at each recovery stage. While waiting for the repair process to be completed, network operators can reroute disrupted network connections that traverse the broken links using other unaffected links. [59] proposed an ILP formulation for rerouting disrupted network connections upon the occurrences of disasters, such that the network services can still be satisfied even after the occurrences of disasters.

Since rerouting may not be possible under high network utilization due to insufficient link bandwidth, [60] proposed that the bandwidth used by certain unaffected network connections be degraded as such to permit more rerouting

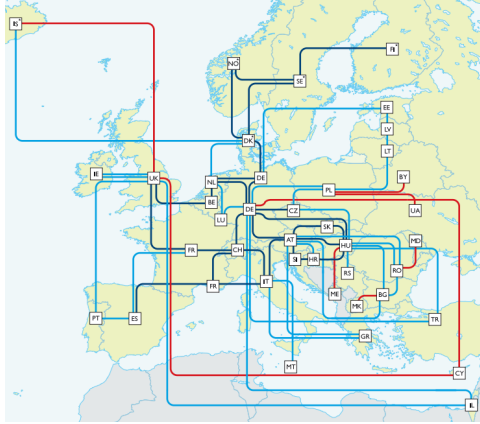


Figure 1.8: GÉANT's pan-European network [65].

of disrupted connections. Certain connections (e.g., first responder communications or air traffic controls) may also need to be prioritized during the connection rerouting process [62]. Existing unaffected connections may thus need to be preempted to make space for rerouting the high priority disrupted connections [63]. If the damage to the nodes and links is too significant, it might also be needed to create a temporary emergency network by interconnecting surviving network nodes and links using portable fiber spans [64].

1.3. MOTIVATIONS AND CONTRIBUTIONS

In telecommunication networks, communication data are transmitted between network nodes using the network links. For example, Figure 1.8 shows an optical network that serves as one of the backbones for the telecommunication network on the European scale. The physical layer of an optical network can be regarded as an interconnection of important network equipment (e.g., optical switches) that are located at the network Points-of-Presence (PoPs) by optical fiber spans. Network nodes (locations where fiber spans terminate [66]) represent network equipment and sometimes part of equipment, such as a chassis or shelf. Network elements at PoPs can also be considered as nodes, where different network elements serve a different function such as routing, switching and traffic grooming. Long distance communications are made possible between the network nodes by encoding digital data onto analog pulses of light on the optical fibers (very thin strand of doped glass), which have very low attenuation compared to older

copper wires. The data signals remain in optical form until the destination node is reached, and can have a very long lifetime if uninterrupted, even in the order of years. Each optical fiber can support a number of different wavelength channels (via Dense Wavelength-Division Multiplexing (DWDM)) with each wavelength channel capable of supporting extremely high bandwidth services, e.g., 100 Gbps [67], between different network nodes (i.e., optical connections). The number of wavelength channels available per optical fiber depends on the wavelength channel spacing defined by the network operator. Additional benefits of optical communications are low signal attenuation and distortion, low power requirements, fast service restoration capabilities, small equipment footprints, and the advantage of higher level of security against undetected data tapping. An excellent read on optical networks can be referred from [68].

Previous studies in the topic of routing have laid out the foundation for more advanced and sophisticated routing algorithms that are more problem-specific and useful in their respected applications. On the other hand, previous studies in the topic of disaster awareness have also highlighted the importance of recognizing the danger that disasters pose to the network services. The first part of this thesis will thus focus on three application-specific advanced routing problems, namely the technology-aware routing problem, the impairment-aware routing problem, and the spatiotemporal risk-averse routing problem. The second part of this thesis will continue with the topic of disaster awareness, particularly in modeling the disaster risk profiles of a network area, identifying network connections that are vulnerable to an emerging disaster risk, identifying the spatially-close fiber segments, computing the spatially-close intervals of different fibers, and grouping spatially-close fibers. In doing so, the thesis will answer the following research questions, which we divide into four different sets:

- Network connections may need to be established across multiple network domains, with each network domain managed by different network operators. In this context, the technology-aware routing problem arises due to the fact that there are no de-facto standards in the technology used by each network domain, since they are managed by different network operators. Establishing a network connection between these network domains (possibly spanning multiple intermediate network domains) is not a trivial task due to the technology incompatibilities of the network domains. How can the technology incompatibilities of network domains and inter-domain links be modeled, and how can network connections be routed accordingly under the technology continuity constraints?

- In optical networks, data are transferred between network nodes using network connections that are established as lightpaths. A lightpath is an optical path of a single wavelength channel [69], established between two network nodes over multiple fiber spans. Signals along these lightpaths accumulate transmission impairments (such as attenuation, dispersion, and distortion) and can be unreadable if the accumulated impairments are too high. Different network equipment (e.g., optical switches, optical fibers, optical amplifiers, and optical dispersion compensator) contribute differently to the transmission impairments, and thus affect the accumulated impairments differently. How can the different contribution of accumulated impairments of different network equipment be modeled, and how can network connections be routed optimally in the presence of transmission impairments?
- Network connections can cease to function due to the failure of optical fibers, especially in the event of disasters. Disasters may also have spatiotemporal characteristics, such that link availabilities vary in time. When the spatiotemporal impact of disasters can be predicted, how can disaster impacts be modeled, how can network connections that are most likely to be disrupted by the disasters be identified, and how can network connections be routed accordingly under spatiotemporal disaster impacts?
- Spatially-close optical fiber spans have a significant chance of failing simultaneously in the event of man-made or natural disasters within their geographic area. How can these spatially-close optical fiber spans be identified? Furthermore, how can the spatially-close intervals of spatially-close optical fiber spans be computed? When the information of all the spatially-close optical fiber spans can be acquired, how can the optical fiber spans be grouped (with each group representing the set of optical fiber spans that are vulnerable to fail simultaneously) optimally?

1.4. THESIS OUTLINE

The structure of this thesis and the relations between the chapters are shown in Figure 1.9. In each chapter, the corresponding research questions will be discussed, and relevant exact or heuristics algorithms will be proposed for solving them. The performance of each algorithm will also be studied on randomly generated networks or real-life networks. The remainder of this thesis is organized as follows.

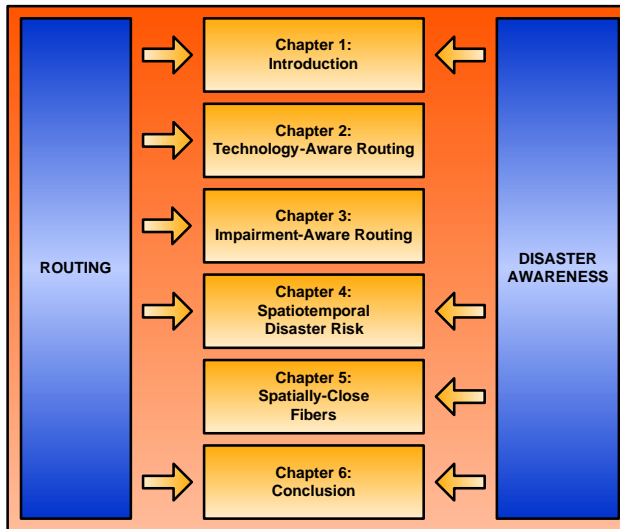


Figure 1.9: The outline of the thesis.

Chapter 2 tackles the first set of our research questions, by studying the problem of representing and finding the most optimal feasible paths in multi-domain multi-layer optical networks with technology incompatibilities. In the chapter, we propose (1) a model for representing different technology incompatibilities, and (2) an exact routing algorithm and two heuristic routing algorithms for finding most optimal feasible paths in such networks. We show that our exact algorithm is correct and always returns the most optimal technology-aware path, if such path exists. On the other hand, one of our heuristic algorithms is fast (even in absence of a feasible path) and often finds the most optimal feasible path, while the other heuristic algorithm is designed to return only a feasible path instead of the most optimal feasible path, allowing it to terminate earlier.

Chapter 3 focuses on the second set of our research questions, by studying the problem of representing and finding the most optimal feasible paths in networks with transmission impairments. In the chapter, we propose (1) a realistic link structure to quantify the potential harm of impairments, (2) a new additive routing metric, referred to as the Figure-of-Impact (FoI), that quantifies the potential harm of the non-linear Self-Phase Modulation (SPM) impairment, and (3) a two-phase heuristic for finding the most optimal feasible paths in such networks. We show that our pragmatic approach in handling transmission impairments performs well in a case study of a real-world network topology.

Chapter 4 concentrates on the third set of our research questions, by studying the problem of representing the risk profile of a network area given the prediction of disaster impacts, detecting vulnerable network connections, and finding the most risk-averse path within a given time period under spatiotemporal disaster impacts. In the chapter, we propose (1) a generic grid-based model for representing the risk profile of a network area, (2) a polynomial-time algorithm for identifying connections that are vulnerable to be disrupted by an emerging disaster risk, and (3) a polynomial-time routing algorithm for finding the most risk-averse end-to-end path within a time period under spatiotemporal disaster impacts. We also study the effect of disaster types and sizes, and network utilization to the number of vulnerable and reroutable connections.

Chapter 5 tackles on the last set of our research questions, by studying the problem of detecting spatially-close fiber segments, grouping spatially-close fibers, and differentiating spatially-close fibers by computing their spatially-close intervals. In the chapter, we propose (1) fast polynomial-time algorithms for detecting all the spatially-close fiber segments of different fibers, (2) a polynomial-time algorithm for computing the spatially-close intervals of a fiber to a set of different fibers, and (3) a fast exact algorithm for grouping spatially-close fibers using the minimum number of distinct risk groups. We show that all of our algorithms have a fast running time when simulated on three real-world network topologies.

Finally, Chapter 6 gives a comprehensive conclusion for the thesis, and discusses possible future research directions that can be derived from the thesis. Though the emphasis of this thesis is particularly on optical networks, each chapter can be generalized for applications in other network types as well.

2

TECHNOLOGY-AWARE ROUTING

This chapter is the first of the three chapters in this thesis that focus on the topic of routing. Specifically, we consider the problem of routing Big Data connections across research and education networks (a type of multi-domain optical networks), in the presence of technology incompatibilities. Transporting Big Data requires high-speed connections between end-hosts. Research and educational networks typically are state-of-the-art networks that facilitate such high-speed user-created network connections, possibly spanning multiple network domains. However, there are many different high-speed optical data plane standards and implementations, and vendors do not always create compatible data plane implementations. These technology incompatibilities may prevent direct communication between network domains and therefore complicate the configuration of network connections. However, some network domains may have adaptation capabilities that can lift the technology incompatibility constraint in establishing paths between incompatible network domains. Within this context, we address two problems, namely: (1) how to model the technology incompatibilities of multi-domain multi-layer networks, and (2) how to optimally establish feasible paths in such networks. We introduce the inclusion of the information of the supported technologies and adaptation/encapsulation capabilities of each network domain and inter-domain link in our model. We subsequently propose technology-aware routing algorithms for finding the shortest feasible path in a multi-domain multi-layer network.

Parts of this chapter have been published in Elsevier Computer Communications, vol 62, pp. 85-96, May 2015 [70].

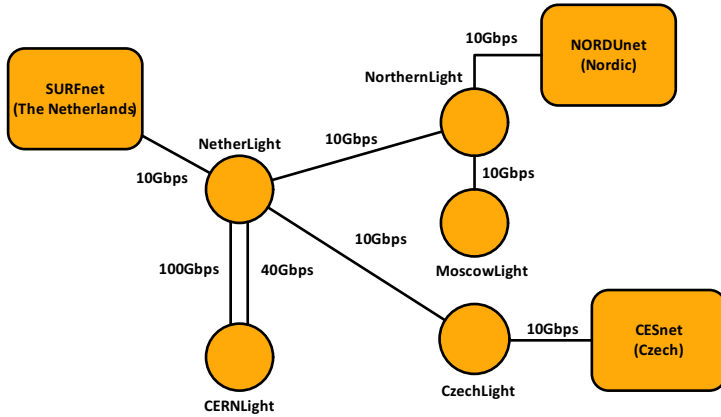


Figure 2.1: Example of a multi-domain optical network.

2.1. INTRODUCTION

Many different scientific research projects are now producing Big Data (massive or complex datasets that require advanced and sophisticated data processing applications). For instance, the fields of physics and astronomy have traditionally been the largest producers of data with projects such as the Large Hadron Collider [71], the Sloan Digital Sky Survey [72] or the planned Square Kilometer Array [73] and the Large Synoptic Survey Telescope [74]. We now see that other fields, such as biology and medical research, are also producing and transporting large data sets. These data sets are often shared between different institutes, within countries, but also across the globe. Most countries have their own National Research and Education Network (NREN) for providing high-speed connections between universities and research institutes within their country using high-speed backbone communication networks. For instance, the Dutch NREN is called SURFnet [75], and the Malaysian NREN is called MYREN [76]. NRENs can be considered as a catalyst of collaboration between research partners in their prospective countries. As becoming more common nowadays, research collaborations are not only confined within countries, but also among research partners in multiple different countries across the globe. One of the main problems faced by NRENs is how to cooperate and pool their resources for setting up international lightpaths to fulfill the ever-increasing worldwide research needs of scientific equipment sharing, data distribution, cloud computing, etc. An example of a worldwide NRENs cooperation is the Global Lambda Integrated Facility (GLIF) [77] initiative.

Traditionally, NRENs are interconnected by inter-domain optical fibers between their border nodes. In the recent years, GLIF has taken the initiative to propose the use of optical exchanges as open and neutral interconnection points between NRENs, as illustrated in Figure 2.1. Figure 2.1 consists of several administrative domains, e.g., NRENs and optical exchanges, where an administrative domain is defined as a network under the control of a single network administrator. Optical exchanges, e.g., the NetherLight [78], CERNLight [79] and CzechLight [80], are Points-of-Presence (PoPs) where all NRENs that are connected to them can communicate with each other. Optical exchanges may also be connected to other optical exchanges. Ideally, the optical exchanges can adapt their client technologies transparently without any restrictions (e.g., client identities, content type or data size).

Multi-domain routing is of interest to several standardization bodies, such as the ITU Telecommunication Standardization Sector (ITU-T), the Internet Engineering Task Force (IETF), and the Open Grid Forum (OGF). These standardization bodies have proposed a number of standards and recommendations on the topic of multi-domain networking, namely the ITU-T G.8080/Y.1304, the Path Computation Element (PCE) framework (IETF RFC4655), and the Network Service Framework (NSF) (OGF GFP173).

In the ITU-T recommendation G.8080/Y.1304 [81], an architecture framework referred to as the Automatically Switched Optical Network (ASON) was proposed for a more intelligent optical network operation. The framework introduces a logical architecture of three planes, the transport plane (i.e., data plane), the control plane and the management plane. The transport plane is made up of a number of optical switches for transporting data via optical connections; the control plane handles the management of network resources and connections, while the management plane manages the control plane. The framework also encompasses the notion of domain, inter-domain links, and several routing approaches.

The IETF RFC4655 [82] aims to decouple the routing function from the control plane such that a dedicated routing component referred to as the Path Computation Element (PCE) is used instead to find more advanced paths, such as impairment-aware paths, multi-domain-paths, and multi-layer paths. The PCE architecture can be either centralized or distributed. Multiple PCEs work together via the use of the PCE protocol (PCEP). The standard covers inter-domain routing, intra-domain routing, and inter-layer routing. Munoz et al. [83] provided a good overview of the PCE functionality.

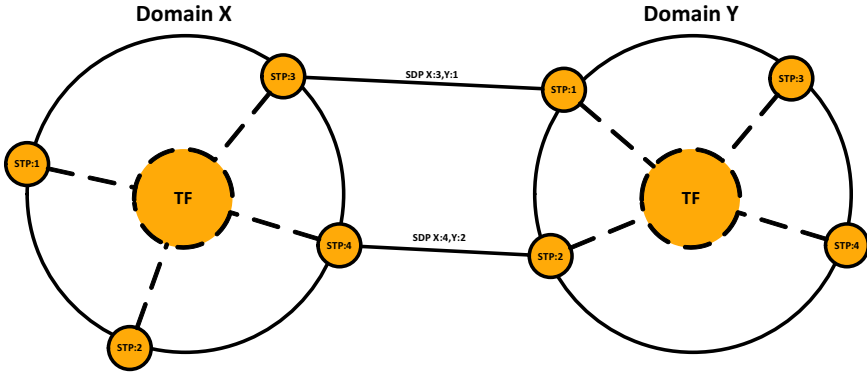


Figure 2.2: An NSI multi-domain network topology.

The OGF GFP173 [84] proposes the Network Service Interface (NSI) protocol [85] for network domains to cooperate in servicing multi-domain connection requests. NSI has been implemented by various research partners of GLIF, e.g., AutoBAHN by GÉANT, G-Lambda/A by AIST, G-Lambda/K by KDDI R&D Labs, DynamicKL by KISTI, OpenNSA by NORDUnet, OSCARS by ESnet and BoD by SURFnet [86]. Each domain is associated with a software-based management system referred to as the Network Service Agent (NSA). Multiple NSAs work collectively to establish, maintain, and terminate multi-domain connections spanning their network domains. Domains are interconnected at their Service Termination Points (STPs), which represent ports on a switch, border nodes, or specific VLANs on a port as illustrated in Figure 2.2. A grouping of two STPs is referred to as a Service Demarcation Point (SDP). Unlike the IETF PCE framework, the OGF NSF has not yet defined any specific standard for multi-domain routing.

Administrators usually build and upgrade their domain according to their preferences for vendors and technologies. These preferences could be based on capital expenditure, equipment availability, maintenance ease, etc. The wide selection of vendors and technologies leads to no de-facto standard in building domains, rendering possible technology incompatibilities between domains. Technology incompatibilities can occur in the data plane, which contains a number of switches interconnected by physical interfaces. A path between two domains is possible only if they support at least a similar technology, can adapt between the technology incompatibilities, or if there is another domain with suitable technology adaptation capability between them. Hence, routing between domains is not a trivial task. Examples of technology incompatibilities are:

Architecture incompatibilities (e.g., IP over WDM network [87, 88], SONET/SDH over WDM network [89, 90], EoS over WDM network [91], or Ethernet over WDM network [92]) imply the needs for common lowest-layer technology and adaptation feasibility to upper layers.

Switching type incompatibilities (e.g., wavelength, waveband and fibre channel at layer 1, Ethernet, Fast Distributed Data Interface (FDDI) and cell switching (ATM) at layer 2, (Generalized) Multi-Protocol Label Switching ((G)MPLS) and Internet Protocol (IP) at layer 3) can exist at various layers.

Interface incompatibilities (e.g., 1 GE Ethernet can be encapsulated into VC-3-21v SDH, VC-4-7v SDH, STS-1-24c SONET, or STS-3c-7v SONET), imply possible adaptation and deadaptation problems [93].

Rate incompatibilities (e.g., 1, 10, 40, or 100 Gbps) imply the need for data-rate conversion.

Optical incompatibilities (e.g., wavelength differences, Forward Error Correction (FEC) coding, modulation formats and symbol mappings).

Since the notion of technology-aware multi-domain multi-layer routing is not yet fully addressed in both IETF PCE framework and OGF NSE, and vendor interoperability issues remain an open research [94], we address this problem in this chapter. First, we propose a generic network model that incorporates technology incompatibilities information using technology matrices and vectors. Our model scales well with the increase of graph size and number of technology incompatibilities, and is applicable for use in modeling variety of technology incompatibilities that can occur in multi-domain multi-layer networks. Our network model would also be a useful addition to existing multi-domain standards, and existing technology representation approaches (e.g. NML [95]). Secondly, we propose exact and heuristic algorithms to find technology-aware loopless path from a source node to a destination node in networks with technology incompatibilities. Although triggered by a realistic problem in the NREN community, our work applies to multi-domain multi-layer networks in general.

The remainder of this chapter is organized as follows. Section 2.2 gives an overview of related work and our contributions. In Section 2.3, we introduce our network model and give some application examples. In Section 2.4, we define the problem formally, for which routing algorithms are proposed in Section 2.5. We present a simulative performance analysis of our algorithms in Section 2.6, and summarize the chapter in Section 2.7.

2.2. RELATED WORK

In a network with limited wavelength conversion, only a subset of nodes can convert between wavelengths. A path between two distinct nodes is feasible (without facing any technology incompatibility) if the wavelength of the path is continuous, or if appropriate wavelength conversion is conducted along the path. Chlamtac et al. [96] modeled wavelength incompatibilities by introducing a wavelength graph of $|N||W|$ nodes. The graph contains $|N|$ columns and $|W|$ rows, where $|N|$ is the number of nodes in the original network, and $|W|$ is the number of wavelengths. Link existence between nodes depends on the wavelength availability (horizontal links), and the wavelength conversion (vertical nodes). Though their work focuses on the intra-domain routing, their model can also be applied to multi-domain networks.

The ITU-T ASON framework does not include any specific control plane protocol, since it was meant to be a generic architectural framework. In the IETF RFC3945 [100], a control plane protocol suite referred to as the Generalized Multi Protocol Label Switching (GMPLS) [101] was proposed to support multi-layer applications that consist of different switching technologies. A GMPLS node may support several switching technologies, e.g., Packet Switch Capable (PSC), Layer 2 Switch Capable (L2SC), Time Division Multiplex (TDM), Lambda Switch Capable (LSC), and Fiber Switch Capable (FSC). A connection may traverse multiple nodes with different switching technologies by the nesting of Label Switched Paths (LSPs). The order of nesting is PSC, L2SC, TDM, LSC and FSC. [97, 98, 102] have studied modeling and routing under GMPLS switching incompatibilities.

Jabbari et al. [97] proposed a channel graph of $\sum_{(u,v) \in L} |Z_{uv}|$ nodes, where L is the set of links and Z_{uv} is the set of switching types supported at link $(u, v) \in L$. Each node in the graph corresponds to a switching type supported by a link. Link existence between nodes depends on the switching capability (horizontal links), and switching adaptation (vertical links). They used a variant of Yen's algorithm [17] as the routing algorithm. Their work was later extended in [102]. However, their solution does not consider the encapsulation order, which is important to ensure proper decapsulation. For instance, if technology z_1 is encapsulated in technology z_2 , and later in technology z_3 , decapsulation of z_3 is required before z_2 to get z_1 back. Shirazipour and Pierre [98] have used a graph of $|N|$ nodes and $|L|$ links as the model. Each link has a number of possible switching types, and each node has an adaptation function between the switching types. Similar to [97], they have also used Yen's algorithm [17], and later optimized the returned solution by a Binary Integer Program (BIP).

Table 2.1: Related work.

Authors	Network Model	Encapsulation Order	Node Looping	Routing Algorithm
Chlamtac et al. [96]	Wavelength graph	No	Yes	Polynomial algorithm
Jabbari et al. [97]	Channel graph	No	No	A variant of Yen's algorithm [17]
Kuipers and Dijkstra [93]	Device-based, layer-based, and stack-based graphs	Yes	Yes (with bandwidth constraint)	A variant of BFS [3, 4], exact algorithm and heuristic
Shirazipour and Pierre [98]	Simple graph with technology information	Yes	No	Yen's algorithm [17], and optimized by a Binary Integer Program (BIP)
Lamali et al. [99]	Push Down Automaton (PDA)	Yes	Yes	Polynomial algorithm based on PDA
This paper	Simple graph with technology information	Yes	No	Exact algorithm with look-ahead function and heuristics

GMPLS has a limited concept of adaptation [103], which may lead to technology adaptation and deadadaptation complications as highlighted by [93, 103]. Responses to GMPLS are also mixed. For example, while [97, 102] have deemed it promising, Das et al. in [104] have argued that GMPLS is unusable as an intelligent unified control plane for various technologies in wide-area networks. Instead of GMPLS, Lamali et al. [99] have considered the Pseudo-Wire architecture, and have proposed a language-based Push Down Automaton (PDA) model. Each protocol is represented by an alphabet, and an adaptation function between alphabets is maintained at each domain. They also developed a polynomial routing algorithm based on the PDA. Their work has been extended in [105].

Kuipers and Dijkstra [93] proposed three methods to model technology incompatibilities. Device-based, where there are $|N|$ devices, with links if two devices are connected. Layer-based, where there are $|N|$ devices and $|L|$ technology layers. Each node corresponds to a device that is aware of its technology layer. Links are either physical links or adaptation capability between technology layers. Stack-based, of at most $|N||Z|$ nodes, where $|N|$ is the number of devices, and $|Z|$ is the number of technology layers. Contrary to the layer-based model, each technology incompatibility is modeled using a different layer. Hence, there are no parallel links in this model. Nodes connected by a horizontal link in a layer can communicate directly without needing any technology adaptation, while nodes connected by a vertical link in different layers can adapt between the technologies represented by the corresponding layers. The layer-based model is unidirectional, while the device-based and stack-based models are bidirectional. A variant of BFS [3, 4] was proposed for the layer-based model, and an exact algorithm and a heuristic were proposed for the stack-based model. The layer-based model was later implemented in [106]. The problem of [93] is NP-complete, because of the imposed bandwidth constraint when traversing a node multiple times. If the bandwidth constraint in [93] were relaxed while looping is still allowed, the problem will reduce to a polynomial complexity as in [96, 99].

Similar to [93], we consider the more broad term of adaptations instead of confining to encapsulations. Contrary to the work of [93, 96, 99], which allow a connection to traverse a node multiple times, we allow only simple paths (no repeating domains) as in [97, 98]. Although confining to a simple path may lower the chance of finding feasible paths, utilizing only simple paths would lower the signaling complexity between domains in servicing connections. Our model scales well with the increase of graph size and number of technology incompatibilities, while the graph transformation approaches of [93, 96, 97, 102] may not.

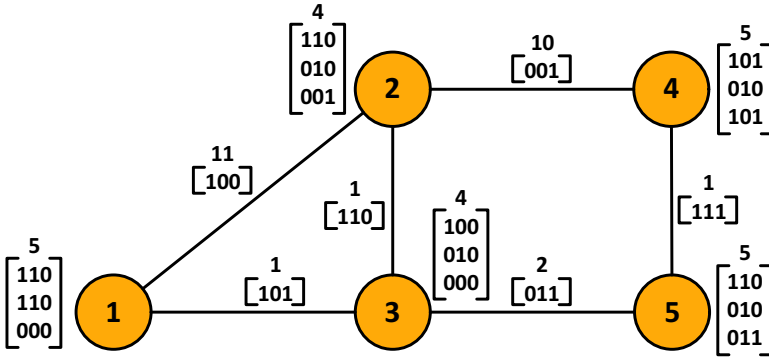


Figure 2.3: Our proposed model.

2.3. NETWORK MODEL

To enable our model, NSAs should maintain and share the knowledge of the supported technologies and (de)adaptation capabilities of their domain, and the technology supported by inter-domain links connected to STPs of their domain. We propose that each domain d be characterized with a single positive additive weight ℓ_d and a binary technology matrix X_d , while each inter-domain link (u, v) connecting domain u and v , is characterized by a single positive additive weight ℓ_{uv} and a binary technology vector X_{uv} . ℓ_d can be assumed as the largest intra-domain shortest path cost between any of the STPs of the domain d . X_d represents the technology adaptations and encapsulations supported by domain d , while X_{uv} represents the technologies supported by inter-domain link (u, v) .

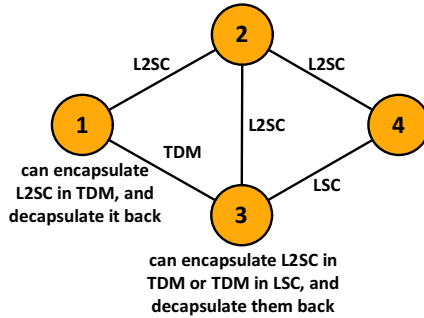
Domains can only support a finite set of technologies due to the limitations of network components. From this finite set of technologies, only some adaptations might be possible, e.g., domains can never adapt to or from unsupported technologies and the technology adaptations may or may not be reciprocal. Inter-domain links have no technology adaptation capabilities. Adjacent domains can communicate with at least one technology supported by both domains and the inter-domain link connecting them. We assume that similar technologies are supported by all intra-domain resources, since each domain is managed by a single network administrator. Thus, technology incompatibilities is most likely to be faced in an inter-domain routing problem, where we consider that each domain is aggregated into a single node view. For further reading on the benefit and overview of other topology aggregation options, we refer the readers to Uludag et. al [107], which provided a good overview on the topic of topology aggregation.

For example, in Figure 2.3, inter-domain link (1,3) with a weight of 1 supports technology 1 and 3 ($X_{1,3}[1] = X_{1,3}[3] = 1$), while domain 1 with a weight of 5 supports technology 1 and 2 ($X_1[1][1] = X_1[2][2] = 1$), and can adapt technology 1 to 2 or vice versa ($X_1[1][2] = X_1[2][1] = 1$). One denotes that the technology is supported (or can be adapted to/from) and zero, otherwise. Domains 1 and 3 can communicate directly using technology 1. Instead of using binary values to denote technology adaptation capabilities, we could also use technology adaptation cost as the values. In the remainder of the chapter, when presenting our algorithms, we will confine to binary values. We provide a generic approach to model technology incompatibilities in a multi-domain multi-layer network. Our model is applicable for various application scenarios. We proceed with two application examples of our model.

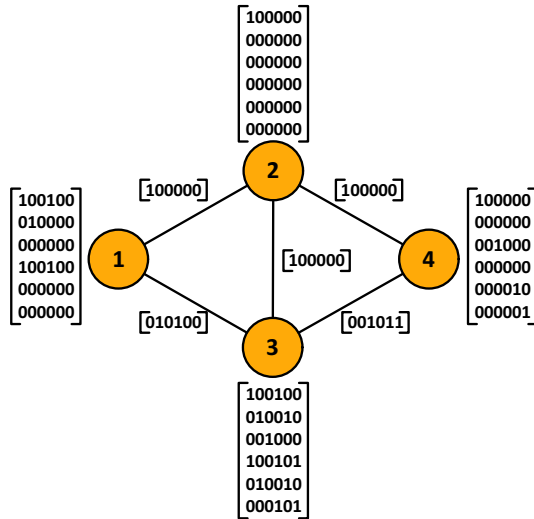
In the case of GMPLS switching incompatibilities [97, 98, 102], a domain may support one or more GMPLS switching technologies discussed in Section 2.2, and some domain may be able to encapsulate and decapsulate between the switching technologies, as illustrated in Figure 2.4. To model the network, six distinct technology representations are needed:

- Technology 1 : L2SC
- Technology 2 : TDM
- Technology 3: LSC
- Encapsulation 4 : L2SC encapsulated in TDM
- Encapsulation 5 : TDM encapsulated in LSC
- Encapsulation 6 : L2SC encapsulated in TDM encapsulated in LSC

Though originally only three switching technologies were considered, we need to also consider the encapsulation order such that proper decapsulation can be made. To explain Figure 2.4, we take domain 3 as an example. Domain 3 supports L2SC, TDM and LSC, so $X_3[1][1] = X_3[2][2] = X_3[3][3] = 1$. Supporting z_2 would imply the support of z_4 , and supporting z_3 would imply the support of z_5 and z_6 as well. Hence, $X_3[4][4] = X_3[5][5] = X_3[6][6] = 1$. Since domain 3 can encapsulate L2SC in TDM, decapsulate L2SC from TDM, encapsulate TDM in LSC, and decapsulate TDM from LSC, $X_3[1][4] = X_3[4][1] = X_3[2][5] = X_3[5][2] = X_3[4][6] = X_3[6][4] = 1$.



(a) GMPLS switching incompatibilities



(b) Corresponding representations

Figure 2.4: Modeling of GMPLS switching incompatibilities.

Another example would be the SONET (de)adaptation incompatibilities studied in [93, 103]. Considering that 1 Gigabit/second Ethernet may be encapsulated in either 21 SONET STS channels or in 24 SONET STS channels as illustrated in Figure 2.5, three distinct technology representations are needed:

- Technology 1 : Ethernet
- Encapsulation 2 : Ethernet in 21 STS
- Encapsulation 3 : Ethernet in 24 STS

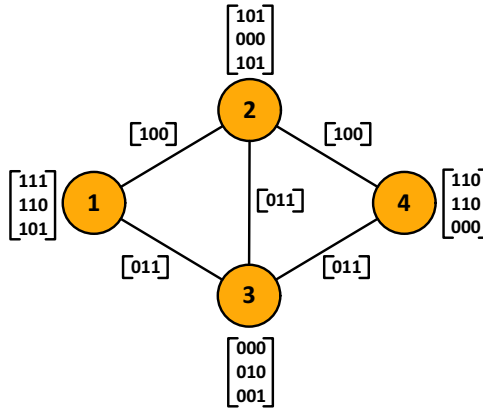
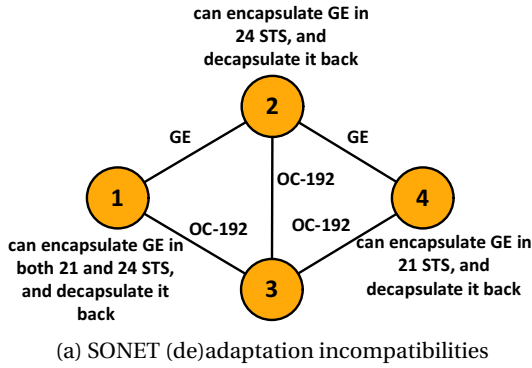


Figure 2.5: Modeling of SONET incompatibilities.

We take domain 1 as an example. Domain 1 supports both GE and SONET, so $X_1[1][1] = X_1[2][2] = X_1[3][3] = 1$. Supporting SONET would imply the support of z_2 , and z_3 . Since domain 1 can encapsulate GE in both 21 STS and 24 STS and decapsulate it back, $X_1[1][2] = X_1[2][1] = X_1[1][3] = X_1[3][1] = 1$.

Based on the given examples, we showed that our model is generic and can be applied to model various types of technology incompatibilities. However, particular insights on the distinct technology representations are needed such that proper technology representations are considered. This can vary on a case-to-case basis. Many multi-layer and hybrid devices exist, which already solve some of the incompatibilities mentioned in this subsection. These devices are exactly what makes current multi-layer networking possible, and also so complex.

2.4. PROBLEM FORMULATION

Problem 1 *Technology-Aware Shortest Path (TASP) problem:*

Given a graph $G = (D, L, Z)$ consisting of a set D of $|D|$ domains, a set L of $|L|$ inter-domain links, and a set Z of $|Z|$ incompatible technologies. Each domain $d \in D$ is characterized by a single positive additive weight ℓ_d and a binary technology matrix X_d , while each inter-domain link $(u, v) \in L$ is characterized by a single positive additive weight ℓ_{uv} and a binary technology vector X_{uv} . Find a simple feasible path from a source domain x to a destination domain y such that the total path weight is minimized.

To prove that the TASP problem is NP-hard, we show that any instance of the NP-hard Min-Sum Disjoint Paths (MSDP) problem [108] can be transformed in polynomial time to an instance of the TASP problem. Though the MSDP problem was originally intended for intra-domain routing, we refer to the problem in a multi-domain context.

Problem 2 *Min-Sum Disjoint Paths (MSDP):*

Given a graph $G = (D, L)$ consisting of a set D of $|D|$ domains and a set L of $|L|$ inter-domain links, and k source-destination domain pairs $(x_1, y_1), \dots, (x_k, y_k) \in D$. Each inter-domain link $(u, v) \in L$ is characterized by a single positive additive weight ℓ_{uv} . Find k disjoint paths to connect all the source-destination domain pairs with minimized total length.

Figure 2.6 shows the transformation of an instance of the MSDP problem to an instance of the TASP problem. We assume that each source-destination domain pairs (x_i, y_i) from the original graph supports only technology z_i . Thus, domains x_{2i} and x_{2i+1} with $1 \leq i \leq \lfloor \frac{k-1}{2} \rfloor$ have incompatible technologies and cannot communicate directly. Similarly, domains y_{2i-1} and y_{2i} with $1 \leq i \leq \lceil \frac{k-1}{2} \rceil$ have incompatible technologies and cannot communicate directly. All other domains and inter-domain links from the original graph support all technologies. We add a new domain x that supports all technologies, connecting x to x_1 by an inter-domain link supporting technology z_1 . For each domain pair (x_{2i}, x_{2i+1}) , we add an adaptation domain d_{2i} that can adapt technology z_{2i} to technology z_{2i+1} . Each domain d_{2i} is connected to x_{2i} by an inter-domain link supporting technology z_{2i} , and to x_{2i+1} by an inter-domain link supporting technology z_{2i+1} . The domain pairs can thus communicate. Similarly, for each domain pair (y_{2i-1}, y_{2i}) , we add an adaptation domain d_{2i-1} that can adapt technology z_{2i-1} to technology z_{2i} . Each domain d_{2i-1} is connected to domain y_{2i-1} by an inter-domain link supporting technology z_{2i-1} , and to domain y_{2i} by an inter-domain

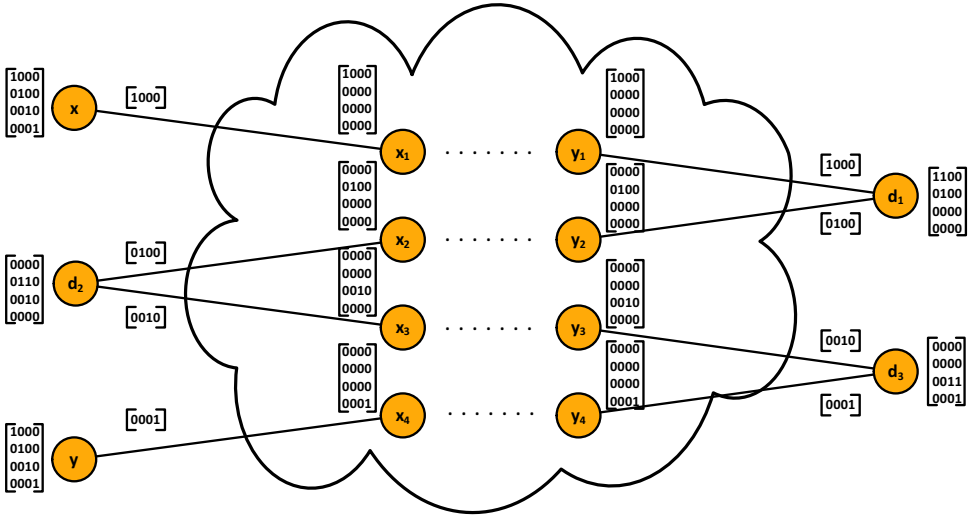


Figure 2.6: Transformation of an MSDP instance to an TASP instance.

link supporting technology z_{2i} . Either domain x_k or y_k with no connection to any of the new domains will be connected to a new destination domain y that supports all technologies by an inter-domain link supporting technology z_k .

A solution to both the MSDP and TASP problems exists if a simple feasible path exists from domain x to domain y . According to [108], the unweighted MSDP problem (i.e., all links have weight 1) is hard to approximate within $\Omega(|L|^{1-\epsilon})$ for any constant $\epsilon > 0$. Since a fully polynomial-time approximation scheme for the TASP problem is unlikely to exist, we focus on developing exact and heuristic algorithms.

2.5. ROUTING ALGORITHMS

A feasible path does not succumb to technology incompatibilities. For instance, although domains 1 and 3 can communicate directly using technology 1, and domains 3 and 5 can communicate directly using technologies 2 and 3 in Figure 2.3, $P_1 = 1 - 3 - 5$ of weight 17 is unfeasible since domain 3 cannot adapt technologies 1 to technology 2. The actual shortest simple feasible path from domain 1 to domain 5 is $P_2 = 1_1 - 2_2 - 3_2 - 5_2$ of weight 32. Although P_2 is longer than P_1 , technology 1 can be adapted to technology 2 at domain 2 before proceeding to domain 5 through domain 3. Path $P_3 = 1_1 - 3_1 - 2_2 - 3_2 - 5_2$ of weight 27 is ignored since it is not a simple path.

We propose Algorithm 1, which we refer to as the Exact Technology-Aware Routing Algorithm (*ETARA*), to solve the TASP problem. *ETARA* implements a k -shortest paths approach [109, 110] by maintaining a list of feasible subpaths at each intermediate domain. To reduce the number of subpaths maintained, we prune out subpaths that use unnecessary technology adaptation. For instance, path $P_4 = 1_1 - 3_1 - 2_2$, which adapts technology 1 to 2 at domain 2 is pruned, since path $P_5 = 1_1 - 3_2 - 2_2$ does not use technology adaptation at domain 2. However, if the identical subpaths use different technologies, e.g., $P_6 = 1_1 - 2_1 - 3_1$ and $P_7 = 1_1 - 2_2 - 3_2$, both of them will be kept since further subpath extension might need to use either of them. The subpaths of the shortest feasible path may not necessarily be shortest paths themselves. For instance, P_2 uses subpath $P_8 = 1_1 - 2_2$ with a weight of 20, which is longer than subpath P_4 of weight 15. Using subpath P_4 instead of P_8 would however lead to a path P_3 with loops. The shortest feasible path may also be unidirectional, and may not be redirected to find the shortest feasible path in the reversed direction, due to unidirectional technology adaptations of domains.

2.5.1. PSEUDOCODES

ETARA uses algorithms *SPT* in line 1 and *LOOK – AHEAD* in line 15 to reduce its search space and improving its running time. *ETARA* proceeds by initializing all the entries counter \mathcal{C}_{dz} of each domain and technology pair to zero in lines 2-4. *ETARA* maintains k subpath entries for each domain and technology pair. k could grow exponentially (albeit bounded by the maximum number of possible simple paths between two domains). The optimum weight Δ is set to infinity since no feasible path has been found so far in line 5. For each technology supported by the source domain, the tentative weight of the corresponding entry w_{xzk} is updated with the weight of the source domain ℓ_x , its predecessor entry π_{xzk} set to empty in line 8, and inserted into the queue Q in line 9. While Q is not empty, the entry u_{zk} with the lowest tentative weight w_{uzk} is extracted in line 11. If u is the destination domain, the optimum path P is returned. Else, if w_{uzk} is lower than Δ , *ETARA* proceeds with algorithm *LOOK – AHEAD* in line 15 to tighten the value of Δ . *ETARA* then checks if the current subpath of the u_{zk} can be extended to its adjacent domains in line 16. *ETARA* ensures the feasibility of the subpath in line 18, the subpath tentative weight is less than Δ in line 19, the subpath has no unnecessary technology adaptation in lines 20, and the subpath is simple in line 21. If a subpath extension is feasible, the corresponding entry v_{ij} is updated in lines 22-24, and inserted into Q in line 25.

Algorithm 1 ETARA

```

1:  $Y = \text{SPT}(G, y)$ 
2: for each domain  $d \in D$ 
3:   for each technology  $z \in Z$ 
4:      $\mathcal{C}_{dz} = 0$ 
5:  $\Delta = \infty$ 
6: for each technology  $z \in Z$ 
7:   if  $X_x[z][z] = 1$ 
8:      $\mathcal{C}_{xz} = \mathcal{C}_{xz} + 1, k = \mathcal{C}_{xz}, w_{xzk} = \ell_x, \pi_{xzk} = \text{NIL}$ 
9:      $Q \leftarrow (x_{zk}, w_{xzk}, \pi_{xzk})$ 
10: while  $Q$  is not empty
11:    $(u_{zk}, w_{uzk}, \pi_{uzk}) = \text{MIN}(Q)$ 
12:   if  $u = y$ 
13:     return solution
14:   if  $w_{uzk} < \Delta$ 
15:      $\Delta = \text{LOOK-AHEAD}(y_{zk}, \Delta, Y)$ 
16:     for each domain  $v$  that is adjacent to domain  $u$ 
17:       for each technology  $i \in Z$ 
18:         if  $X_u[z][z] = X_{uv}[z] = X_v[z][i] = X_v[i][i] = 1$ 
19:           if  $w_{uzk} + \ell_{uv} + \ell_v < \Delta$ 
20:             if  $!(i \neq z \text{ and } !(X_u[i][i] = 0 \text{ or } X_{uv}[i] = 0 \text{ or } \mathcal{C}_{ui} = 0))$ 
21:               if  $v$  is not in the current subpath of  $u_{zk}$ 
22:                  $\mathcal{C}_{vi} = \mathcal{C}_{vi} + 1, j = \mathcal{C}_{vi}$ , where  $j \leq k_{max}$  for  $kTARA$ 
23:                  $w_{vij} = w_{uzk} + \ell_{uv} + \ell_v$ 
24:                  $\pi_{vij} = u_{zk}$ 
25:                  $Q \leftarrow (v_{ij}, w_{vij}, \pi_{vij})$ 

```

SPT functions to compute a shortest feasible paths tree Y rooted at the destination domain. *SPT* may not span all domains since it opts only for the best subpath that may lead to the shortest feasible path and ignores subpaths with higher weight. *SPT* first initializes the tentative weight w'_{dz} and predecessor π'_{dz} of all entries d_z (i.e., domain and technology pairs) in lines 1-3. For each technology supported by the destination domain, the tentative weight of the corresponding entry w'_{yz} is updated with the weight of the destination domain ℓ_y in line 6, and inserted into the queue Q' in line 7. While Q' is not empty, the entry u_z with the lowest tentative weight is extracted in line 9. *SPT* checks if the current

Algorithm 2 SPT

```

1: for each domain  $d \in D$ 
2:   for each technology  $z \in Z$ 
3:      $w'_{dz} = \infty, \pi'_{dz} = NIL$ 
4:   for each technology  $z \in Z$ 
5:     if  $X_y[z][z] = 1$ 
6:        $w'_{yz} = \ell_y$ 
7:        $Q^j \leftarrow (y_z, w'_{yz}, \pi'_{yz})$ 
8:   while  $Q^j$  is not empty
9:      $(u_z, w'_{uz}, \pi'_{uz}) = \text{MIN}(Q^j)$ 
10:    for each domain  $v$  that is adjacent to domain  $u$ 
11:      for each technology  $i \in Z$ 
12:        if  $X_u[z][z] = X_{uv}[z] = X_{vu}[i] = X_v[z][i] = X_u[i][z] = X_v[i][i] = 1$ 
13:          if  $w'_{uz} + \ell_{uv} + \ell_v < w'_{vi}$ 
14:            if  $!(i \neq z \text{ and } !(X_u[i][i] = 0 \text{ or } X_{uv}[i] = 0))$ 
15:              if  $v$  is not in the current subpath of  $u_z$ 
16:                 $w'_{vi} = w'_{uz} + \ell_{uv} + \ell_v$ 
17:                 $\pi'_{vi} = u_z$ 
18:                 $Q^j \leftarrow (v_i, w'_{vi}, \pi'_{vi})$ 

```

Algorithm 3 LOOK-AHEAD

```

1: if  $u_z \in Y$ 
2:   let  $P$  be the set of domain-technology pairs in the current subpath of  $u_z$ 
3:   GO = TRUE
4:   for each domain  $d_i \in P$ 
5:     if  $d_i$  lies on the shortest path from  $u_z$  to any  $y_j \in Y$ 
6:       GO  $\leftarrow$  FALSE
7:   if  $w_{uzk} + w'_{uz} - \ell_u < \Delta$  and GO = TRUE (FTARA terminates here)
8:      $\Delta = w_{uzk} + w'_{uz} - \ell_u$ 

```

subpath of u_z can be extended to its adjacent domains in line 10. For each subpath extension, *SPT* ensures the bidirectional feasibility of the subpath in line 12, the subpath has no unnecessary technology adaptation in lines 14, and the subpath is simple in line 15. If a subpath extension is feasible, the corresponding entry v_i is updated in lines 16-17, and inserted into Q^j in line 18.

LOOK – AHEAD functions to tighten the value of Δ such that any subpath extension with higher tentative weight can be ignored, thus saving the running time of *ETARA*. *LOOK – AHEAD* uses the shortest feasible path tree Y returned by *SPT* while doing so. For each extracted entry u_{zk} of Q , *LOOK – AHEAD* checks whether u_z is a part of Y in line 1. *LOOK – AHEAD* confirms that the predecessors of the u_{zk} do not coincide with any of the entries in the branch of u_z in Y , in lines 2-6. If so, *LOOK – AHEAD* tightens Δ to the weight of the stitched end-to-end feasible path.

Although a feasible path has been found by *LOOK – AHEAD*, *ETARA* will still proceed since this might not be the shortest feasible path from x to y . However, if only a feasible path is required (not necessarily the shortest feasible path), one could terminate with the path as the solution. We call this variant the Feasible Technology-Aware Routing Algorithm (*FTARA*).

By limiting the maximum number of maintained entries k_{max} for each domain and technology pair (similarly to the limiting approach of [110] or that of a k -shortest path algorithm [109]), a heuristic form of *ETARA*, which we refer to as (k) Technology-Aware Routing Algorithm (*kTARA*), is obtained. *kTARA* is heuristic, because we do not know upfront how big to choose k_{max} to find an exact result (while *ETARA* automatically adapts to the appropriate value). Hence, if we choose k in *kTARA* smaller than the k_{max} used by *ETARA* on the same instance, *kTARA* will fail to find the optimal feasible path.

2.5.2. ILLUSTRATIVE EXAMPLE

Consider the problem of finding the shortest simple feasible path from domain 1 to domain 5 in the network shown in Figure 2.3. *ETARA* starts by invoking *SPT*. Since the destination domain 5 supports z_1, z_2 and z_3 , the three valid entries (i.e., domain-technology pair) $5_1, 5_2$ and 5_3 of domain 5 will have a tentative weight of $\ell_y = 5$, $w'_{5,1} = w'_{5,2} = w'_{5,3} = 5$. The entries are inserted into the queue Q' . Then, the three entries are extracted from Q' one by one.

Since domain 5 can communicate with domain 3 using technology 2, and with domain 4 using all technologies, $w'_{3,2}, w'_{4,1}, w'_{4,2}$ and $w'_{4,3}$ are relaxed, added to Q' and their predecessor is set, as illustrated in Figure 2.7a. Then, entry 3_2 with $w'_{3,2} = 11$ is extracted from Q . Path $3_2 - 1_2$ is not feasible since inter-domain link (2, 1) does not support technology 2, and path $3_2 - 5_2$ contains a loop. However, domain 3 can communicate with domain 2 using technology 2, as illustrated in Figure 2.7b. After that, as illustrated in Figure 2.7c, no further subpath extensions are feasible or optimal.

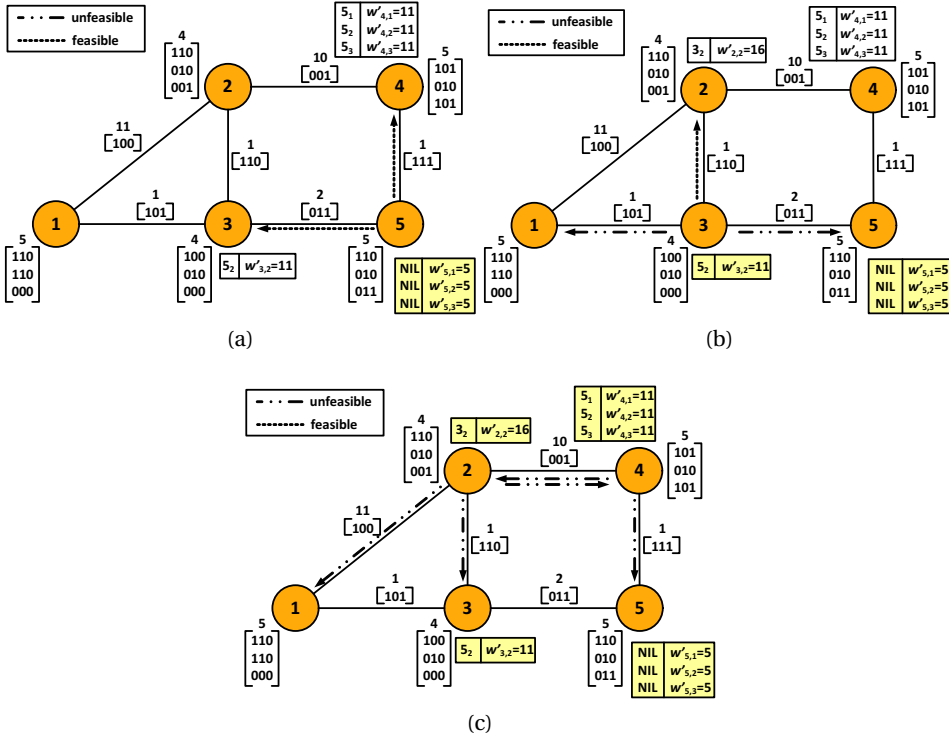


Figure 2.7: Illustrative example of SPT.

After utilizing SPT, ETARA proceeds by initializing all the valid entries (i.e., domain-technology-number pair) of the source domain, $1_{1,1}$ and $1_{2,1}$, updating their tentative distance, $w_{1,1,1} = w_{1,2,1} = 5$, and inserting them into the queue Q as illustrated in Figure 2.8a. Unlike SPT, a maximum number of k_{max} entries could be maintained by ETARA for each domain-technology pair. The two entries are then extracted from Q one by one while checking whether the subpath could be extended to domains 2 or 3. Since domain 1 can communicate with domain 2 using technology 1, with possible adaptation to technology 2, and with domain 3 using technology 1, entries $2_{1,1}$, $2_{2,1}$ and $3_{1,1}$ are inserted into Q , as illustrated in Figure 2.8a. Δ remains at infinity since these entries are not in Z . Then, entry $3_{1,1}$ with $w_{dzk} = 10$ is extracted from Q , which is also not part of Y . Path $1_1 - 3_1 - 5_1$ is not feasible due to technology restriction of inter-domain link (3, 5), and paths $1_1 - 3_1 - 1_1$ and $1_1 - 3_1 - 1_2$ contain a loop. However, domain 3 can

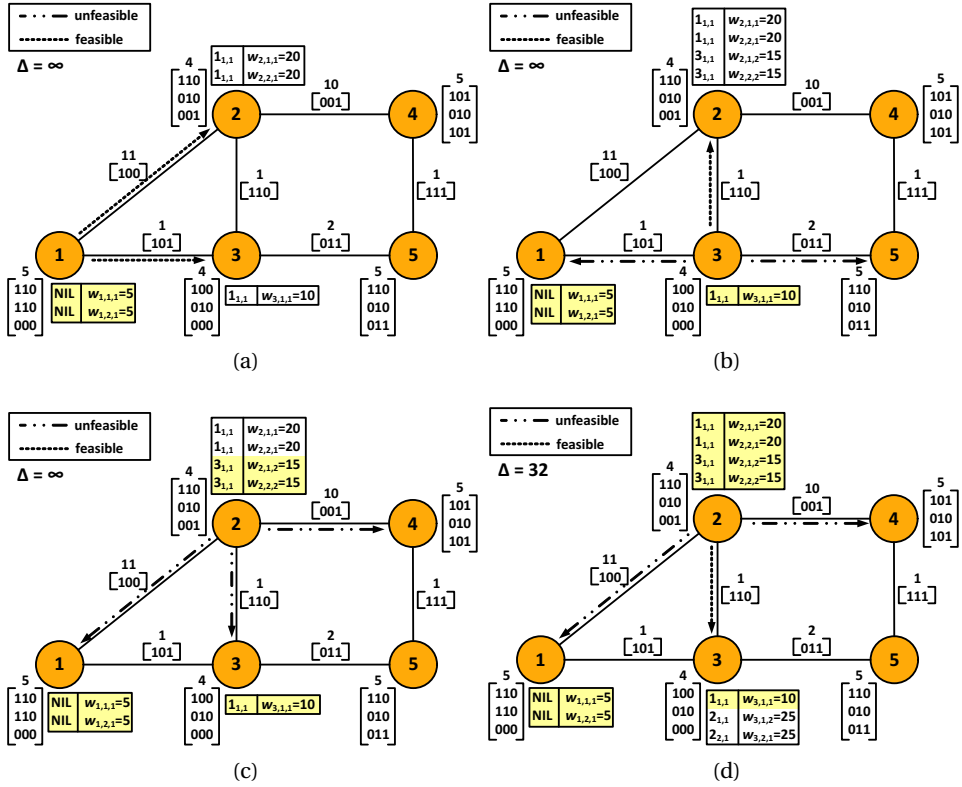


Figure 2.8: Illustrative example of *ETARA*.

communicate with domain 2 using technology 1 and further adapt it to technology 2 as in Figure 2.8b. Then, entries $2_{1,2}$ and $2_{2,2}$ with $w_{dzk} = 15$ are extracted from Q as illustrated in Figure 2.8c. Paths from domain 3 to domains 1, 2 and 4 are not feasible due to looping or technology incompatibility. Although entry 3_2 exists in F , the existence of domain 2 among its predecessors when checked by *LOOK-AHEAD* prevents *ETARA* from updating Δ . When entry $3_{2,2}$ is extracted from Q in Figure 2.8d, Algorithm 3 confirms that the predecessors of the entry do not coincide with any of the entries in the branch of $3_{2,2}$ in Y . Hence, *ETARA* tightens Δ to 32, the weight of the stitched feasible path $1_1 - 2_2 - 3_2 - 5_2$. Then, entries $3_{1,2}$ and $3_{2,1}$ are extracted. However, all subpath extensions from them are not feasible or non-optimal. Hence, *ETARA* terminates and the shortest feasible path of weight 32 can be traced back from the earlier stitched path.

2.5.3. TIME COMPLEXITY

The initialization in lines 1-9 of *ETARA* has a worst-case time complexity of $O(|D||Z| \log(|D||Z|) + |D||L||Z|)$. The extract procedure in line 11 has a worst-case time complexity of $O(k_{max}|D||Z| \log(k_{max}|D||Z|))$, since Q contains at most $k_{max}|D||Z|$ entries. Algorithm 3 in line 15 takes at most $O(D)$ time. The for loop in line 16 takes at most $O(k_{max}|L||Z|)$ time, since it is invoked at most $k_{max}|Z|$ times for each side of each inter-domain link. Lines 17-24 take at most $O(|D|)$ time. Summing up all the contributions, the worst-case time complexity of *ETARA* is $O(k_{max}|D||Z| \log(k_{max}|D||Z|) + k_{max}|D||L||Z|)$. k_{max} can grow exponentially with the input, implying that *ETARA* has an exponential running time. However, when k_{max} is bounded, as in *kTARA*, the complexity is polynomial.

2.5.4. CORRECTNESS PROOF

A brute force approach would consider all possible subpath extensions from x to y , which can be time and memory consuming. In order to make the searching process more efficient, *ETARA* prunes out all subpath extensions that is unfeasible, have loops, or with $w_{ntk} > \Delta$. Our search-space reduction will never remove any subpath of the shortest feasible path, if it exists.

If a subpath violates the technology continuity constraint, use unnecessary technology adaptations, or has loops, it can never be a part of the shortest feasible path and thus is safe to be ignored.

If a domain could be reached directly using a technology, then it is safe to ignore any subpaths with the exact domain sequence so far that use the technology adaptation capability at the domain to adapt it to the technology.

Whenever a feasible subpath is found by stitching the current subpath with the branch containing the current entry in Y , its w_{dzk} is compared with Δ . If w_{dzk} is lower, then Δ is updated to w_{dzk} . If w_{dzk} is higher, the feasible subpath could safely be ignored since another shorter subpath with the weight of Δ has already been found. We do not need to consider any extracted entry or subpath extension with $w_{dzk} > \Delta$.

Upon termination, *ETARA* will always find the solution by retracing the shortest feasible path, if it exists. *ETARA* is thus guaranteed to be exact. When limiting k_{max} using *kTARA*, exactness can no longer be guaranteed. If we stop once a feasible path is found using *FTARA*, the feasible path may not be the shortest feasible path.

2.6. SIMULATIONS

We study the performance of our algorithms in four network topologies, namely the Erdős-Rényi random network [111, 112], the lattice network, the Waxman network [113], and the GÉANT network [114]. We use $\frac{2\log|D|}{|D|}$ as the probability of an inter-domain link existence in the Erdős-Rényi random network. In the lattice network, all interior domains have the same degree and the exterior domains are connected to its closest exterior domain neighbours. This property is useful in representing grid-based networks, that may resemble the inner core of an ultra-long-reach optical data plane systems [115]. We use a square lattice network of $i \times i$ dimension where $i = \sqrt{|D|}$. The Waxman network is frequently used to model communication networks [116], optical transport networks [117], and the Internet topology [118], due to its unique property of decaying link existence over distance. In the Waxman network, the domains are uniformly positioned in the plane, and the inter-domain link existence is reflected by $ie^{\frac{\ell_{uv}}{ja}}$, where ℓ_{uv} is the Euclidean distance between nodes u and v , a is the maximum distance between any two domains in the plane, and we set $i = 0.3$ and $j = 0.55$. Higher i leads to higher link densities, and lower j leads to shorter links. The GÉANT network is a realistic pan-European network interconnecting multiple countries. We refer to [119] for the GÉANT network topology.

We consider only connected graphs, such that there is at least one path between each domain. We choose that a domain has a random weight in the range of 0.1 to 0.3, while an inter-domain link has a random weight in the range of 0.2 to 0.5 (except for the Waxman network, where the link's weight depends on the coordinates between the endpoints). No self-loops or parallel inter-domain links are allowed. The probability that a domain or an inter-domain link supports a technology is reflected by κ and $\sqrt{\kappa}$ respectively. The probability that a domain supports a unidirectional technology adaptation is κ^2 , and the probability that a domain supports a bidirectional technology adaptation is κ^3 . A domain can only adapt between its supported technologies.

We compare the performance of *ETARA*, *1TARA*, *FTARA* and the classical Dijkstra's algorithm [5] in finding the shortest simple feasible path from a random domain x to a different random domain y , while varying several network characteristics. Simulations were conducted on an Intel(R) Core i7-4600U 2.1GHz machine of 16GB RAM memory, and all results are averaged over a thousand runs. In all simulations, we terminate when k_{max} exceeded two thousand, since a solution might not exist in the randomly generated multi-domain networks.

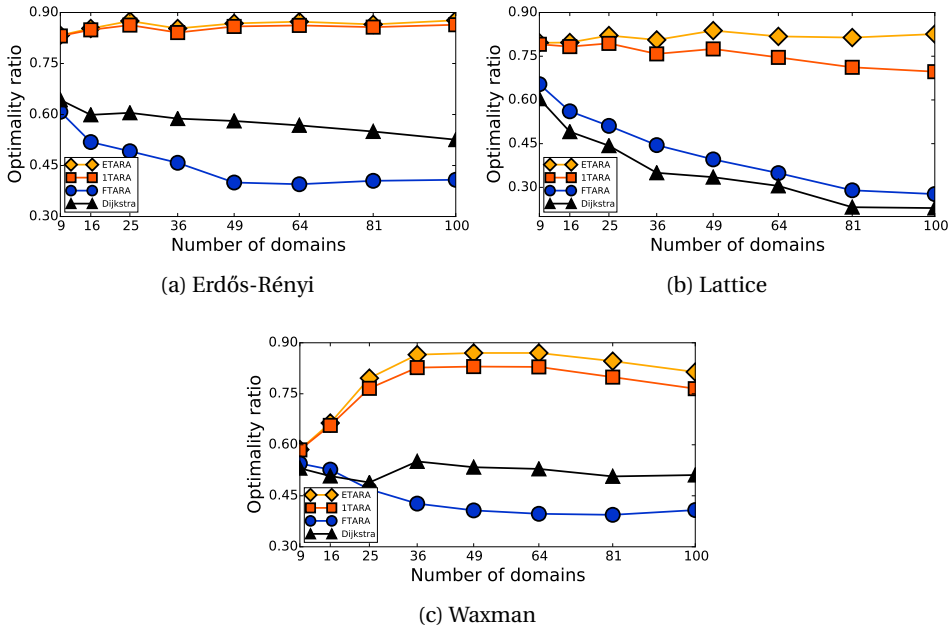


Figure 2.9: Effect of $|D|$ on the optimality ratio ($|Z| = 3$ and $\kappa = 0.6$).

Figure 2.9 illustrates the performance of *ETARA*, *1TARA*, *FTARA*, and Dijkstra’s algorithm as a function of $|D|$. The optimality ratio reflects how often the algorithm was able to retrieve the shortest feasible path. Since *ETARA* is exact, an optimality ratio for *ETARA* below one indicates that in some instances, no feasible path existed. *ETARA* performs best in finding the optimal feasible path while *1TARA* comes second due to the limitation of the number of maintained entries at each domain. The Dijkstra’s algorithm performs badly because the probability that the shortest path being also the shortest feasible path decreases as the network size increases. *FTARA* has lower optimality ratio since it terminates whenever a feasible path is found, even though the feasible path may be sub-optimal.

Figure 2.10 illustrates the optimality ratio of *ETARA*, *1TARA*, *FTARA*, and Dijkstra’s algorithm as a function of $|Z|$. As the number of technologies increases, the optimality ratio for finding the optimal path increases for both *ETARA* and *1TARA*, since we assumed an identical probability of technology existence for all technologies. Having higher number of technologies with similar κ increases the

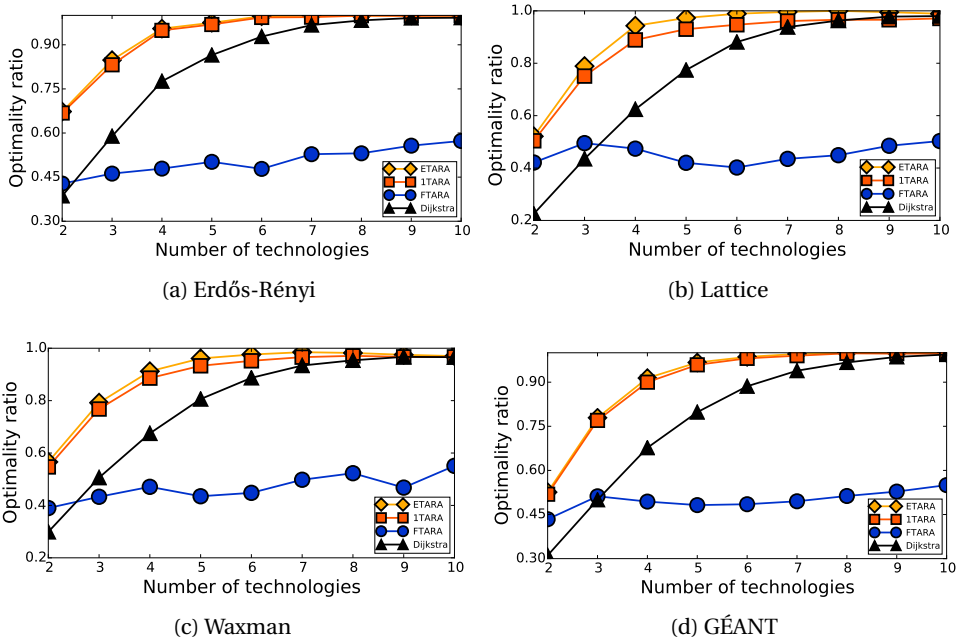


Figure 2.10: Effect of $|Z|$ on the optimality ratio ($|D| = 25$ (23 for GÉANT network) and $\kappa = 0.6$).

chance of technology continuity from x to y , thus increasing the performance of Dijkstra's algorithm. Different results may be observed if each technology has a different probability of existence.

Figure 2.11 illustrates the optimality ratio of *ETARA*, *1TARA*, *FTARA*, and Dijkstra's algorithm as a function of the technology probability κ . We notice an improved performance as κ increases. With the increase of the technology probability, the number of possible feasible paths between each network domain increases, thus increasing the chance of having a feasible multi-domain path with lower path length. Vice versa, when κ decreases, the multi-domain networks are more likely to break into islands of technologies, reducing the optimality ratio.

Figure 2.12 plots the average running time per feasible request for *ETARA*, *FTARA*, and *1TARA*. When *ETARA* is able to find an optimal feasible path, then *FTARA* also is guaranteed to find a (not necessarily optimal) feasible path. Generally, the number of entries processed from Q' increases as $|D|$ increases because more subpaths need to be considered. With the increase of the number of subpaths due to the increase of $|D|$, $|Z|$ or κ , the benefit of using Algo-

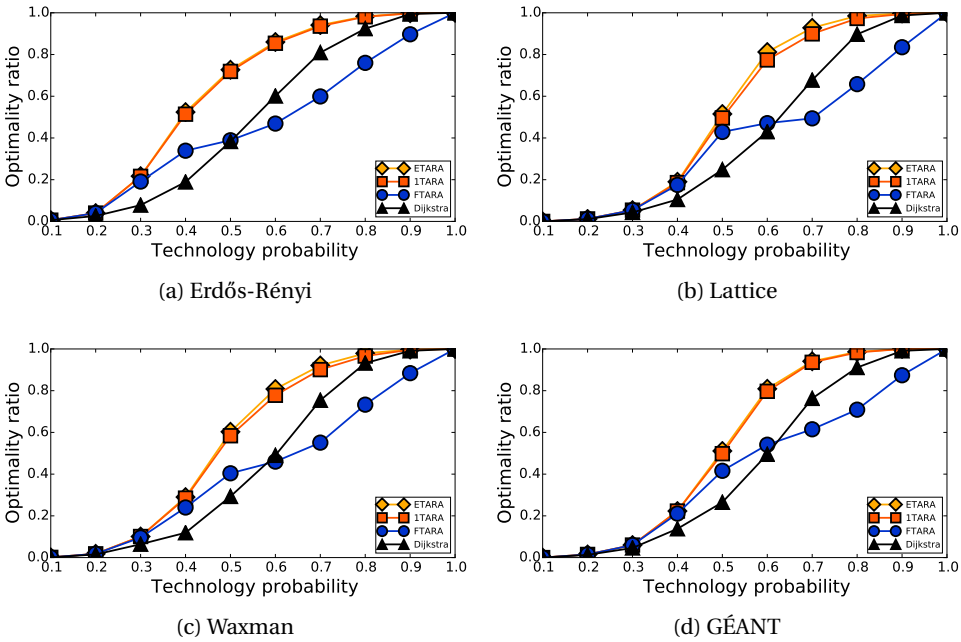


Figure 2.11: Effect of κ on the optimality ratio ($|D| = 25$ (23 for GÉANT network) and $|Z| = 3$).

rithm 3 increases. *ETARA* has highest running time, while *1TARA* will becomes faster than *FTARA* as the network average path length becomes longer. Although *FTARA* can be faster than *1TARA*, *FTARA* seldom returns the most optimal path, since *FTARA* always terminates early whenever a feasible path has been found, regardless of whether the feasible path is optimal in terms of path length or not, as shown earlier in Figure 2.9. An important advantage of *ktARA* over *ETARA* and *FTARA* is that it always terminates fast, even when no solution in the multi-domain network exists, while *ETARA* and *FTARA* may continue searching for a considerable time to come to that conclusion.

Since *ktARA* is fast (even in absence of a feasible path) and often finds the shortest feasible path, it is our recommended algorithm for multi-domain routing with technology incompatibilities.

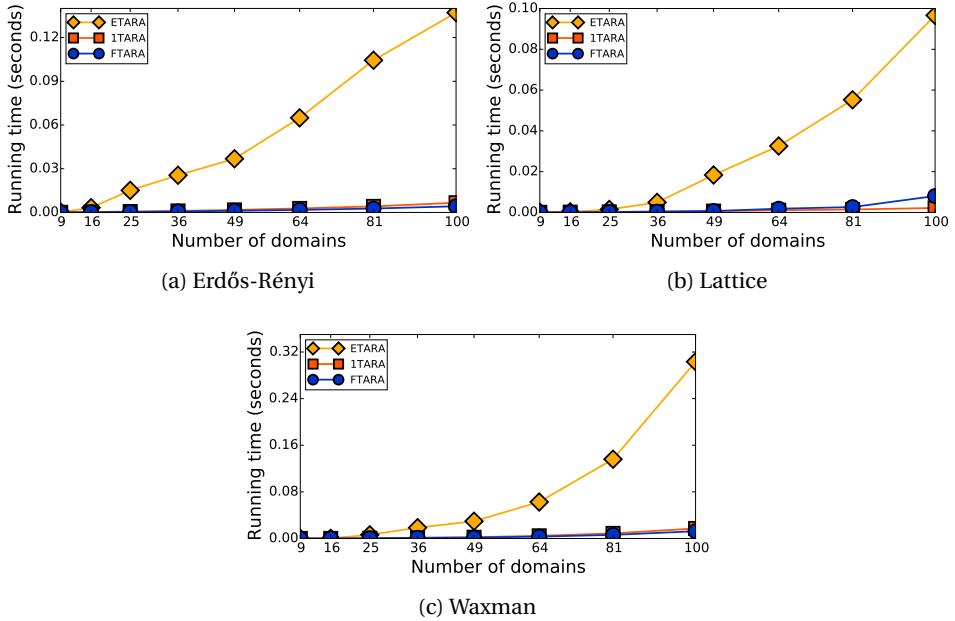


Figure 2.12: Effect of $|D|$ on the running time ($|Z| = 3$ and $\kappa = 0.6$).

2.7. CHAPTER CONCLUSION

In this chapter, we have studied the problem of finding paths in multi-domain multi-layer optical networks with technology incompatibilities. We have proposed a technology representation consisting of a technology matrix at each domain and a technology vector at each inter-domain link. In combination with costs (which could represent available bandwidth, monetary costs, impairment values, etc.) assigned to domains and inter-domain links, the technology matrices and vectors allow for flexibility in including also conversion costs, (different adaptation) policies, etc. We subsequently proposed an exact path-finding algorithm *ETARA* and heuristic *kTARA* to compute a technology-aware shortest feasible path from a source domain to a destination domain. The algorithms can be easily modified to take different objective functions (e.g., maximizing bandwidth) or QoS constraints into account. For future work, our conceptual contributions/algorithms in dealing with technology incompatibilities could also be helpful in the Software-Defined Networking (SDN) context as well.

3

IMPAIRMENT-AWARE ROUTING

Following the previous chapter, this chapter continues on the topic of routing, by focusing on the problem of routing in the presence of transmission impairments, which are common in optical networks. Optical networks are networks of nodes that are interconnected by optical fibers (the NRENs discussed in the previous chapter are examples of optical networks). The Points-of-Presence (PoPs) of optical networks are interconnected by lightpaths capable of carrying Terabits of data. However, signals along those lightpaths accumulate transmission impairments and thus can be unreadable at the receiver if the accumulated impairments are too high. Our contributions in this chapter are three-fold: (1) we propose the use of a realistic link structure to quantify the potential harm of impairments, (2) we propose a new additive routing metric, referred to as the Figure-of-Impact (FoI), that quantifies the potential harm of the non-linear Self-Phase Modulation (SPM) impairment, and (3) we propose a two-phase heuristic for solving the multi-constrained impairment-aware routing and wavelength assignment problem and apply it to a realistic network.

Parts of this chapter have been published in the 21st European Conference of Networks and Optical Communications (NOC 2015), London, United Kingdom, June 2015 [120].

3.1. INTRODUCTION

A lightpath [69] is a preconfigured transmission path on a single wavelength channel between two network nodes, possibly spanning multiple optical fiber spans. In the absence of electronic regeneration [121], signals accumulate transmission impairments [122, 123] over their lightpath and become unusable when those accumulated impairments surpass the tolerable limit at the destination node [124]. Impairment limitations are one of the major concerns for network operators when establishing lightpaths across their network.

Linear impairments (e.g., loss, noise and dispersion) are independent of the signal power and affect each wavelength individually. On the other hand, non-linear impairments (e.g., Self-Phase Modulation (SPM) and Cross-Phase Modulation (XPM)) depend on the signal power, and may cause disturbance and interference between wavelengths. Quantifying the negative effects of impairments often requires complex procedures that are computationally intensive. For instance, a high fidelity network simulator could take days to compute a path when considering impairments. In some cases, e.g., service restoration upon simultaneous failure of both the primary and backup paths of a connection, time-consuming computation may incur additional service penalty to the network operator. We thus propose a fast, pragmatic approach that quantifies the potential harm of impairments, as an alternative to the high fidelity calculation, albeit with reduced fidelity of the accumulated impairments.

Often, a simplified and rigid link structure is used to represent network links (e.g., [121, 125] consider a link as a single optical fiber, [126] considers a link as an optical fiber with attached amplifiers at each end, and [127] considers a link as a concatenation of a multiplexer, an amplifier, a fiber span, an amplifier and a demultiplexer, in that order, all of which are not representative enough for practical use). In realistic networks, different links comprise different network equipment with different impairment effects. In Section 3.2, we consider a network link as a concatenation of different link blocks (each corresponding to a network equipment), and quantify the potential harm of impairments at each link block.

In Section 3.3, we propose a new metric referred to as the Figure-of-Impact (FoI) to represent the potential harm of SPM. The FoI enables the consideration of the non-linear SPM impairment as an additive routing metric, which is useful in finding feasible lightpaths, without needing to estimate the SPM effect of each link as part of the link metric before finding paths as done in [128, 129].

In Section 3.4, we propose a two-phase heuristic, based on the formulation of an ILP and an exact algorithm, for solving the multi-constrained impairment-

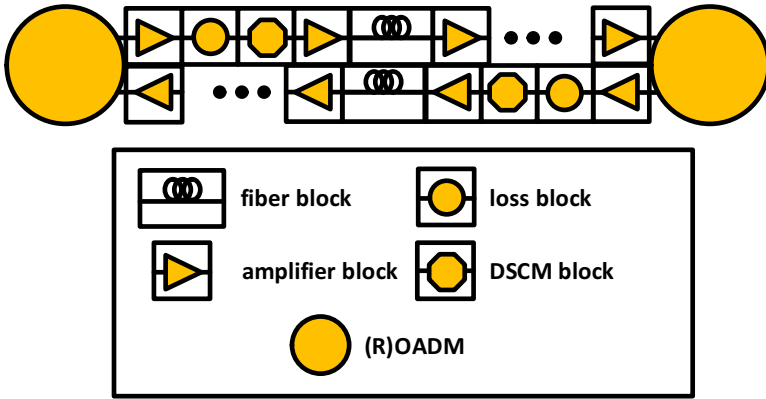


Figure 3.1: An example of a link structure.

aware routing and wavelength assignment problem. We consider multiple impairment constraints, instead of only a single impairment as done in [126]. Contrary to [121, 125–127] which consider unidirectional connections, we consider bidirectional connections (each with a feasible lightpath from the source node to the destination node, and another feasible lightpath from the destination node to the source node).

3.2. LINK STRUCTURE

We propose the link structure illustrated in Figure 3.1. Each network node is equipped with an optical add-drop multiplexer (OADM) or a reconfigurable optical add-drop multiplexer (ROADM) [91]. (R)OADMs add, drop and/or optically pass signals. Each directed link consists of a concatenation of link blocks. A directed link from node u to node v can have link blocks that are different from the directed link from node v to node u . We consider four types of link blocks,

Fiber block represents an optical fiber span (e.g., Non Dispersion-Shifted Fiber (NDSF) [130] or Non-Zero Dispersion-Shifted Fiber (NZDSF) [131]). A fiber is a very thin strand of pure glass, capable of carrying multiple lightpaths of certain wavelengths with very high bandwidth.

Amplifier block represents an optical amplifier [132]. An optical amplifier amplifies optical signals that passes through it directly, without the need for optical-electrical-optical (OEO) conversion.

DSCM block represents a Dispersion Slope Compensating Module (DSCM) [133].

A DSCM module is a fiber-based dispersion compensation module that useful in compensating the dispersion effect of a long span of fiber.

Loss block represents an attenuator [134], non-amplifier line interface module, connector transitions, or any other equipment that produces loss.

Our link structure enables the quantification of various signal parameters at each link block during path computation. For example, we consider four types of signal parameters in this chapter, namely power level, dispersion, Figure of Merit (FoM) [126], and Figure of Impact (FoI) (explained later in Section 3.3). We also address XPM in Section 3.4.

3.2.1. POWER LEVEL

The power level of signals is gradually attenuated along their lightpath due to the loss at (R)OADMs, fiber blocks, DSCM blocks and loss blocks. To compensate these losses, amplifier blocks are placed at strategic points along the link to boost the signal power to its initial power level.

(R)OADM loss - The signal power is reduced by the insertion loss α_x^{in} of the source node (R)OADM, the pass-through loss α_n^{pass} of the (R)OADM of each intermediate node n , and the outgoing loss α_y^{out} of the destination node (R)OADM.

Fiber block loss - A fiber block i reduces signal power by $\alpha_i \ell_i$ due to absorption by glass particles, heat conversion, etc, where α_i is the fiber loss coefficient in dB/km, and ℓ_i is the length of the fiber block in km.

DSCM block loss - A DSCM block i reduces signal power by $(1.7 + 0.06 \times \ell_i)$, where ℓ_i is the length of the DSCM block in km.

Loss block loss - A loss block i reduces signal power by the equipment loss, e.g., 1 dB loss for non-amplifier line interface modules, 0.5 dB loss for connector transitions, or the loss of attenuators. Attenuators ensure that the signal power is kept below a certain level to satisfy the minimum amplifier, and avoid a more serious SPM effect due to high signal power.

Amplifier block gain - An amplifier block i boosts signal power to its initial launch power (e.g., 10 Gbps signals have a 0 dBm typical launch power, while 100 Gbps

signals have a 3 dBm typical launch power). We limit the number of signals that traverse each amplifier block i , such that its total output power does not exceed its power saturation limit p_{sat} . Above p_{sat} , the amplifier gain reduces, affecting the signal's output power and noise.

3.2.2. DISPERSION

Dispersion reduces signal power within the bit slot, and spreads the signal power beyond the allocated bit slot, leading to inter-symbol interference. Dispersion occurs due to the fiber block, where light of different wavelengths travel at different speeds within the fiber thus spreading the pulse, but can be compensated by the DSCM block (or via appropriate parametric wavelength conversion [135]). For ease of implementation and without loss of generality, only chromatic dispersion is considered. Polarization Mode Dispersion (PMD) can be included in the model in a similar fashion.

Fiber block dispersion - A fiber block i increases signal dispersion by $\mathcal{D}_i \ell_i$, where \mathcal{D}_i is the fiber dispersion coefficient in ps/nm·km, and ℓ_i is the length of the fiber block in km.

DSCM block compensation - A DSCM block i reduces signal dispersion by $\beta_i \ell_i$, where β_i is the DSCM compensation coefficient in ps/nm·km, and ℓ_i is the length of the DSCM block in km.

3.2.3. FIGURE-OF-MERIT (FOM)

Though amplifiers are useful for compensating loss, they introduce Amplifier Spontaneous Emission (ASE) noise. Beshir et al. [126] proposed the Figure-of-Merit (FoM) metric to represent the potential harm of noise. We extend the use of FoM to adapt to our link structure. The FoM between two amplifier blocks a_i and a_j can be computed as,

$$\text{FoM} = 10^{\frac{\mathcal{L}_{ij}}{10}} \quad (3.1)$$

where \mathcal{L}_{ij} is the total loss in dB between a_i and a_j . The FoM of a lightpath is the sum of the FoMs between each consecutive amplifier along the lightpath.

3.2.4. FIGURE-OF-IMPACT (FOI)

In Section 3.3, we introduce a new metric referred to as the Figure-of-Impact (FoI) for quantifying the potential harm of SPM. Only SPM is considered as the

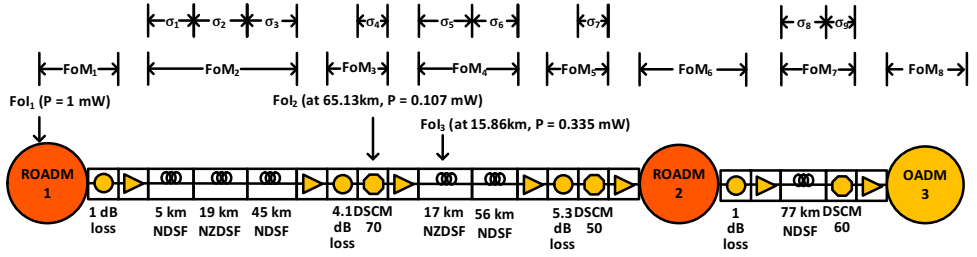


Figure 3.2: Computation example.

dominant effect caused by fiber non-linearity. XPM and FWM can be added in a similar fashion without significantly increasing the model. The total FoI of a lightpath is computed as the sum of the FoI at points along the path where the signal dispersion is zero. Examples of possible zero dispersion points are at the beginning of the lightpath, within the DSCM block and within the fiber block. At these points, the signal power is computed and the FoI is computed by Equation 3.13.

3.2.5. COMPUTATION EXAMPLE

Consider a 10 Gbps Amplitude-Shift Keying (ASK) signal that uses a lightpath P of wavelength 1530 nm from node 1 to node 3 via node 2 as illustrated in Figure 3.2. All the parameters required for computing the total path dispersion σ , the total path FoM, and the total path FoI are shown in Table 3.1.

$$\begin{aligned}\sigma_P &= \sigma_1 + \sigma_2 + \sigma_3 - \sigma_4 + \sigma_5 + \sigma_6 - \sigma_7 + \sigma_8 - \sigma_9 \\ &= \mathcal{D}_1 l_1 + \mathcal{D}_2 l_2 + \mathcal{D}_3 l_3 - \beta_4 l_4 + \mathcal{D}_5 l_5 + \mathcal{D}_6 l_6 - \beta_7 l_7 + \mathcal{D}_8 l_8 + \mathcal{D}_9 l_9 \\ &= 604.65 \text{ ps/nm}\end{aligned}$$

$$\begin{aligned}\text{FoM}_P &= \text{FoM}_1 + \text{FoM}_2 + \text{FoM}_3 + \text{FoM}_4 + \text{FoM}_5 + \text{FoM}_6 + \text{FoM}_7 + \text{FoM}_8 \\ &= 694.991\end{aligned}$$

$$\begin{aligned}\text{FoI}_P &= \text{FoI}_1 + \text{FoI}_2 + \text{FoI}_3 \\ &= \nu P_1 + \nu P_2 + \nu P_3 \\ &= 0.118\end{aligned}$$

Table 3.1: Simulation parameters.

Parameter	Symbol	Value
Amplifier maximum output power	p_{sat}	20 dBm
DSCM compensation coefficient	β	13.15 ps/nm·(1530 nm), 14.95 ps/nm·km (1565 nm)
NDSF dispersion coefficient	\mathcal{D}	15.55 ps/nm·km (1530 nm), 17.78 ps/nm·km (1565 nm)
NZDSF dispersion coefficient	\mathcal{D}	3.5 ps/nm·km (1530 nm), 5.12 ps/nm·km (1565 nm)
NDSF and NZDSF effective core area	A_{eff}	80 μm^2
NDSF and NZDSF loss coefficient	α	0.25 dB/km (or 31.66 μ Np/m)
NDSF and NZDSF non-linear refractive index coefficient	η_2	$3.2 \times 10^{-20} \text{ m}^2/\text{W}$ [136]
Initial signal power	p_{in}	0 dBm (10 Gbps signal), 3 dBm (100 Gbps signal)
(R)OADM insertion loss	α^{in}	10 dB (OADM), 16 dB (ROADM)
(R)OADM outgoing loss	α^{out}	6 dB (OADM), 10 dB (ROADM)
(R)OADM pass-through loss	α^{pass}	varies between 6 dB and 16 dB based on nodes
Signal dispersion constraint	σ_{max}	must be between -400 and 1600 ps/nm
Signal FoM constraint	FoM_{max}	720 (10 Gbps), 900 (100 Gbps)
Signal FoI constraint	FoI_{max}	0.4

3.3. THE FIGURE-OF-IMPACT (FOI)

Self-Phase Modulation (SPM) occurs due to the Kerr effect, a variation of the fiber refractive index over distance to the signal power. Different optical pulse parts undergo different phase shift, chirping the pulse. The spectral broadening due to SPM contributes to greater temporal broadening due to dispersion. SPM is a concern for signals operating at 10 Gbps or more, especially at high signal power.

We introduce a new metric referred to as the Figure-of-Impact (FoI) for quantifying the potential harm of SPM. FoI represents the ratio of the non-linear phase shift due to SPM to the linear phase shift due to dispersion. The total FoI_P of a lightpath P is computed as the sum of the FoI at points along the path where dispersion σ is fully compensated,

$$\text{FoI}_P = \sum_{i=1, \dots, j} \text{FoI}_i \mid \sigma_i = 0 \quad (3.2)$$

where j is the number of times the dispersion becomes zero in the lightpath. The more frequently a signal is fully dispersion compensated, and the higher the signal power is at these points, the higher the total FoI of the lightpath FoI_P will be.

The accumulated phase shift ϕ of a signal over a transmission distance i can be expressed as,

$$\begin{aligned} \phi &= \frac{2\pi}{\lambda} \eta_{eff} \ell_{eff} \\ &= \frac{2\pi}{\lambda} (\eta_0 + \eta_2 I_i) \ell_{eff} \\ &= \frac{2\pi}{\lambda} \eta_0 \ell_{eff} + \frac{2\pi}{\lambda} \eta_2 I_i \ell_{eff} \end{aligned} \quad (3.3)$$

where η_{eff} is the fiber effective refractive index coefficient, η_0 is the fiber linear refractive index coefficient, η_2 is the fiber non-linear refractive index coefficient, I_i is the pulse intensity at distance i and ℓ_{eff} is the effective fiber length where the signal power is assumed to be constant up to that length. I_i can be computed as,

$$\begin{aligned} I_i &= \frac{p_i}{A_{eff}} \\ &= \frac{p_1 e^{-\alpha_f i}}{A_{eff}} \end{aligned} \quad (3.4)$$

where p_i is the signal power in W at distance i , p_l is the optical launch power, A_{eff} is the effective fiber core area (i.e., the size of the area where optical power is confined within the fiber core), and α is the fiber loss coefficient.

The effective fiber length, ℓ_{eff} can be computed as,

$$\begin{aligned}\ell_{eff} &= \int_0^{\ell} e^{-\alpha l} dl \\ &= \frac{1}{\alpha} (1 - e^{-\alpha \ell})\end{aligned}\quad (3.5)$$

where ℓ is the fiber length. For a long fiber, $\ell_{eff} \sim \frac{1}{\alpha}$.

The right part of the phase shift ϕ is the non-linear phase shift ϕ_{NL} due to SPM. ϕ_{NL} can be expressed as,

$$\begin{aligned}\phi_{NL} &= \frac{2\pi}{\lambda} \eta_2 \frac{P_i}{A_{eff}} \ell_{eff} \\ &\sim \frac{2\pi}{\lambda} \frac{\eta_2}{\alpha A_{eff}} P_i\end{aligned}\quad (3.6)$$

where λ is the signal wavelength. The corresponding amount of chirp $\Delta\phi_{NL}$ due to ϕ_{NL} is,

$$\begin{aligned}\Delta\phi_{NL} &= \frac{\partial\phi_{NL}}{\partial t} \\ &= \frac{2\pi}{\lambda} \frac{\eta_2}{\alpha A_{eff}} \frac{\partial p_i}{\partial t}\end{aligned}\quad (3.7)$$

We can use a Taylor-based expansion to convert changes in optical frequency to a change in optical wavelength for obtaining a measure for the amount of power that is dispersed in time as the cause of Inter-Symbol Interference (ISI). The impact of fiber non-linearity can then be expressed as a time interval in which the signal power is dispersed,

$$\begin{aligned}\Delta\tau_{NL} &= \sigma \ell \frac{-\lambda^2}{c} \Delta\phi_{NL} \\ &= -\sigma \ell \frac{2\pi\lambda}{c} \frac{\eta_2}{\alpha A_{eff}} \frac{\partial p_i}{\partial t}\end{aligned}\quad (3.8)$$

where c is the speed of light. Assume that p_i is a raised cosine at the symbol rate of the modulating signal.

In order to evaluate the maximum dispersion induced time shift, the derivative of a typical signal p_i with respect to time is needed. In general, the largest frequency component that can be expected in the signal is the frequency that corresponds to half the symbol rate \mathcal{B} ,

$$p_i = \frac{1}{2} p_l (1 + \sin(\pi \mathcal{B} \tau)) \quad (3.9)$$

where p_l is the optical launch power.

The maximum value of the derivative is

$$\frac{\partial p_i}{\partial t} = \frac{1}{2} p_l \pi \mathcal{B} \quad (3.10)$$

$$\Delta \tau_{NL} = -\sigma \ell \frac{2\pi^2 \lambda}{c} \frac{\eta_2}{\alpha A_{eff}} p_l \mathcal{B} \quad (3.11)$$

Equation 3.11 indicates the time shift experienced by a signal when propagating across a distance ℓ caused by a launch power p_l where the signal itself is not assumed to become dispersed. Hence, dispersion is not a mechanism that reduces the non-linear phase shift.

If we consider this, it can be seen that the non-linear phase shift adds to the time shift resulting only from dispersion $\Delta \tau_\sigma$ already present in the fiber,

$$\Delta \tau_\sigma = -\sigma \ell \frac{\lambda^2}{c} \mathcal{B} \quad (3.12)$$

Let us determine the ratio of these two time shifts, which we shall refer to as the Figure of Impact (FoI),

$$\begin{aligned} \text{FoI} &= \frac{\Delta \tau_{NL}}{\Delta \tau_\sigma} \\ &= \frac{\pi^2}{\lambda} \frac{\eta_2}{\alpha A_{eff}} p_l \\ &= \nu p_l \end{aligned} \quad (3.13)$$

where ν is the FoI coefficient. It becomes clear that the more power is launched into the fiber the higher the FoI will be. For instance, a power level of 5mW which

corresponds to a FoI of 0.40 will start to deteriorate NRZ signals in an observable way, and should be avoided. Since the degree of impairment may differ per modulation type [137], different value of FoI constraint would apply to different modulation type.

3.4. APPLICATION

We define the Multi-constrained Impairment-aware Routing and Wavelength Assignment (MIRWA) problem:

Problem 3 *Multi-constrained Impairment-aware Routing and Wavelength Assignment (MIRWA) problem:*

Given a directed graph $G = (N, L)$ consisting of a set N of $|N|$ nodes and a set L of $|L|$ links, a set C of $|C|$ connection requests, and a set $\Delta = \{\sigma_{max}, FoM_{max}, FoI_{max}\}$ of three impairment constraints. Each unidirectional link $(u, v) \in L$ that connects node u to node v is associated with a set B of $|B|$ link blocks, and a set W of $|W|$ wavelengths. Each connection request $c \in C$ is associated with a tuple (x_c, y_c, δ_c) , where x_c is the source node, y_c is the destination node and δ_c is the transmission rate. Assign each $c \in C$ with a bidirectional lightpath (from x_c to y_c , and from y_c to x_c) at a wavelength $\lambda \in W$ that satisfy Δ , such that the number of used wavelengths is minimized.

The MIRWA problem is NP-hard, since it consists of two NP-hard problems, namely multi-constraint routing problem [138], and routing and wavelength assignment problem [69]. Hence, we develop a two-phase heuristic for the MIRWA problem. Phase 1 solves the multi-constrained impairment aware routing problem exactly, and Phase 2 solves the wavelength assignment problem exactly.

3.4.1. PHASE 1

In Phase 1, we propose the Multi-constrained Impairment-aware Routing (MIR) algorithm that is based on the k -shortest paths approach [109, 110] to find at most k bidirectional connections for each $c \in C$ that satisfy Δ . When there exist less than k number of feasible bidirectional connections, the MIR algorithm will still return all the feasible connections. The MIR algorithm can also be used independently to find a single connection ($k = 1$) for path restoration purposes. In the context of the MIRWA problem, we use the minimum wavelength ($\lambda = 1530$ nm) as an input to the MIR algorithm, and also ensure that the returned connections are also feasible at the maximum wavelength ($\lambda = 1565$ nm) in line 8 of

the MIR algorithm. Hence, all the k connections of each $c \in C$ will satisfy Δ at all possible wavelengths in the set W .

The pseudocode of the MIR algorithm is given in Algorithm 4. Each node n will keep at most i subpaths, with each subpath denoted by P_{ni} . A set of subpaths maintained by n is denoted by P_n . Each P_{ni} is paired with its last visited node, total hop count h_{ni} , latest signal power p_{ni} , total dispersion σ_{ni} , total loss since last amplifier \mathcal{L}_{ni} , total FoM $_{ni}$ and total FoI $_{ni}$. A subpath consisting of only the source node P_{x1} is initialized in lines 1-2, and inserted into the queue Q in line 3. While Q contains at least a subpath, the subpath with the lowest h_{ni} is extracted from Q as P_{ui} in line 5. If the last visited node of P_{ui} is y , and Δ are satisfied by both P_{ui} and the reverse subpath P'_{ui} , P_{ui} is recorded as a feasible connection in line 9. When k feasible connections have been recorded, the algorithm terminates in line 11. If not, each adjacent node v of u is checked for possible subpath extension P_{vi} . Line 16 ensures that P_{vi} is simple. The signal parameters for P_{vi} are updated accordingly to each link block $b \in B_{uv}$ of link (u, v) in lines 17-36. P_{vi} is inserted into Q in line 37. If k feasible connections do not exist, the recorded connections (less than k) are returned in line 38.

Line 5 takes at most $O(i_{max}|N| \log(i_{max}|N|))$ time, since Q contains at most $i_{max}|N|$ subpaths. Line 8 takes at most $O(|L||B|)$ time. The for loop in line 13 takes at most $O(i_{max}|L|)$ time, since the for loop is invoked at most i_{max} times for each side of each link. Summing up all contributions, the worst-case time complexity of the MIR algorithm is $O(i_{max}|N||L||B| \log(i_{max}|N|))$. Since i_{max} can grow exponentially with the input, the MIR algorithm has an exponential running time. However, a polynomial-time tuneable heuristic for the MIR algorithm can be derived by fixing i_{max} as done in [70].

3.4.2. PHASE 2

In Phase 2, we use the pre-computed k connections of Phase 1 as input to an Integer Linear Programming (ILP) formulation. The ILP returns an optimal wavelength assignments for all connection requests while minimizing the number of used wavelengths. Minimizing the number of used wavelengths leads to lower network resource consumption, and saving up the costs incurred in deploying wavelength transceiver at the network nodes. We also tailored the ILP objective such that requests with 10 Gbps transceivers are assigned starting from low wavelengths while requests with 100 Gbps transceivers are assigned starting from high wavelengths. The separation will reduce the XPM effect between 10 Gbps and 100 Gbps signals, and since connections with different data rate are assigned

Algorithm 4 MIR

```

1:  $P_{x1} = x, p_{s1} = p_{in} - \alpha_x^{in}$ 
2:  $h_{x1} = 0, \sigma_{x1} = 0, \mathcal{L}_{x1} = 0, \text{FoM}_{x1} = 0, \text{FoI}_{x1} = \nu p_{in}$ 
3:  $Q \leftarrow (x, P_{x1}, h_{x1}, p_{x1}, \sigma_{x1}, \mathcal{L}_{x1}, \text{FoM}_{x1}, \text{FoI}_{x1})$ 
4: while  $Q$  is not empty
5:    $(u, P_{ui}, h_{ui}, p_{ui}, \sigma_{ui}, \mathcal{L}_{ui}, \text{FoM}_{ui}, \text{FoI}_{ui}) \leftarrow \text{EXTRACT-MIN}(Q)$ 
6:   if  $u = y$ 
7:      $p_{ui} = p_{ui} - \alpha_y^{out}, \text{FoM}_{ui} = \text{FoM}_{ui} + 10 \frac{\alpha_y^{out}}{10}$ 
8:     if  $P_{ui}$  and  $P'_{ui}$  both satisfy  $\Delta$  at  $\lambda$ 
9:       record as a feasible connection
10:      if  $k$  connections have been recorded
11:        return the  $k$  connections
12:    if  $u \neq y$ 
13:      for each node  $v$  adjacent to node  $u$ 
14:         $P_{vi} = P_{ui} + \nu, h_j = h_{ui}, p_j = p_{ui}, \sigma_j = \sigma_{ui}, \mathcal{L}_j = \mathcal{L}_{ui}$ 
15:         $\text{FoM}_j = \text{FoM}_{ui}, \text{FoI}_j = \text{FoI}_{ui}$ 
16:        if  $P_{vi}$  is simple
17:          for each link block  $b \in B_{uv}$ 
18:            if  $b$  is a fiber block
19:               $p_j = p_j - \alpha_b \ell_b, \sigma_j = \sigma_j + \mathcal{D}_b \ell_b$ 
20:              if  $\sigma_j = 0$  at point  $a$  of the fiber block
21:                compute the signal power  $p_a$  at point  $a$ 
22:                 $\text{FoI}_j = \text{FoI}_j + \nu p_a$ 
23:                 $\mathcal{L}_j = \mathcal{L}_j + \alpha_b \ell_b$ 
24:              if  $b$  is an amplifier block
25:                 $\text{FoM}_j = \text{FoM}_j + 10 \frac{\mathcal{L}_j}{10}, p_j = p_{in}, \mathcal{L}_j = 0$ 
26:              if  $b$  is a DSCM block
27:                 $p_j = p_j - (1.7 + 0.06 \ell_b), \sigma_j = \sigma_j - \beta_b \ell_b$ 
28:                if  $\sigma_j = 0$  at point  $a$  of the DSCM block
29:                  compute the signal power  $p_a$  at point  $a$ 
30:                   $\text{FoI}_j = \text{FoI}_j + \nu p_a$ 
31:                   $\mathcal{L}_j = \mathcal{L}_j + 1.7 + 0.06 \ell_b$ 
32:              if  $b$  is a loss block
33:                 $p_j = p_j - \alpha_b, \mathcal{L}_j = \mathcal{L}_j + \alpha_b$ 
34:            if  $v \neq y$ 
35:               $p_j = p_j - \alpha_v^{pass}, \mathcal{L}_j = \mathcal{L}_j + \alpha_v^{pass}$ 
36:               $p_v = p_{vi}, h_j = h_j + 1$ 
37:               $Q \leftarrow (v, P_{vi}, h_j, p_j, \sigma_j, \mathcal{L}_j, \text{FoM}_j, \text{FoI}_j)$ 
38: return the connections

```

from each end of the wavelength spectrum, their XPM effects will be reduced due to the higher separation.

ILP Constants and Variables:

- $a_{ck\lambda}$ is 1 if connection c uses its k -th path and λ ; else 0
- b_c is 1 connection c has a 10 Gbps rate; else 0
- d_c is 1 connection c has a 100 Gbps rate; else 0
- e_{ckuv} is 1 if the k -th path of connection c uses link (u, v) ; else 0

ILP Objective:

$$\text{minimize } \sum_{c \in C, i \in k, \lambda \in W} (\lambda a_{ci\lambda} b_c + (W - \lambda)(a_{ci\lambda} d_c)) \quad (3.14)$$

ILP Constraints:

Each request has one connection and one wavelength

$$\sum_{i \in k, \lambda \in W} a_{ci\lambda} = 1 \quad \forall c \in C \quad (3.15)$$

One path is picked from the k -paths

$$\alpha_{ci\lambda} \leq \sum_{u \in N, v \in N} e_{ciuv} \quad \forall \lambda \in W, c \in C, i \in k \quad (3.16)$$

A wavelength can only be used once per link

$$\sum_{c \in C, i \in k} e_{ciuv} a_{ci\lambda} \leq 1 \quad \forall \lambda \in W, (u, v) \in L \quad (3.17)$$

Amplifier saturation gain limit

$$p_{sat} \geq \sum_{c \in C, i \in k, \lambda \in W} e_{ciuv} a_{ci\lambda} p_{in,c} \quad \forall (u, v) \in L \quad (3.18)$$

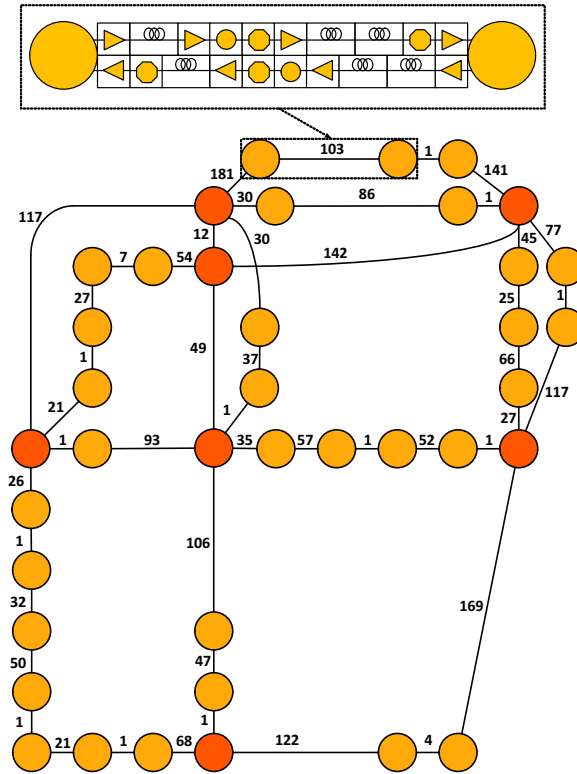


Figure 3.3: An example of a zoom-in view of a link in the SURFnet7 network.

3.4.3. SIMULATION AND ANALYSIS

For our analysis, we use a realistic set of link blocks, one realistic traffic matrix (Traffic Matrix 1) of 195 requests and one projected traffic matrix (Traffic Matrix 2) of 200 requests of the SURFnet7 network [139]. A sample zoom-in view of a link in the SURFnet7 network is illustrated in Figure 3.3. The other links also consist of a number of different link blocks. Dark shaded nodes have (R)OADMs, while light shaded nodes have OADMs. Our simulation parameters are given in Table 3.1. Simulations were conducted on an Intel(R) Core i7-4600U 2.1GHz machine of 16GB RAM memory.

The simulation results are shown in Table 3.2. The optimality of the solution and running time of the two-phase approach can be tuned by adjusting the value of k . As k is increased, the solution gradually becomes better at the cost of higher running time. For all the simulated k , Phase 1 takes as little as four seconds, and

Table 3.2: Simulation Results (with Phase 2).

k	Traffic Matrix 1		Traffic Matrix 2	
	Wavelengths Needed	Running Time (minutes)	Wavelengths Needed	Running Time (minutes)
1	47	1.53	29	1.38
2	33	3.72	25	2.98
3	29	6.05	25	4.08
4	27	8.95	24	5.38
5	27	12.18	24	6.53

Table 3.3: Simulation Results (with First-Fit instead of Phase 2).

k	Traffic Matrix 1		Traffic Matrix 2	
	Wavelengths Needed	Running Time (minutes)	Wavelengths Needed	Running Time (minutes)
1	51	0.47	32	0.18
2	51	1.51	32	1.18
3	51	2.58	32	1.33
4	51	3.40	32	1.65
5	51	3.68	32	1.95

at most one and half minutes, to be solved. Phase 2 then contributes most to the simulation running time. As an alternative, Phase 2 can be substituted with a variant of the first-fit wavelength assignment approach [140]. In the increasing order of path hop counts of its k connections, each connection $c \in C$ is assigned with a bidirectional connection and a wavelength while ensuring that all of the conditions imposed by the ILP of Phase 2 are also satisfied. The simulation results are shown in Table 3.3. Though this approach is fast, the solution is not as good as our Phase 2. The additional candidate paths provided by Phase 1 also do not improve the solution, while significant improvement due to the k connections can be observed when using our two-phase approach.

3.5. CHAPTER CONCLUSION

In this chapter, we have proposed a pragmatic approach for quantifying the potential harm of various impairments in realistic networks; a new metric referred to as the Figure-of-Impact (FoI) that quantifies the Self-Phase Modulation (SPM) impairment; and a two-phase heuristic for solving the impairment-aware routing and wavelength assignment problem. Our pragmatic approach performs well in a realistic case study of the SURFnet7 network.

4

SPATIOTEMPORAL DISASTER RISKS

This chapter falls in both the topics of routing and disaster awareness, thus bridging our transition into the topic of disaster awareness. We focus on the problems of modeling spatiotemporal disasters and routing connections accordingly under the presence of such disasters. Regardless of the preventive measures taken for ensuring the survivability of network services, network services are bound to fail eventually, especially in the event of disasters. Disasters tend to display spatiotemporal characteristics, and consequently link availabilities may vary in time. Yet, the requested connection availability of traffic must be satisfied at all times, even under disasters. In this chapter, we argue that often the spatiotemporal impact of disasters can be predicted, such that suitable actions can be taken, before the disaster manifests, to ensure the availability of connections. Our main contributions are three-fold: (1) we propose a generic grid-based model to represent the risk profile of a network area, and relate the risk profile to the availability of links and connections, (2) we propose a polynomial-time algorithm to identify connections that are vulnerable to an emerging disaster risk, and (3) we consider the predicted spatiotemporal disaster impact, and propose a polynomial-time algorithm based on an auxiliary graph to find the most risk-averse path under a time constraint.

Parts of this chapter have been published in IEEE INFOCOM Workshop on Cross-Layer Cyber-Physical Systems Security (CPSS 2016), San Francisco, United States, April 2016 [141].

4.1. INTRODUCTION

Optical networks can be managed via the Software-Defined Networking (SDN) framework, enabling the system of advanced network elements to be managed and controlled from a central location for ease of injecting information pertaining to potential disaster risks into the control system and react accordingly by reconfiguring the network upon potential issues with the network services. One of the important aspects in managing optical networks is that the availability of network services, e.g., network connectivity, is ensured at all times. A network connection between two nodes is often provided via an end-to-end path (a sequence of links) between the nodes. For instance, a lightpath in an optical network provides a secure and fast connection between nodes, enabling data transmission by network clients between the nodes. Network clients often care only about their connection availability (the probability that the connection is functioning at a random time in the future), and are often oblivious to how the end-to-end path is assigned. Different network clients may request different connection availability [142] and the assigned end-to-end path must satisfy that requested availability, even under the failure of network links. Connection availability is typically defined in the Service Level Agreements (SLAs), where a SLA is a contract between the network operator and the network clients [143].

The availability of a connection depends on the availability of the links constituting its assigned end-to-end path. Although links are designed to be as robust as possible, link failures are still a recurring problem [32], especially due to natural disasters (adverse events due to the force of nature, e.g., earthquakes, hurricanes and floods) and anthropogenic disasters [37] (adverse events due human actions, negligence or errors, e.g., construction works, nuclear explosions and sabotage). Safeguarding connections against disaster risks is important for satisfying the requested connection availability.

Certain disaster risks may be anticipated beforehand, e.g., by disaster early warning systems (e.g., hurricanes may be anticipated hours [144] or days [61] in advance, while earthquakes may be anticipated tens of seconds in advance [145]), warnings from intelligence agencies, or by predicting near-future disaster occurrences from earlier statistics. For instance, Donnellan et al. [146] conducted a study to estimate the probability that an earthquake of certain magnitude occurs near Los Angeles between May 2015 and May 2018, based on the earlier March 2014 earthquake. When the geospatial impact of disaster risks can be foreseen, network operators can configure new connections with safer end-to-end paths or reroute vulnerable existing connections through safer net-

work areas. Disaster risks may also display spatiotemporal behavior by moving around in the network area, affecting different parts of the network area at different times. Hence, the spatiotemporal nature of disaster risks needs also be considered in ensuring the availability of connections.

Our main contributions in this chapter can be summarized as follows.

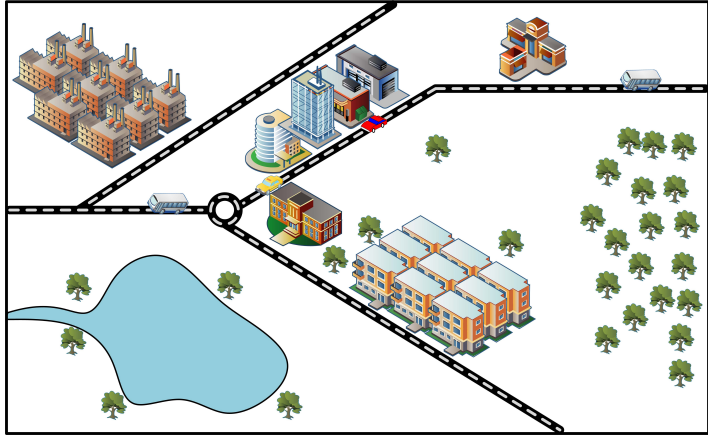
- We develop a generic grid-based model to represent the risk profile of a network area and relate the risk profile to the availability of links and connections.
- We propose a polynomial-time algorithm to identify connections that are vulnerable to an emerging disaster risk.
- We propose a polynomial-time algorithm, based on the generation of a flexible auxiliary graph, for finding the most risk-averse end-to-end path under a time constraint, when disaster risks are spatiotemporal.

The remainder of this chapter is organized as follows. In Section 4.2, we introduce our proposed grid-based model, discuss possible approaches for assigning the risk profiles, and relate the risk profiles to the availability of links and connections. We propose an approach for identifying connections that are vulnerable to an emerging disaster risk in Section 4.3 and analyze the effect of different disaster sizes on the number of vulnerable connections and for different network utilization levels. Section 4.4 explains our approach for finding the most risk-averse path under a time constraint. We discuss related work in Section 4.5 and conclude in Section 4.6.

4.2. GRID-BASED MODEL

4.2.1. AVAILABILITY OF GRID RECTANGLES

We propose a grid-based model of equally-sized rectangles for representing the network area (e.g., a terrestrial network area, an undersea network area, an urban network area or any combination of them). Assuming that the network area can be projected onto a two-dimensional Cartesian plane, the grid can be generated by partitioning the Cartesian plane into a set F of $|F|$ equally-sized rectangles. Each grid rectangle $f \in F$ is assigned with a risk in the form of an availability value A_f between zero to one, which represents the probability that the network area bounded by rectangle f is free from the impact of disasters during a specific time period. The risk that is assigned to each grid rectangle depends on the geospatial attributes of the network area bounded by the grid rectangle.



(a) network area

0.95	0.95	0.95	0.97	0.97	0.97	0.97	0.99	0.99	0.97	0.97	0.99	0.99
0.95	0.95	0.95	0.95	0.97	0.97	0.97	0.97	0.99	0.97	0.97	0.99	0.99
0.95	0.95	0.95	0.95	0.97	0.97	0.97	0.99	0.99	0.99	0.99	0.99	0.99
0.97	0.95	0.95	0.97	0.97	0.97	0.97	0.99	0.99	0.99	0.99	0.99	0.99
0.90	0.90	0.90	0.90	0.97	0.97	0.97	0.97	0.97	0.97	0.99	0.99	0.99
0.90	0.90	0.90	0.90	0.90	0.90	0.97	0.97	0.97	0.97	0.99	0.99	0.99
0.90	0.90	0.90	0.90	0.90	0.90	0.97	0.97	0.97	0.97	0.99	0.99	0.99
0.90	0.90	0.90	0.90	0.90	0.90	0.97	0.99	0.99	0.99	0.99	0.99	0.99

(b) grid model

Figure 4.1: An example of a grid of risk profiles.

Adjacent grid rectangles may or may not be assigned with equal risk value. For instance, almost ninety percent of the world's earthquakes occur along the Pacific Ring of Fire [55]. Link failures also occur more frequently in areas with higher populations, such that a grid rectangle in a city should be assigned with a grid availability that is lower than a grid rectangle in a rural area. Optical fibers are also often buried along roads and railways, such that the links are vulnerable to failure due to road and railway maintenance. Figure 4.1 shows an example

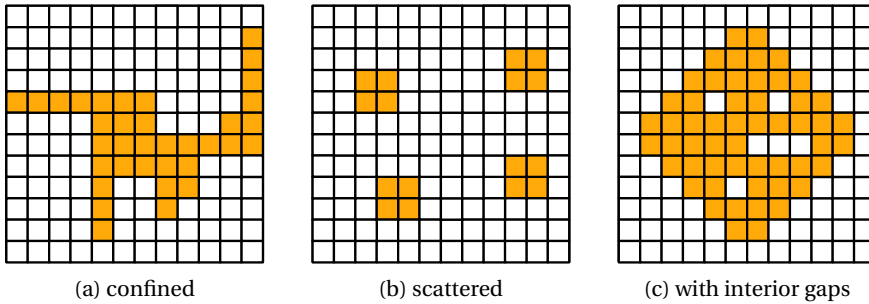


Figure 4.2: Different risk boundaries.

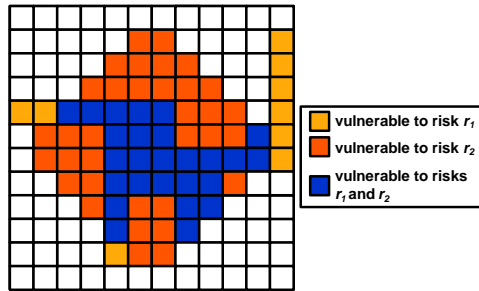


Figure 4.3: Overlapping disaster risks.

of a network area modeled by 104 grid rectangles. The accuracy of the grid in representing a network area can always be tuned by adjusting the granularity of the grid (the value of $|F|$).

The availability of a grid rectangle can also be determined by the risk of disasters in the grid rectangle. A disaster risk r is characterized by its occurrence probability $\Pr(r^o)$ and impact probability $\Pr(r^i)$. Both probabilities are equally important since although natural disasters have less occurrence probability than anthropogenic disasters, natural disasters often have higher impact probability than anthropogenic disasters [40]. Disasters can also occur without enough impact to damage their area-of-effect, e.g., an earthquake of magnitude below 2.5 poses no harm to buildings. The probability $\Pr(r)$ of a disaster r occurring and damaging its area-of-effect is

$$\Pr(r) = \Pr(r^o) \times \Pr(r^i) \quad (4.1)$$

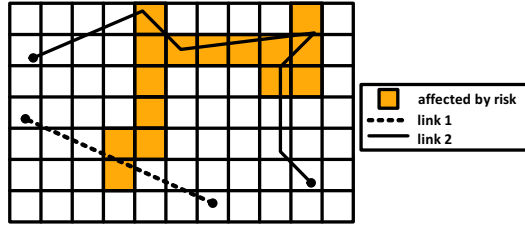


Figure 4.4: Example two different link representations.

Our grid-based model also eases the representation of various risk boundaries (e.g., confined risks, scattered risks and risks with unaffected interior gaps as shown in Figure 4.2). Confined risks, e.g., controlled demolitions and electromagnetic pulse attacks, have contained area-of-effect with regular or irregular boundaries. Scattered risks, e.g., heat waves and thunderstorms, have scattered area-of-effects. A grid rectangle f can be affected by a set of disasters R as shown in Figure 4.3, with each disaster $r \in R$ occurring independently of one another, but can occur simultaneously. The availability A_f of a grid rectangle f is

$$A_f = \prod_{r \in R} (1 - \Pr(r_f)) \quad (4.2)$$

where $\Pr(r_f)$ is the probability of disaster risk $r \in R$ occurring and damaging grid rectangle f .

4.2.2. AVAILABILITY OF LINKS AND PATHS

A network G consists of a set N of $|N|$ network nodes and a set L of $|L|$ network links. We focus on link availability, since link failures are more frequent than node failures [147]. Each link $(u, v) \in L$ can be represented as a straight line between nodes u and v , or as non-straight concatenations of multiple straight line segments of irregular lengths between nodes u and v [148], as shown in Figure 4.4. Each link $(u, v) \in L$ overlaps a set of grid rectangles $O_{uv} \subseteq F$. The failure of any grid rectangle $f \in O_{uv}$ causes the failure of link (u, v) , irrespective of the other grid rectangles in O_{uv} that do not fail. For instance, if an optical fiber is cut by a construction backhoe at a specific grid rectangle, the optical fiber ceases to function regardless of the state of other grid rectangles that the optical fiber overlaps. We consider the availability A_{uv} of each link $(u, v) \in L$ as the product of the availability of all the grid rectangles that link (u, v) crosses.

$$A_l = \prod_{f \in O_l} A_f \quad (4.3)$$

Since each connection is assigned with an end-to-end path, the availability of a connection equals the availability of its assigned end-to-end path. If the path fails, the connection ceases to function. Considering that a path P consists of a number of links, the availability of the path A_P is the product of the availability of its links.

$$A_P = \prod_{(u,v) \in P} A_{uv} \quad (4.4)$$

If multiple (maximally) disjoint paths are assigned for each network connection, Equation 4.4 can also be extended similar to the approach discussed in [149, 150].

4.3. DETECTION OF VULNERABLE CONNECTIONS

In the emergence of a risk of disaster to parts of the network area at a point in time, vulnerable existing connections (connections that cannot satisfy their requested availability once the disaster manifests) need to be detected and properly rerouted using safer paths. Only then can the availability of connections be ensured if the disaster manifests.

4.3.1. PROBLEM DEFINITION

Problem 4 *Detection of Vulnerable Connections (DVC) problem:*

Given a network G of a set N of $|N|$ nodes and a set L of $|L|$ links, a grid F of $|F|$ grid rectangles representing the area into which G is embedded, a set C of $|C|$ existing connections, and a set $F' \subseteq F$ of $|F'|$ grid rectangles that are vulnerable to disaster risk r . Each grid rectangle $f \in F$ is characterized by a grid availability A_f , and each grid rectangle $f \in F'$ is characterized by a projected worst-case reduced grid availability A'_f due to disaster risk r . Each link $(u, v) \in L$ connects nodes u and v , and overlaps a set $O_{uv} \subseteq F$ of $|O_{uv}|$ grid rectangles. Each connection $c \in C$ is characterized by a requested connection availability A_c and an end-to-end path P_c . Identify the set $C' \subseteq C$ of connections that are vulnerable to disaster risk r .

The DVC problem is polynomially solvable when the grid-based model of Section 4.2 is considered.

Algorithm 5 Detecting Vulnerable Connections

-
- 1: populate an R-tree Y with all the grid rectangles $f \in F$
 - 2: **for** each link $(u, v) \in L$
 - 3: compute its minimum bounding rectangle MBR_{uv}
 - 4: find the set $O_{uv} \in Y$ that overlaps MBR_{uv}
 - 5: **for** each grid rectangle $f \in O_{uv}$
 - 6: **if** f does not overlaps link (u, v)
 - 7: remove f from O_{uv}
 - 8: compute the projected availability A'_{uv} of link (u, v)
 - 9: **for** each connection $c \in C$
 - 10: compute its projected path availability A'_{P_c}
 - 11: **if** $A'_{P_c} < A_c$
 - 12: add c into the vulnerable connection set C'
-

4.3.2. OUR APPROACH

We propose Algorithm 5 for solving the DVC problem. In line 1 of Algorithm 5, an R-tree [151] (a depth-balanced data structure for organizing objects using bounded rectangles) is populated with all the grid rectangles. Lines 3-4 use the minimum bounding rectangle (MBR) of each link for performing a window query on the R-tree Y , by recursively checking the R-tree nodes for grid rectangles that overlap the MBR of the link. Lines 5-7 confirm that the grid rectangles overlap the link and not just the MBR of the link. The R-tree eliminates the need for checking pairwise overlap between all possible link and grid rectangle pairs, by identifying beforehand the grid rectangles that may overlap each link. The projected availability of links is computed using Equation 4.3 in line 8, and the projected availability of existing connections is computed using Equation 4.4 in line 10. If the projected path availability A'_{P_c} of a connection c is less than its requested connection availability A_c , c is vulnerable to disaster risk r .

Populating the R-tree takes at most $O(|F| \log |F|)$ time [152]. Finding the grid rectangles that overlap each link takes at most $O(|F|)$ time, since in the worst case, a link can overlap all grid rectangles. Computing the availability of connections and identifying vulnerable connections takes at most $O(|C||L|)$ time. Summing up all contributions, the worst-case time complexity of Algorithm 5 is $O(|F| \log |F| + |L|(|F| + |C|))$.

4.3.3. ANALYSIS

We analyze the effect of the size of the disaster risk to the number of vulnerable connections for different levels of network utilization in three network topologies, namely the Erdős-Rényi random network [111, 112], the lattice network, and the Waxman network [113]. In all three topologies, $|N|$ nodes are placed uniformly at random coordinates in the grid. We use $\frac{2\log|N|}{|N|}$ as the probability of a link existence in the Erdős-Rényi random network. In the lattice network, all interior nodes have the same degree and the exterior nodes are connected to its closest exterior node neighbours. This property is useful in representing grid-based networks, that may resemble the inner core of an ultra-long-reach optical data plane systems [115]. We use a square lattice network of $i \times i$ dimension where $i = \sqrt{|N|}$. We generate Waxman graph [113] in a grid F of $|F|$ grid rectangles. The Waxman graph is frequently used for representing spatial networks, e.g., communication networks [116], optical transport networks [117], and the Internet topology [118], due to its unique property of decaying link existence over distance. The link existence is reflected by $ie^{-\frac{\ell_{uv}}{ja}}$, where ℓ_{uv} is the Euclidean distance between nodes u and v , and a is the maximum Euclidean distance between any nodes. Higher i leads to higher link densities, and lower j leads to shorter links. We consider only connected graphs, such that there is at least one path between each node. Each grid rectangle $f \in F$ is assigned with a random availability A_f between 0.9999 and 1.0000. Simulations are conducted on an Intel(R) Core i7-4600U 2.1GHz machine of 16GB RAM memory, with $|F| = 2500, |N| = 25, i = 0.6$ and $j = 0.6$. All results are averaged over five thousand runs.

We generate a random set $|C|$ of C existing connections according to the network utilization level for each simulation run. The network utilization is the average utilization of all links, with each link having $|W| = 50$ capacity. In an iterative manner (until the network utilization is reached), a connection c is assigned with a random source-destination node pair (x_c, y_c) , and an end-to-end path P_c with the highest possible availability A_{P_c} (using Dijkstra's algorithm [5] with $-\log A_{uv}$ as the link weight of each link $(u, v) \in L$). Each connection $c \in C$ is then assigned with a random requested connection availability A_c between 0.7000 and A_{P_c} .

We consider both confined and scattered risks in our analysis. We generate a confined emerging risk by randomly selecting a grid rectangle as the epicenter, and randomly expanding set F' with one of the adjacent grid rectangles until the required $|F'|$ is achieved. We ensure that confined emerging risks of different sizes have the same epicenter for each simulation run for a fair analysis. We gen-

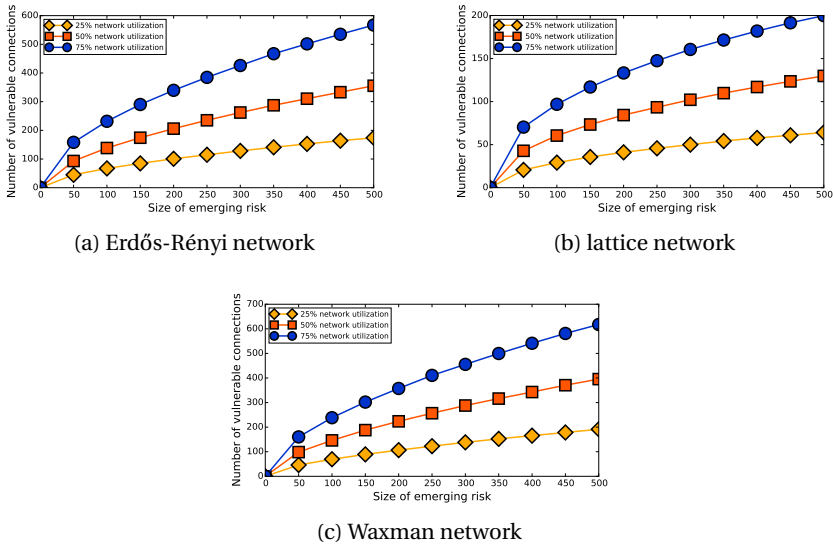


Figure 4.5: Effect of disaster size to the number of vulnerable connections (confined risk).

erate a scattered emerging risk by randomly selecting $|F'|$ grid rectangles from F . The projected reduced availability (once the risk manifests) of each grid rectangle $f \in F'$ is assumed to be half of its original value.

Figures 4.5 and 4.6 show the effect of the size of the emerging risk on the number of vulnerable connections. As the size of the emerging risk increases, more connections are vulnerable to the emerging risk. A scattered emerging risk is more detrimental to connections than a confined emerging risk. More connections are also vulnerable to the emerging risk as the network utilization level increases, as shown in Figures 4.7 and 4.8.

Vulnerable connections need to be rerouted through safer network areas, such that the connection availability can be satisfied when the risk manifests. Figures 4.9, 4.10, 4.11 and 4.12 categorize vulnerable connections into reroutable and unroutable connections. A vulnerable connection is reroutable if there is at least an alternate path in the network that can satisfy the requested connection availability. Else, the connection is unroutable. The number of reroutable connections increases with the disaster size since more connections are affected by the disasters, but fell after a certain increase since the possibility of rerouting decreases with the increase of disaster size. Although the number of reroutable

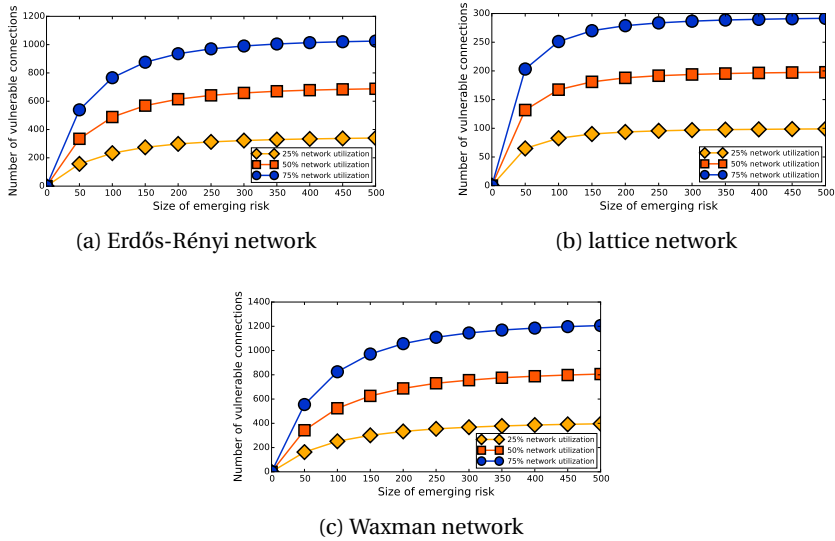


Figure 4.6: Effect of disaster size to the number of vulnerable connections (scattered risk).

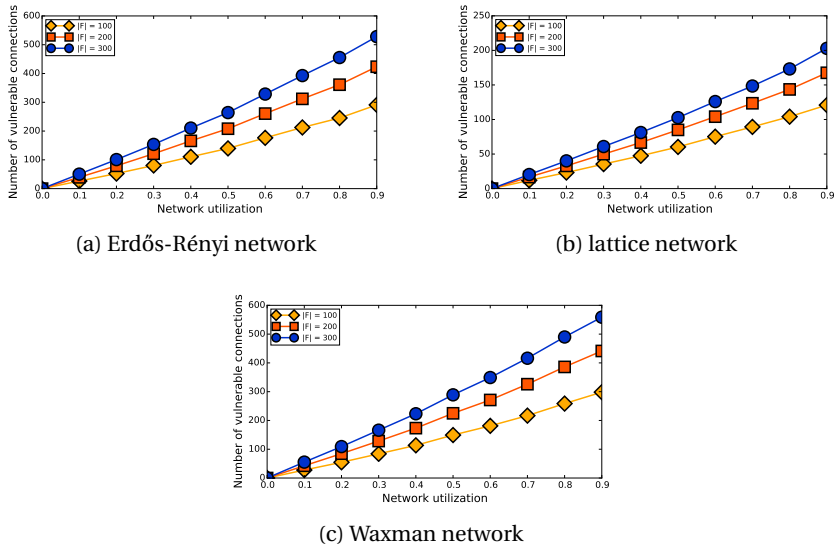


Figure 4.7: Effect of network utilization to the number of vulnerable connections (confined risk).

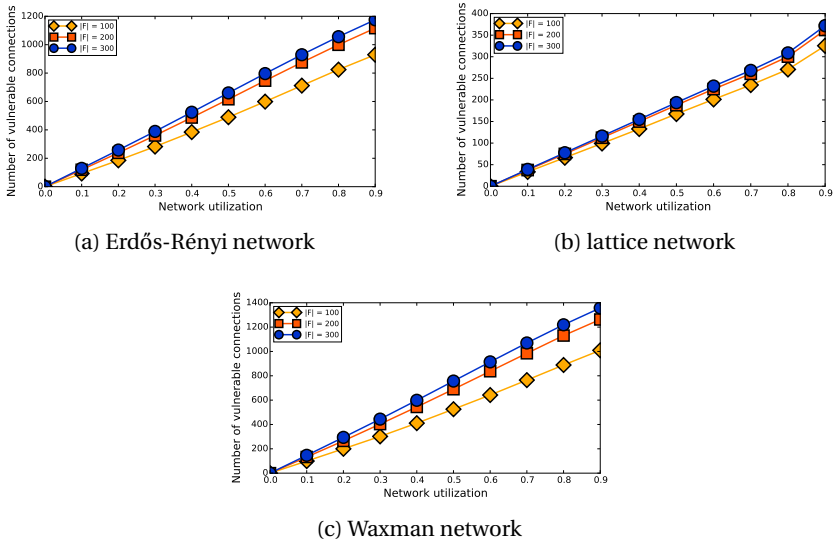


Figure 4.8: Effect of network utilization to the number of vulnerable connections (scattered risk).

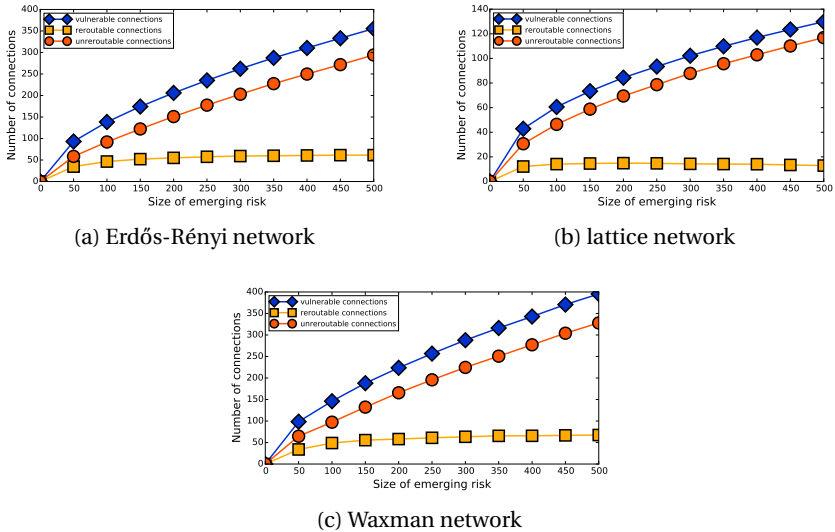


Figure 4.9: Effect of $|F|$ to the status of connections (network utilization = 0.5, confined risk).

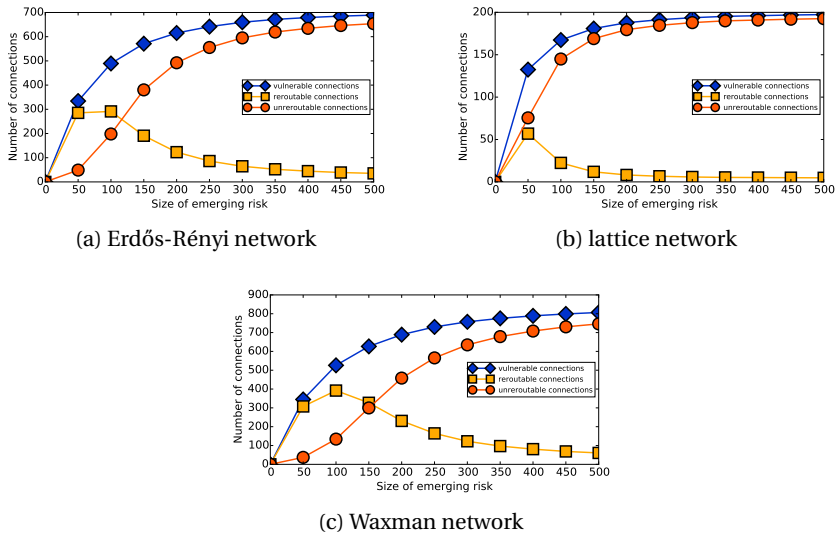


Figure 4.10: Effect of $|F|$ to the status of connections (network utilization = 0.5, scattered risk).

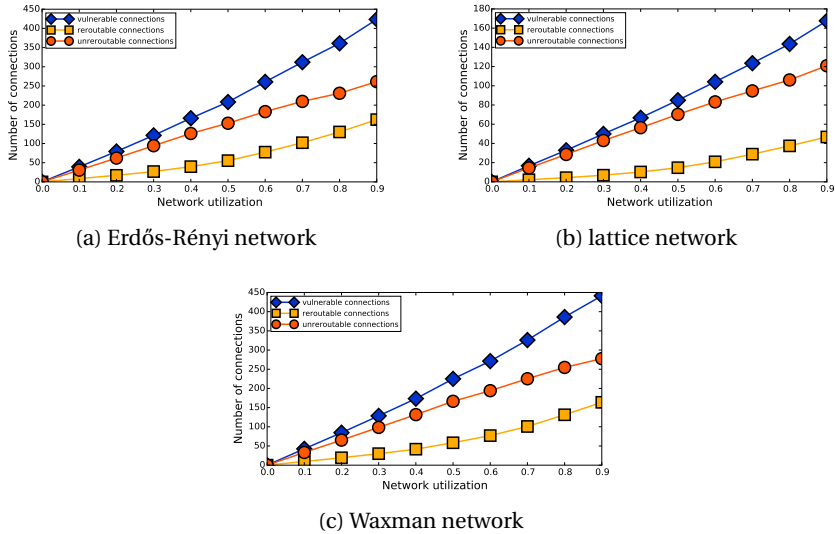


Figure 4.11: Effect of network utilization to the status of connections ($|F| = 200$, confined risk).

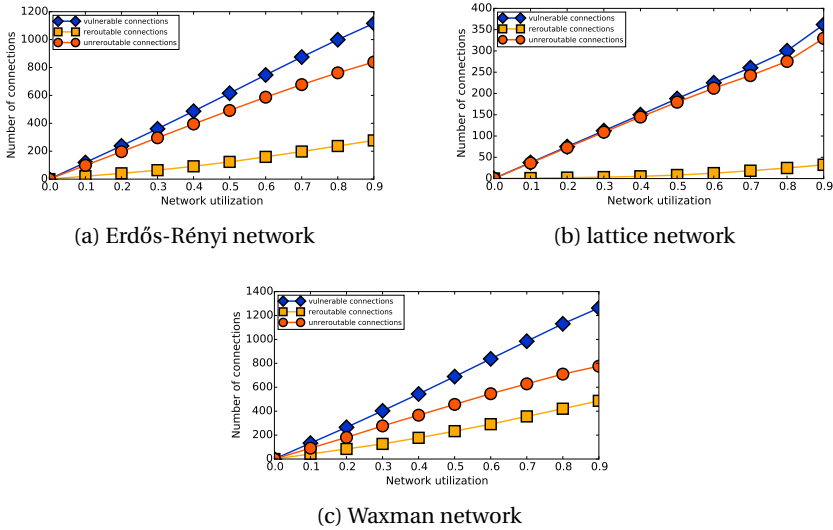


Figure 4.12: Effect of network utilization to the status of connections ($|F| = 200$, scattered risk).

connections increases with network utilization, the ratio between the number of reroutable connections and the number of unreroutable connections increases as well. In order to increase the possibility of rerouting under high network utilization, least-loaded routing algorithms [153] can also be used instead. Since the possibility of rerouting after the disaster risk has manifests is low, we focus on finding the most risk-averse path in the next section such that connections can be rerouted accordingly through safer network area before the disaster risk manifests.

4.4. SPATIOTEMPORAL RISK-AVERSE ROUTING

Disasters may also travel within or pass through the network area, such that its impact on the risk profiles of the network area differs in time. For example, consider the network area shown in Figure 4.13. The network consists of four nodes and four links, and the network area is represented as a grid of 36 grid rectangles. It takes one time slot to traverse links (1,3) and (3,4), and two time slots to traverse links (1,2) and (2,4). At time slot t_0 , a hurricane manifests at the upper right part of the network area, reducing the availability of the grid rectangles in its area-of-effect. After a time slot, the hurricane moves towards the lower middle of the network area with stronger impact, while affecting links (1,3), (2,4) and

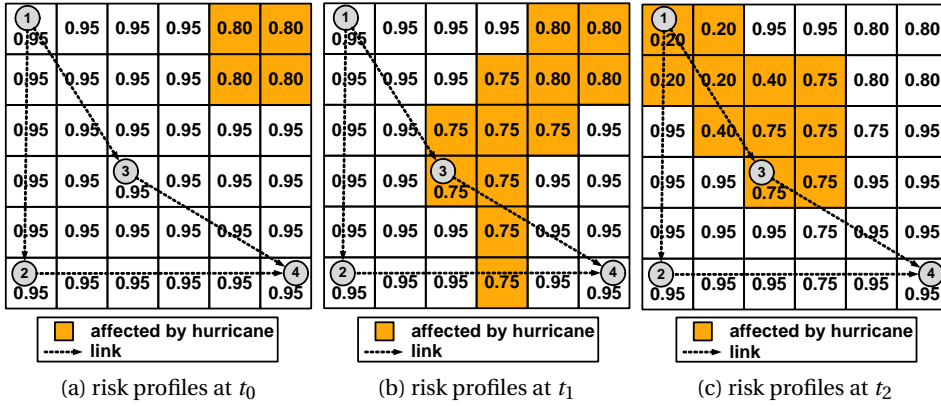


Figure 4.13: An example of a grid with spatiotemporal risk profiles.

(3,4). After another time slot, the hurricane grows stronger and moves towards the upper left part of the network area, while affecting links (1,2), (1,3) and (3,4). Hence, some grid rectangles have different availabilities at different time slots.

4.4.1. PROBLEM DEFINITION

Problem 5 *Spatiotemporal Risk-Averse Routing (SRR) problem:*

Given a network G of a set N of $|N|$ nodes and a set L of $|L|$ links, a grid F of $|F|$ grid rectangles representing the area of G , a source node $x \in N$, a destination node $y \in N$, and a time window T of $|T|$ time slots. Each grid rectangle $f \in F$ is characterized by a grid availability A_{ft} , for each time slot $t \in T$. Each link $(u, v) \in L$ connects nodes u and v , is characterized by a link delay ℓ_{uv} (in the unit of time slots) and overlaps a set of grid rectangles $O_{uv} \subseteq F$ of $|O_{uv}|$ grid rectangles. Find a path P from node x to node y , between the time period $t_{\Delta_1} \in T$ and $t_{\Delta_2} \in T$, such that the path availability A_P is maximized.

The time window is assumed to be discretized into discrete time slots (e.g., by using the common divisor among all link delays as the unit of the time slots). Each link delay represents the number of time slots required to traverse the link. A routing decision is made before the travel commences, and traffic follows the assigned end-to-end path irrespective of any further network state change. Waiting may be allowed at certain or all nodes, such that traffic can stay for a duration of time slots at the nodes before leaving the nodes. By waiting at a node, the link availability of an adjacent link might increase or decrease in time. We consider

Algorithm 6 Auxiliary Graph Generation

-
- 1: initialize an empty graph $H = (V, E)$
 - 2: **for** each node $n \in N$
 - 3: **for** each time slot $t \in T$ where $t < t_{\max}$
 - 4: add nodes n_t and n_{t+1} into V
 - 5: **if** waiting is allowed at node n at time slot t
 - 6: add link (n_t, n_{t+1}) into E where $A_{n_t n_{t+1}} = 1$
 - 7: **for** each link $(u, v) \in L$
 - 8: **for** each time slot $t \in T$ where $t + \ell_{uv} \leq t_{\max}$
 - 9: insert link $(u_t, v_{t+\ell_{uv}})$ into E
 - 10: **for** each link $(u, v) \in E$
 - 11: compute the worst-case availability A_{uv} of link (u, v)
 - 12: $\ell'_{uv} = -\log A_{uv}$
-

only simple paths such that each link can only be traversed once in a path.

The SRR problem finds the most risk-averse path (the path with the highest possible availability), while ensuring that the traffic reaches the destination node at least at t_{Δ_2} . In the SRR problem, links have fixed delay but spatiotemporal availability (since the availabilities of grid rectangles are spatiotemporal). The SRR problem is thus a multi-criteria problem that maximizes the path availability under a path delay constraint. The SRR problem is polynomially solvable when the grid model of Section 4.2 and the notion of time slots are considered.

4.4.2. OUR APPROACH

We propose a polynomial-time graph transformation algorithm (shown in Algorithm 6) that uses an auxiliary graph to reflect the notion of time slots. Using our auxiliary graph, the SRR problem can be solved by a polynomial-time min-cost routing algorithm (e.g., Dijkstra's algorithm [5]). For instance, the auxiliary graph for the network in Figure 4.13 is shown in Figure 4.14. In lines 2-6, each node $n \in N$ is represented by $|T|$ auxiliary nodes. Vertical unidirectional auxiliary links with perfect availability are added between the different time slots of an auxiliary node when waiting is allowed at the node during that time slot. In lines 7-9, each link $(u, v) \in L$ is represented by at most $|T|$ unidirectional auxiliary links, which also reflect the time slots needed to traverse the link. We consider the availability of an auxiliary link to be the worst-case availability of the link during the time slots spent to traverse the link. The auxiliary graph contains at

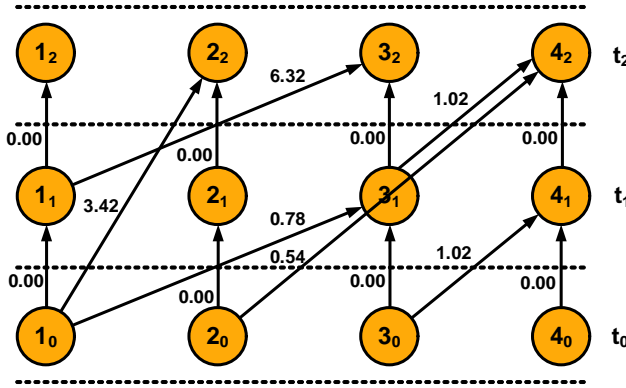


Figure 4.14: Example of an auxiliary graph.

most $|N||T|$ auxiliary nodes and $(|N| + |L|)(|T| - 1)$ auxiliary links. In line 12, the auxiliary link weight ℓ'_{uv} of each auxiliary link $(u, v) \in E$ is set to the negative logarithmic value of its availability. The worst-case time complexity of Algorithm 6 is $O(|L||F| + |T|(|N| + |L|))$.

The most risk-averse path from node $x \in N$ to node $y \in N$ between t_{Δ_1} and t_{Δ_2} can be acquired by using an appropriate min-cost routing algorithm (e.g., Dijkstra's algorithm [5]) to find the min-cost path (using ℓ'_{uv} as the cost of each link $(u, v) \in E$) from node $x_{\Delta_1} \in V$ to a temporarily created node $y' \in V$ that is connected from nodes $(y_{\Delta_1}, y_{\Delta_1+1}, \dots, y_{\Delta_2} \in V)$ via directed links with zero link cost, in the auxiliary graph H . y' is temporarily created since traffic may arrive at the destination node earlier than t_{Δ_2} , when waiting is forbidden at the destination node. When disjoint risk-averse paths are needed, appropriate min-cost disjoint paths algorithms (e.g., Suurballe's algorithm [22]) can be used instead.

4.4.3. ANALYSIS

We analyze the effect of the size of the time window on the time required to generate the auxiliary graph and find the most risk-averse path. We again use connected graphs with the properties mentioned earlier in Section 4.3, for each simulation run. Each link $(u, v) \in L$ is randomly assigned with a delay ℓ_{uv} between one to four time slots. Each grid rectangle $f \in F$ is assigned with a random availability A_f between 0.00 and 1.00 for each time slot. We assume that waiting is allowed indefinitely at all nodes, though our auxiliary graph is fully capable of handling the scenario where waiting is allowed only for a finite duration at selected network nodes.

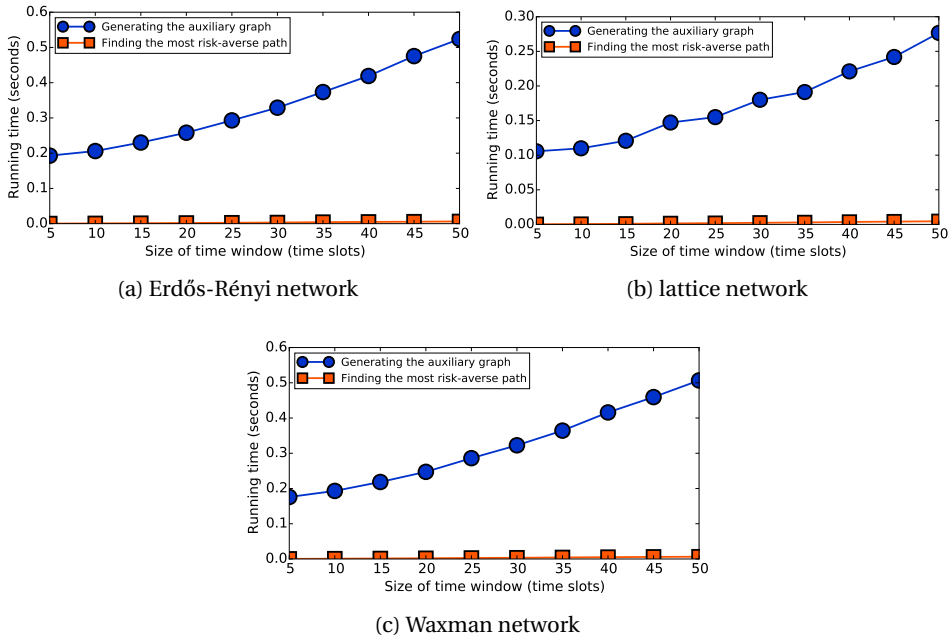


Figure 4.15: Effect of the size of the time window to running time.

The time required to generate the auxiliary graph increases with the increase of the size of the time window, as shown in Figure 4.15, with line 11 of Algorithm 6 dominating the running time. It is worth noting that the auxiliary graph need only be created once for a specific time window, and can be reused to find the most risk-averse path for any other node pair under time constraints that are part of the time window. The time required to find the most risk-averse path (including the time needed to create the temporarily created destination nodes and links), if it exist, in the auxiliary graph is substantially less than the time required to generate the auxiliary graph in all the tested cases.

4.5. RELATED WORK

Kuipers provides an overview of survivability algorithms [154]. Dikbiyik et al. [59] propose risk-aware provisioning of connections to minimize the loss for network operators when a disaster occurs. They also consider a post-disaster re-provisioning scheme to recover disrupted connections. We, however, aim to reduce the number of disrupted connections by detecting vulnerable connections be-

fore the disaster, and route connections using the most risk-averse paths (instead of routing connections using the least-delay paths [155]). We also consider link availability as a function of the spatiotemporal risk profile, instead of link component availabilities [143, 149, 156–158]. Earlier study on temporal routing often aims to minimize the expected end-to-end path delay under temporal link delays [16, 159]. On the other hand, we maximize the path availability under spatiotemporal link availabilities, while also considering a time constraint under fixed link delays. In addition, our grid-based model enables the representation of more complex disaster boundaries, complementing earlier work that assumes specific geometric shapes of disaster boundaries, e.g., circular [41], ellipses [42], general polygons [42] or half-planes [56].

4.6. CHAPTER CONCLUSION

In this chapter, we proposed a generic grid-based model to represent the risk profile of a network area, a polynomial-time algorithm to identify connections that are vulnerable under the risk of a disaster, and a polynomial-time algorithm to find the most risk-averse end-to-end path under a time constraint when disaster risks are spatiotemporal. We also showed that larger disaster size leads to more vulnerable connections, and scattered disasters are more detrimental to network connections than confined disasters. The number of vulnerable connections increases with the increase in network utilization, and the possibility of rerouting vulnerable connections using alternative paths decreases with the increase in network utilization.

Possible future directions that can be derived from this chapter are finding the minimum delay path that satisfies an availability constraint, using a probability density function to represent the risk profile, and extending the grid-based model for use in a three-dimensional Cartesian plane.

5

SPATIALLY-CLOSE FIBERS

This chapter focuses solely on the topic of disaster awareness, where our problem now is finding and grouping spatially-close fiber spans in the network. Spatially-close network fibers have a significant chance of failing simultaneously in the event of natural or anthropogenic disasters within their geographic area. Network operators are interested in the proper detection and grouping of any existing spatially-close fiber segments, to avoid service disruptions due to simultaneous fiber failures. Moreover, spatially-close fibers can further be differentiated by computing the intervals over which they are spatially close. In this chapter, we propose (1) polynomial-time algorithms for detecting all the spatially-close fiber segments of different fibers, (2) a polynomial-time algorithm for finding the spatially-close intervals of a fiber to a set of other fibers, and (3) a fast exact algorithm for grouping spatially-close fibers using the minimum number of distinct risk groups. All of our algorithms have a fast running time when simulated on three real-world network topologies.

Parts of this chapter have been published in the 12th International Conference on Design of Reliable Communication Networks (DRCN 2016), Paris, France, March 2016 [148].

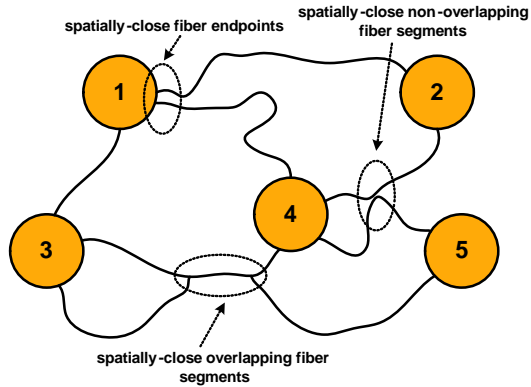


Figure 5.1: Example of spatially-close fiber segments.

5

5.1. INTRODUCTION

Network services rely upon optical fibers to communicate between network Points-of-Presence (PoPs). These fibers carry Terabits of data over long distances. Hence, various measures have been taken to ensure the fibers' robustness, e.g., coating against lateral forces, moisture and mechanical stress. However, fibers can and do still fail due to natural disasters (e.g., earthquakes, floods and volcanic eruptions) or anthropogenic disasters (e.g., electromagnetic pulse attacks, sabotages and terrorist attacks). Fiber failures degrade and interrupt network services in the absence of proper service compensating measures, possibly leading to monetary penalties to network operators due to breached service level agreements.

Spatially-close fibers typically have a higher chance of failing simultaneously, due to a disaster, than fibers that are more distant. For instance, in 2006, an earthquake off southern Taiwan had cut eight undersea fibers in sixteen places, disabling offshore connectivity for China and Southeast Asia [160]. The repair time took months. In 2009, an earthquake off East Taiwan and Typhoon Morakot had cut eight undersea fibers [161]. Taiwan is known to be geographically positioned in the circum-Pacific seismic belt. Proper risk analyses on spatially-close fibers are thus crucial for providing survivable network services across similar risky geographical areas.

Fibers can be spatially close due to a variety of reasons. Fiber segments of different fibers may have been deployed in a single duct (a physical pipe for placing fibers between two locations) due to the high cost of digging ducts. Duct sharing between network operators is also beginning to become a norm [162, 163].

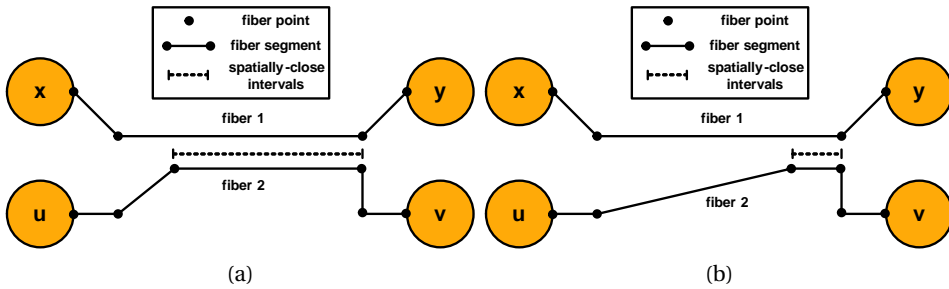


Figure 5.2: Fibers with different spatially-close intervals.

Duct sharing leads to overlapping fiber segments, as shown in Figure 5.1. If the duct is cut, all the fibers within it will fail simultaneously [164]. Fibers originating or terminating from/to a PoP may have spatially-close endpoints due to existing infrastructures or landscapes. For instance, if the PoP is next to a river, the fiber segments may have been placed closely alongside a bridge. Fibers in different ducts may also be spatially close due to the close proximity of their ducts.

Confining to detecting only whether different fibers are spatially close can be misleading in terms of their risk of simultaneous failures. Fibers with longer spatially-close intervals have a higher chance of failing simultaneously compared to fibers with shorter spatially-close intervals, as shown by Figure 5.2. For instance, there is a bottleneck of more than eight spatially-close fibers along the intervals of the Gulf of Suez [165]. Any disaster occurring along these intervals has a high chance of cutting all the fibers simultaneously, possibly leading to connectivity interruptions in many countries.

Our key contributions in this chapter are organized as follows: (1) We propose fast polynomial-time algorithms in Section 5.2 for detecting all the spatially-close fiber segments of different fibers. (2) We propose a fast polynomial-time algorithm in Section 5.3 for detecting the intervals of a fiber that are spatially close to another fiber, and extend it for detecting the intervals of a fiber that are spatially close to a set of other fibers. (3) We propose a fast exact algorithm in Section 5.4 for grouping spatially-close fibers using a minimum number of risk groups. We simulate our algorithms on three real-world network topologies. We discuss related work in Section 5.5 and summarize the chapter in Section 5.6.

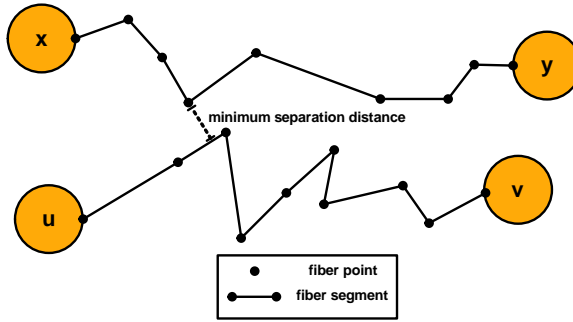


Figure 5.3: Example of two fibers represented by our fiber structure.

5.2. DETECTION OF SPATIALLY-CLOSE FIBER SEGMENTS

5.2.1. FIBER STRUCTURE

Fibers are commonly deployed in a non-straight manner, since deploying fibers in a straight line between PoPs can be cumbersome and impractical due to various reasons, e.g., terrain, existing infrastructure and government rules. Hence, we approximate fibers as non-straight concatenations of multiple fiber segments of irregular lengths, as shown in Figure 5.3. The accuracy of the approximation increases with more fine-grained fiber segments. Each fiber segment is a straight line connecting two fiber points of known geodetic coordinates (latitude and longitude). Latitude specifies a point's angle north or south of the equator, while longitude specifies a point's angle east or west from the Prime Meridian. For easier geospatial calculations, we assume that the geodetic coordinates of all fiber points can be projected into corresponding two-dimensional Cartesian coordinates. Two consecutive fiber segments may not necessarily have collinear fiber points (three or more points are collinear if they lie on a single straight line).

5.2.2. PROBLEM DEFINITION

Problem 6 *Detection of Spatially-Close Fiber Segments (DSCFS) problem:*

Given a set L of $|L|$ fibers and a distance Δ . Each fiber $l \in L$ is associated with a set S_l of $|S_l|$ fiber segments. Each fiber segment $s \in S_l$ is associated with two fiber points (u_{s_1}, v_{s_1}) and (u_{s_2}, v_{s_2}) of known geodetic locations. Find all the fiber segment pairs of different fibers that have a minimum separation distance of at most Δ .

The DSCFS problem is polynomially solvable (in the number of fiber segments) when the fiber structure of Section 5.2.1 is considered. One brute-force

Algorithm 7 DSCFS with k-d Tree Preprocessing

```

1: for each fiber  $l \in L$ 
2:   for each fiber segment  $s \in S_l$ 
3:     compute the segment midpoint  $m_s$ , and insert it into the k-d tree  $Y$ 
4:   for each fiber segment midpoint  $m_s \in Y$ 
5:     find the set  $A$  of the entries of  $Y$  at a distance of at most  $\Delta + a$  from  $m_s$ 
6:     for each fiber segment midpoint  $z_j \in A$ 
7:       if the minimum distance between fiber segments  $s$  and  $j$  is at most  $\Delta$ 
8:         fiber segments  $s$  and  $j$  are spatially close

```

approach of solving the DSCFS problem is by computing the minimum separation distance between all fiber segment pairs of different fibers. If the minimum separation distance between any two fiber segments is at most Δ , they are spatially close. The worst-case time complexity of this brute-force approach is $O(|L|^2|S_{max}|^2)$, where $|S_{max}|$ is the maximum number of fiber segments per fiber.

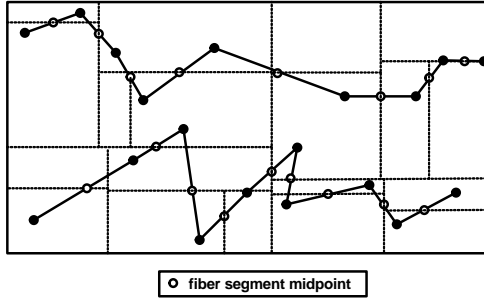
5.2.3. OUR APPROACH

To achieve a faster practical running time, we propose Algorithm 7 that uses a k-d tree [166] to preprocess the fiber segments, and Algorithm 8 that uses an R tree [151] to preprocess the fiber segments for solving the DSCFS problem. A k-d tree is a space-partitioning data structure for organizing points in a k-dimensional space. An R tree is a depth-balanced data structure for organizing objects using bounded rectangles. The trees eliminate the need for computing the minimum separation distance between all fiber segment pairs, thus reducing the running time significantly.

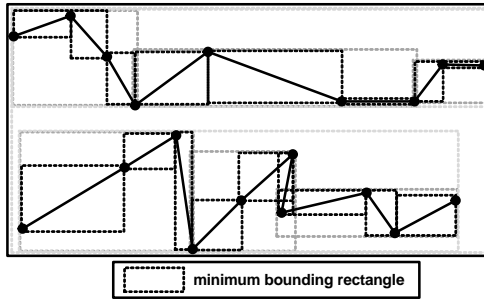
Lines 1-3 of Algorithm 7 find the midpoint of all fiber segments and insert them into the k-d tree, since a k-d tree works with points instead of segments. Line 3 of Algorithm 8 computes the minimum bounding rectangle (MBR) of all fiber segments, and inserts them into the R tree. The MBR of a fiber segment is the smallest rectangle that encloses the fiber segment in the two-dimensional Cartesian plane. For instance, the partitioning of fibers of Figure 5.3 by the k-d tree is shown in Figure 5.4a, or by the R tree is shown in Figure 5.4b. For each fiber segment $s \in S$, lines 4-5 in Algorithm 7 find the set A of fiber segments in Y with midpoints of a distance of at most $\Delta + a$ from the midpoint of fiber segment s , where a is the maximum fiber segment length. Similarly, for each fiber segment

Algorithm 8 DSCFS with R Tree Preprocessing

- 1: **for** each fiber $l \in L$
- 2: **for** each fiber segment $s \in S_l$
- 3: compute the MBR of segment s , MBR_s , and insert it into the R tree Y
- 4: **for** each $MBR_s \in Y$)
- 5: find the set A of the entries of Y at a distance of at most Δ from MBR_s
- 6: **for** each $MBR_j \in A$
- 7: **if** the minimum distance between fiber segments s and j is at most Δ
- 8: fiber segments s and j are spatially close



(a) k-d tree partitioning



(b) R tree partitioning

Figure 5.4: Example of fiber partitioning for tree representations.

$s \in S$, lines 4-5 in Algorithm 8 find the set A of fiber segment MBRs in Y with distance of at most Δ from the MBR of fiber segment s . Lines 6-8 of Algorithm 7 and Algorithm 8 detect all the fiber segments of set A that are spatially close (with minimum separation distance of at most Δ) to fiber segment s .

Two scenarios need to be considered when computing the minimum separation distance between any two fiber segments:

Case 1: For intersecting fiber segments, their minimum separation distance is zero.

Case 2: Else, their minimum separation distance is the minimum distance between any points along the two fiber segments.

The ball tree [167] or newer variants of the R tree [168] can also be used instead with Algorithms 7 and 8. Although the worst-case time complexity of Algorithms 7 and 8 is similar to the naive approach (in the worst-case, all the fiber segments could be spatially close), significant time-savings can be expected in practice in solving the DSCFS problem.

5.2.4. PROOF-OF-CONCEPT

We generate three real-world network topologies, namely the Angola Telecom network, the Ethiopia Telecom network and the Telkom South Africa network, from the Keyhole Markup Language (KML) datasets provided in [169]. We assume each placemark in the KML datasets as a distinct fiber. KML is a language schema of the Open Geospatial Consortium (OGC) [170] for representing geographical information. KML is also often used by other network operators in illustrating their network, e.g., [171, 172]. We use this format in our proof-of-concept since KML datasets can be directly translated to our fiber structure. We use the projection wizard of [173] to generate an equidistant map projection for each network, such that all the two-dimensional plane coordinates (projected using [174]) have proportionally correct distances from the center point of the network geographic bounds.

Of all the studied networks, the Telkom South Africa network has the highest number of fibers and fiber segments, the Angola Telecom network has the highest average length of fibers and fiber segments, while the Ethiopia Telecom network has the highest average number of fiber segments per fiber. Detailed properties of the networks are shown in Table 5.1.

Algorithm 7 and Algorithm 8 are coded in Python and simulations were conducted on an Intel(R) Core i7-4600U 2.1GHz machine of 16GB RAM memory. Parsing the datasets and generating the network took less than a second for all the networks. As shown in Table 5.2, the running time of the naive approach is quite high, even when the minimum separation distance Δ is low. Significant time-savings can be achieved by Algorithm 7 and Algorithm 8, particularly when

Table 5.1: Properties of the studied networks.

Property	Angola Telecom	Ethiopia Telecom	Telkom South Africa
Number of fibers	16	21	343
Total length of fibers	10943.86 km	8162.47 km	27849.70 km
Average length of fibers	683.99 km	388.69 km	81.19 km
Maximum length of fibers	1745.93 km	2105.52 km	479.08 km
Minimum length of fibers	261.53 km	67.35 km	4.01 km
Number of fiber segments	979	2917	4901
Average number of fiber segments per fiber	61.19	138.90	14.29
Maximum number of fiber segments per fiber	238	492	80
Minimum number of fiber segments per fiber	17	10	1
Average length of fiber segments	11.18 km	2.80 km	5.68 km
Maximum length of fiber segments	59.49 km	54.30 km	97.75 km

Δ is low. Algorithm 8 outperforms Algorithm 7 since the performance of Algorithm 7 also relies on the value of a . Although the running times of Algorithm 7 and 8 increase with Δ , Δ is often a small value. The running time of the algorithms is highest on the Telkom South Africa network, due to its high number of fibers and fiber segments.

Table 5.2: The effect of Δ on the time taken for solving the DSCFS problem.

Algorithm	Minimum separation distance (Δ)						
	5 m	50 m	500 m	5 km	50 km	500 km	5000 km
Angola Telecom							
Naive approach	20.16 s	20.16 s	20.16 s	20.16 s	20.16 s	20.16 s	20.16 s
Algorithm 7	1.12 s	1.13 s	1.15 s	1.15 s	1.66 s	11.90 s	19.81 s
Algorithm 8	0.21 s	0.22 s	0.23 s	0.23 s	0.34 s	9.17 s	21.20 s
Ethiopia Telecom							
Naive approach	2.98 min	2.98 min	2.98 min	2.98 min	2.98 min	2.98 min	2.98 min
Algorithm 7	7.12 s	7.37 s	7.55 s	7.80 s	14.79 s	2.12 min	3.05 min
Algorithm 8	0.75 s	0.75 s	0.75 s	0.76 s	2.50 s	2.01 min	3.22 min
Telkom South Africa							
Naive approach	8.60 min	8.60 min	8.60 min	8.60 min	8.60 min	8.60 min	8.60 min
Algorithm 7	30.89 s	31.17 s	31.90 s	31.97 s	50.51 s	5.20 min	8.97 min
Algorithm 8	1.28 s	1.30 s	1.31 s	1.45 s	8.23 s	4.53 min	9.00 min

5.3. INTERVALS OF SPATIALLY-CLOSE FIBERS

In the previous section, we discussed how to detect spatially-close fibers, and pinpoint spatially-close fiber segments. However, viewing spatially-close fibers as a Boolean relation can be misleading in terms of the risk of simultaneous failures. In this section, we find the intervals of spatially-close fibers, to give a better measure of the fibers' spatial proximity. For instance, the fiber pair in Figure 5.2a has longer intervals that are spatially close than the fiber pair in Figure 5.2b.

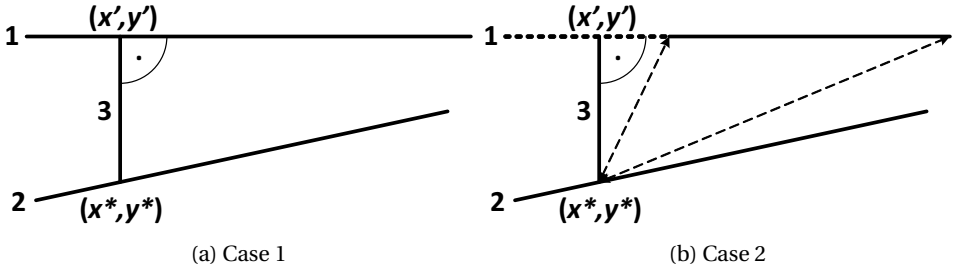


Figure 5.5: Intervals of a pair of spatially-close fiber segments

5.3.1. INTERVALS OF A PAIR OF SPATIALLY-CLOSE FIBER SEGMENTS

We first explain our approach of finding the intervals of a pair of spatially-close fiber segments, before proceeding with the intervals of spatially-close fibers in subsequent sections.

Suppose we have two fiber segments that can each be represented by their slope intercept form $y_1 = k_1 x_1 + n_1$ of $x_1 \in [a, b]$ and $y_2 = k_2 x_2 + n_2$ of $x_2 \in [c, d]$. Let us fix a point $(x^*, y^* = k_2 x^* + n_2)$ on fiber segment 2, as shown in Figure 5.5. The y -intercept m of a line 3 through (x^*, y^*) that is perpendicular to fiber segment 1 is $m = (k_2 + \frac{1}{k_1})x^* + n_2$.

The intersection of line 3 and the line projection of fiber segment 1 defines point (x', y')

$$-\frac{1}{k_1} x' + m = k_1 x' + n_1$$

$$x' = \frac{1}{1 + k_1^2} [(k_1 k_2 + 1)x^* + k_1(n_2 - n_1)] \quad (5.1)$$

For simplicity, consider $A = \frac{k_1 k_2 + 1}{1 + k_1^2}$ and $B = \frac{k_1(n_2 - n_1)}{1 + k_1^2}$. For the distance from all possible (x^*, y^*) to the projected line of fiber segment 1 to be at most Δ , the condition is

$$\Delta^2 \geq (x' - x^*)^2 + (y' - y^*)^2$$

$$= ((A - 1)x^* + B)^2 + ((k_1 A - k_2)x^* + k_1 B + n_1 - n_2)^2 \quad (5.2)$$

From Eq. 5.2, we have a quadratic inequality, whose solution is an interval $x^* \in [i_1, i_2]$. The intersection of this interval and the interval $[c, d]$ gives a necessary condition for x^*

$$x^* \in [z_1, z_2] = [i_1, i_2] \cap [c, d] \quad (5.3)$$

When (x', y') is on fiber segment 1, i.e. $x' \in [a, b]$

$$a \leq Ax^* + B \leq b \quad (5.4)$$

By solving Eq. 5.4 for x^* , we obtain an interval $x^* \in [j_1, j_2]$. The solution is then

$$x^* \in [z_1, z_2] \cap [j_1, j_2] \quad (5.5)$$

On the other hand, when (x', y') is not on fiber segment 1, i.e. $x' \notin [a, b]$, it is sufficient that the minimum of the distances from (x^*, y^*) to the two endpoints of fiber segment 1 is not bigger than Δ . In this case, $x^* \notin [j_1, j_2]$.

$$(x^* - a)^2 + (k_2x^* + n_2 - k_1a - n_1)^2 \leq \Delta^2, \text{ or} \quad (5.6)$$

$$(x^* - b)^2 + (k_2x^* + n_2 - k_1b - n_1)^2 \leq \Delta^2 \quad (5.7)$$

These two inequalities give two intervals $[p_1, p_2]$ and $[q_1, q_2]$. The solution is then

$$x^* \in [[z_1, z_2] \setminus [j_1, j_2]] \cap [[p_1, p_2] \cup [q_1, q_2]] \quad (5.8)$$

The solution gives the intervals of fiber segment 2 that are spatially close to fiber segment 1.

5.3.2. PROBLEM DEFINITION

Problem 7 *Intervals of a Pair of Spatially-Close Fibers (IPSCF) Problem:*

Given two fibers l_i and l_j , and a distance Δ . Each fiber l_i / l_j is associated with a set S_i / S_j of $|S_i| / |S_j|$ fiber segments, respectively. Each fiber segment $s \in S_i / S_j$ is associated with two fiber points (u_{s_1}, v_{s_1}) and (u_{s_2}, v_{s_2}) of known geodetic locations. Find the intervals of fiber l_i that have a minimum separation distance of at most Δ to fiber l_j .

Algorithm 9 IPSCF with R Tree Preprocessing

```

1: for each fiber  $l_j \in L$ 
2:   for each fiber segment  $s \in S_{l_j}$ 
3:      $Y \leftarrow \text{MBR}_s$ 
4:   set  $\mathcal{I}$  as an empty interval
5:   for each fiber segment  $s \in S_{l_i}$ 
6:     compute its  $\text{MBR}_s$ 
7:     find the set  $A$  of the entries of  $Y$  at distance at most  $\Delta$  from  $\text{MBR}_s$ 
8:     for each  $\text{MBR}_a \in A$ 
9:        $J \leftarrow$  intervals of segment  $s$  that are spatially close to segment  $a$ 
10:     $\mathcal{I} \leftarrow \mathcal{I} \cup J$ 

```

The IPSCF problem is an extension of the DSCFS problem. If two fibers are spatially close, detecting their spatially-close intervals is useful for recognizing to which extent they are vulnerable to simultaneous failures. The IPSCF problem is unidirectional, since the intervals of fiber l_i that are spatially close to fiber l_j are not necessarily equal to the intervals of fiber l_j that are spatially close to fiber l_i . When the network operator needs to find the spatially-close intervals of a fiber to a set of other fibers, the following problem is more useful.

Problem 8 *Intervals to a Set of Spatially-Close Fibers (ISSCF) Problem:*

Given a fiber l_i , a set L of $|L|$ fibers and a distance Δ . Each fiber l_i and $l_j \in L$ is associated with a set S_i/S_j of $|S_i|/|S_j|$ fiber segments, respectively. Each fiber segment $s \in S_i/S_j$ is associated with two fiber points (u_{s_1}, v_{s_1}) and (u_{s_2}, v_{s_2}) of known geodetic locations. Find the intervals of fiber l_i that have a minimum separation distance of at most Δ to any fiber $l_j \in L$.

The IPSCF problem is a subset of the ISSCF problem, where L is a single fiber l_j . The IPSCF and ISSCF problems are polynomially solvable in the number of fiber segments.

5.3.3. OUR APPROACH

We propose Algorithm 9 for solving the IPSCF and ISSCF problems. Lines 1-3 insert all the fiber segment MBR of each fiber $l_j \in L$ into an R tree Y . For each fiber segment s of fiber l_i , line 7 finds the set A of fiber segment MBRs in Y with distance of at most Δ from the MBR of fiber segment s . Line 9 then uses the equations of Section 5.3.1 to find the spatially-close intervals of fiber segment s

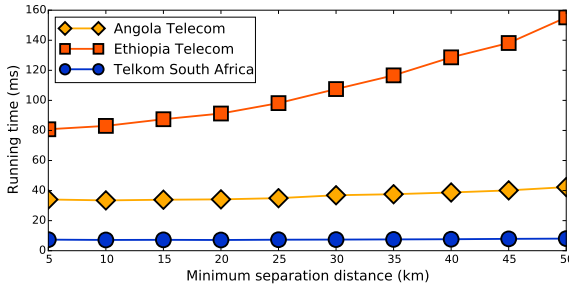


Figure 5.6: Effect of Δ on the time taken to solve the ISSCF problem ($|L| = 5$).

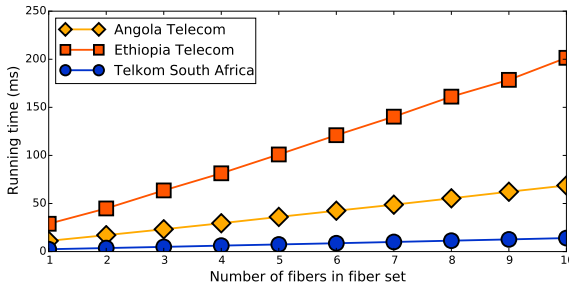


Figure 5.7: Effect of $|L|$ on the time taken to solve the ISSCF problem ($\Delta = 25$ km).

to each fiber segment $a \in A$. Line 10 returns the intervals of fiber l_i that have a minimum separation distance of at most Δ from any fiber $l_j \in L$ by uniting all the intervals acquired by line 9. The worst-case time complexity of Algorithm 9 is $|L||S|^2$, where $|S|$ is the maximum number of fiber segments per fiber.

5.3.4. PROOF-OF-CONCEPT

Algorithm 9 is coded in Python and simulations were conducted on an Intel(R) Core i7-4600U 2.1GHz machine of 16GB RAM memory. All simulation results are averaged over five thousand runs, and we randomly chose the fibers for l_i and L in each simulation run. Figure 5.6 shows the running time of Algorithm 9 as a function of Δ when $|L|$ is 5, while Figure 5.7 shows the running time of Algorithm 9 as a function of $|L|$ when Δ is 25 km. Higher Δ or $|L|$ implies potentially longer intervals, such that the running time increases. The case when $|L| = 1$ corresponds to the IPSCF problem.

To reduce the running time, fiber segments with collinear fiber points can be combined safely. Unfortunately, the number of collinear fiber segments in the

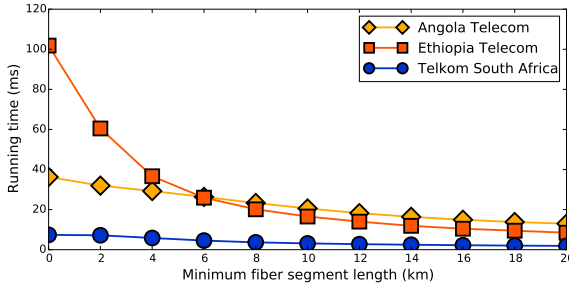


Figure 5.8: Effect of limiting the length of fiber segment on the time taken to solve the ISSCF problem ($\Delta = 25$ km, $|L| = 5$).

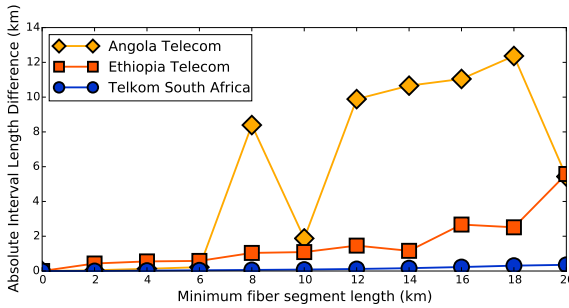


Figure 5.9: Effect of limiting the length of fiber segment on the interval length of the ISSCF problem ($\Delta = 25$ km, $|L| = 5$).

studied datasets are too few for the effect to become apparent. It is also tempting to combine shorter fiber segments by imposing a lower bound on the fiber segment length, which reduces the number of fiber segments and the running time as shown in Figure 5.8. However, by doing so, the network changes unpredictably, affecting the intervals as shown in Figure 5.9.

5.4. GROUPING OF SPATIALLY-CLOSE FIBERS

This section builds upon Section 5.2 by grouping spatially-close fibers in the same risk group. A risk group is often defined as a set of fibers sharing an adjacent node or duct, e.g., [156, 175, 176]. We propose a broader definition of risk groups, such that a risk group is a set of fibers that are spatially close to every other fiber in the same set. Each risk group implies a set of fibers with a high chance of simultaneous failures. A risk group contains multiple fibers, and a

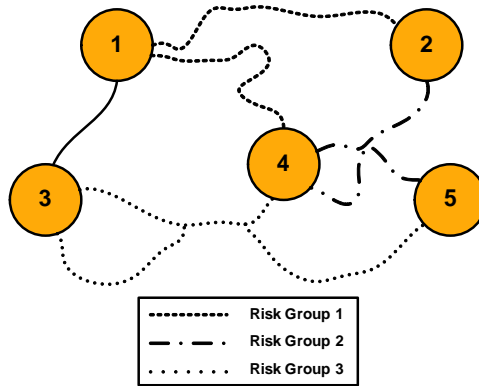


Figure 5.10: An example of risk groups.

fiber may belong to multiple risk groups. For instance, the fibers in Figure 5.1 can be placed into three risk groups, as shown in Figure 5.10.

5

5.4.1. PROBLEM DEFINITION

Problem 9 *Grouping of Spatially-Close Fibers (GSCF) Problem:*

Given a set L of $|L|$ spatially-close fiber pairs (each fiber pair has a minimum separation distance of at most Δ). Group all the fibers that are spatially close to each other, such that the number of distinct risk groups used is minimized.

The GSCF problem is NP-hard due to the complexity of assigning the maximal risk groups. A maximal risk group is a set of fibers that are spatially close to every other fiber in the set, and which is not a subset of any other larger risk group. To prove that the GSCF problem is NP-hard, we show that any instance of the NP-hard Maximal Clique Enumeration (MCE) problem [177] can be transformed in polynomial time to an instance of the GSCF problem, where a clique is a set of nodes that have a link to every other node in the set [178].

Problem 10 *Maximal Clique Enumeration (MCE) Problem:*

Given a graph $H = (V, E)$ of a set V of $|V|$ nodes and a set E of $|E|$ links. Each link $(u, v) \in E$ connects nodes $u \in V$ and $v \in V$. Find all the maximal cliques in H . A maximal clique is a set of nodes that have a link to every other node in the set, and it is not a subset of any other larger clique.

We start our proof by adjusting the interpretation of H such that each node $n \in V$ represents a distinct fiber $l \in L$. H then consist of $|L|$ nodes. If any two

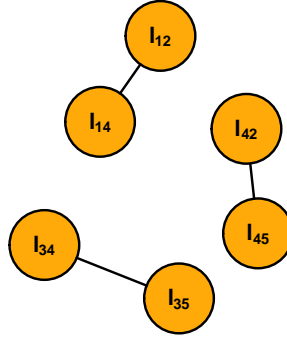


Figure 5.11: Transformation between problems.

Algorithm 10 GSCF

- 1: create an empty graph $H = (V, E)$
- 2: **for** each fiber $l_i \in L$
- 3: **for** each fiber $l_j \in L \setminus l_i$
- 4: **if** fibers l_i and l_j are spatially close
- 5: add node l_i and l_j in H
- 6: connect node l_i and l_j by a link in H
- 7: find all the maximal cliques in H

nodes $u \in V$ and $v \in V$ are connected by a link $(u, v) \in E$ in H , the two fibers $l_u \in L$ and $l_v \in L$ are spatially close. For instance, the corresponding H for the fibers in Figure 5.10 is shown in Figure 5.11. By solving the GSCF problem in H , the MCE problem is solved as well, since each maximal risk group is equivalent to a maximal clique. Since the MCE problem (and thus the GSCF problem as well) is hard to approximate [179], we focus on a practically efficient exact approach to solve the GSCF problem.

5.4.2. OUR APPROACH

We propose Algorithm 10, which is based on a graph transformation approach to solve the GSCF problem. An empty graph $H = (V, E)$ is created in line 1. For each fiber pair in L , a node is created for each of them in H in line 5, if a node representing them does not yet exist in H . Both nodes in H are connected by a link in line 6. The maximal risk groups can then be acquired by finding all the maximal cliques of graph H in line 7. Each resultant maximal clique represents a distinct

maximal risk group. The maximal cliques can be acquired by the Bron-Kerbosch algorithm [180]. The variant of the Bron-Kerbosch algorithm by [181] has the best worst-case time complexity of $O(3^{\frac{|V|}{3}})$, since any graph with $|V|$ nodes can have at most $3^{\frac{|V|}{3}}$ maximal cliques [182]. Using the implementation of [181], the worst-case complexity of Algorithm 10 is $O(3^{\frac{|L|}{3}})$ since there are at most $|L|$ nodes in H .

5.4.3. PROOF-OF-CONCEPT

Algorithm 10 is coded in Python and simulations were conducted on an Intel(R) Core i7-4600U 2.1GHz machine of 16GB RAM memory. We vary the minimum separation distance Δ (thus varying L via the DSCFS problem) while finding the maximal risk groups. The maximal risk group assignment takes a very short amount of time, less than a second in most of the tested cases as shown in Table 5.3, with at most ten seconds for the Telkom South Africa network.

The maximum and minimum numbers of fibers per maximal risk group increase with the increase of Δ . Higher Δ increases the possibility of more fibers being identified as being spatially close to each other, and which consequently are assigned into the same maximal risk group. On the other hand, the total number of maximal risk groups can either increase or decrease with the increase of Δ . Higher Δ increases the possibility of more fibers being identified as being spatially close to each other, thus creating more risk groups, in which some of them are maximal. However, by having more fibers within each risk group, the possibility of a maximal risk group being a superset of another smaller risk group also increases, possibly reducing the number of maximal risk groups.

5.5. RELATED WORK

The survivability of network services in the event of disasters has received increasing interest in recent years, e.g., [32, 41, 42, 46, 56, 59, 154]. The effect of disasters on network services can be studied from an attacker perspective, e.g., disconnecting two nodes under a disaster [56], how many disasters are needed to cut connectivity between different nodes [41] or the geographic area that brings the worse effect to the network connectivity when confronted by a disaster [42]. From an attacker perspective, the knowledge of the vulnerable network geographic areas (often modeled as a circular disk [41], an ellipse or a general polygon [42] or a half-plane [56]) is highly appealing. However, from a network operator perspective, knowing the vulnerable geographic areas without enough information on resolving the problem can be frustrating. There are endless possibilities of

Table 5.3: The effect of Δ on the sizes of maximal risk groups.

Property	Minimum separation distance (Δ)						
	5 m	50 m	500 m	5 km	50 km	500 km	5000 km
Angola Telecom							
Total number of maximal risk groups	9	13	16	15	12	9	1
Average number of fibers per maximal risk groups	2.22	2.15	2.25	2.60	3.00	8.11	16
Maximum number of fibers per maximal risk groups	3	3	3	3	4	9	16
Minimum number of fibers per maximal risk groups	2	2	2	2	2	7	16
Ethiopia Telecom							
Total number of maximal risk groups	12	16	17	17	15	11	1
Average number of fibers per maximal risk groups	2.08	2.25	2.41	2.41	2.67	11	21
Maximum number of fibers per maximal risk groups	3	3	3	3	4	14	21
Minimum number of fibers per maximal risk groups	2	2	2	2	2	10	21
Telkom South Africa							
Total number of maximal risk groups	210	230	311	271	281	3659	1
Average number of fibers per maximal risk groups	2.03	2.05	2.47	2.82	4.97	80.31	343
Maximum number of fibers per maximal risk groups	3	3	5	8	9	108	343
Minimum number of fibers per maximal risk groups	2	2	2	2	2	19	343

disaster shapes, and protecting against all of them is hard. In this chapter, more attention is given to the fiber geodetic locations instead of the disaster shape. Spatially-close fibers have a high chance of failing simultaneously, regardless of the disaster shape.

We have proposed fast approaches on finding spatially-close fiber segments for any arbitrary positioning or length of fiber segments. While the work of [41, 42] may also be used out of context to solve a similar problem, their time complexity is much higher than ours, even without our practical time-saving preprocessing routines. [41] limits the fiber segments to be non-intersecting and two adjacent fiber segments are not collinear, while we do not impose such limitations. [42] is more suited for wireless networks instead of fiber networks, since they consider that only links adjacent to nodes inside a disaster area fail, while links merely passing through the area remain intact. Consider two perpendicular fibers with minimum separation distance from one of the fiber endpoints to the middle of the other (much longer) fiber. [42] would have not considered the fiber pair to be spatially close.

[40, 46] focus on a greenfield planning of placing new fibers in a geographic area. Our approach on solving the ISSCF problem is useful in complementing their work by verifying that the new fibers are not spatially close to any existing fibers. [59] groups fibers by matching their locations to specific disaster maps. On the other hand, we focus on grouping fibers based on their spatial proximity. We also find the maximal risk groups, such that the number of risk groups needed are greatly reduced, which is favorable since many applications, e.g., risk-group-based routing, are NP-hard [66, 183], thus the running time can grow exponentially with the number of risk groups.

5.6. CHAPTER CONCLUSION

We have proposed fast polynomial-time approaches for detecting spatially-close fiber segments. Network operators can adapt their existing network physical maps to our fiber structure for detecting spatially-close fiber segments in their network. We also showed that the algorithm based on R tree preprocessing far outperforms the algorithm with k-d tree preprocessing and the intuitive naive approach.

We have also proposed a polynomial-time approach for finding the intervals of a fiber that are spatially close to another fiber, i.e., the span of a fiber that is unsafe from the other fiber. These intervals can be used to differentiate spatially-close fibers according to their proximity. We also extended the problem

to find the intervals of a fiber that are spatially close to at least one fiber in a set of fibers. We also showed that maintaining the granularity of fiber segments is important, since combining non-collinear fiber segments changes the intervals unpredictably, albeit with significant time savings.

We have also proposed a fast exact approach for grouping spatially-close fibers using the minimum number of distinct risk groups. Our risk group classification enables ample knowledge of existing risk-group-disjoint paths algorithms to be used in finding disaster-disjoint paths, and leads to a unified risk group classification when combined with existing risk group classification approaches. We showed that the number of maximal risk groups can increase or decrease with the increase of the minimum separation distance between fibers.

Examples of possible future work that can be derived from this chapter are, 1) finding two paths P_1 and P_2 between two network nodes such that the minimum separation distance of the two paths is maximized, and 2) finding two paths P_1 and P_2 between two network nodes such that the total interval length of P_1 that is spatially close to P_2 is minimized.

6

CONCLUSION

In optical networks, data are transmitted over optical fibers of very long lengths, in the form of light pulses between the network nodes. Optical networks often play the role as the backbone of most telecommunication networks, such that they play a pivotal role in communication of critical network services as banking and emergency services. Thus, society heavily depends on the optical networks to be managed efficiently and be as reliable as possible, underlying the importance of the research topics studied in this thesis. The thesis has studied two important research topics related to the management and survivability of network services, namely routing and disaster awareness. Routing enables the optimal end-to-end path to be assigned to each network connection, while disaster awareness increases the survivability of network connections against the risk of failing due to the occurrences of disasters. The first part of this thesis, namely Chapters 2, 3 and 4 have dealt with advanced routing algorithms for configuring network connections with paths that are optimal in their respective criteria and conditions, while the second part of this thesis, namely Chapters 4 and 5 have dealt with approaches for disaster awareness in ensuring the survivability of network connections. Each chapter has proposed valuable insights to new research problems in their respective topic, and the proposed solutions for the problem have been tested in a variety of randomly generated networks and real-life networks. Though the thesis emphasizes particularly on optical networks, the provided insights and contributions in each chapter are general enough to be extended for application in other network types as well.

6.1. THESIS CONTRIBUTIONS

The main contributions of this thesis are thus as follows:

- Network connections may need to be established across multiple optical network domains, with each network domain managed by different network operators. In this context, the technology-aware routing problem arises due to the fact that there are no de-facto standards in the technology used by each network domain, since they are managed by different network operators. Establishing a network connection between these network domains (possibly spanning multiple intermediate network domains) is not a trivial task due to the technology incompatibilities of the network domains. This thesis has proved that routing connections in multi-domain networks with technology incompatibilities are NP-hard, proposed a new model for modeling the technology adaptations and conversions of network domains and inter-domain links, and proposed an exact algorithm and two heuristics for routing connections using simple paths that are optimal in length while satisfying the technology continuity constraints.
- Data are transferred between network nodes using network connections that are established as lightpaths. Signals along these lightpaths accumulate transmission impairments (such as attenuation, dispersion, and distortion) and can be unreadable if the accumulated impairments are too high. Different network equipment (e.g., optical switches, optical fibers, optical amplifiers, and optical dispersion compensator) contribute differently to the impairments, and thus affect the accumulated impairments differently. This thesis has proposed the use of a realistic link structure to quantify the potential harm of impairments according to respective network equipments, a new additive routing metric referred to as the Figure-of-Impact (FoI) that quantifies the potential harm of the non-linear Self-Phase Modulation (SPM) impairment, and a two-phase heuristic for solving the multi-constrained impairment-aware routing and wavelength assignment problem. This thesis also showed that the proposed pragmatic approach performs well in a realistic case study of the SURFnet7 network.
- Network connections can cease to function due to the failure of optical fibers, especially in the event of disasters. Disasters may also have spatiotemporal characteristics, such that link availabilities vary in time. By considering that the spatiotemporal impact of disasters can be predicted,

this thesis provided the means for representing the spatiotemporal risk profile of a network area to the occurrences of disasters using a grid-based model, a polynomial-time algorithm for identifying network connections that are vulnerable to an emerging disaster risk, and a polynomial-time routing algorithm for finding the most risk-averse end-to-end path under a time constraint. This thesis also showed that larger disaster size leads to more vulnerable connections, and scattered disasters are more detrimental to network connections than confined disasters. The number of vulnerable connections increases with the increase in network utilization, and the possibility of rerouting vulnerable connections using alternative paths decreases with the increase in network utilization (or disaster size).

- Spatially-close optical fibers have a significant chance of failing simultaneously in the event of man-made or natural disasters within their geographic area. This thesis provided polynomial-time algorithms for detecting all the spatially-close fiber segments of different fibers, a polynomial-time algorithm for finding the spatially-close intervals of a fiber to a set of other fibers, and a fast exact algorithm for grouping spatially-close fibers using the minimum number of distinct risk groups. Network operators can adapt their existing network physical maps to the proposed fiber structure for detecting spatially-close fiber segments in their network. This thesis showed that the algorithm based on R tree preprocessing far outperforms the algorithm with k-d tree preprocessing and the intuitive brute-force approach in finding all the spatially-close fiber segments. The proposed spatially-close intervals can be used to differentiate spatially-close fibers according to their proximity. This thesis also showed that maintaining the granularity of fiber segments in computing the spatially-close intervals is important, since combining non-collinear fiber segments changes the intervals unpredictably, albeit with significant time savings. The proposed risk group classification enables ample knowledge of existing risk-group-disjoint paths algorithms to be used in finding disaster-disjoint paths, and leads to a unified risk group classification when combined with existing risk group classification approaches. This thesis showed that the number of maximal risk groups can increase or decrease with the increase of the minimum separation distance between fibers.

The contributions of the thesis tally with the four sets of research questions mentioned earlier in Chapter 1.3.

6.2. DIRECTIONS FOR FUTURE WORK

Various directions for future work that can be derived from this thesis are:

- Chapter 2 dealt with the technology-aware routing problem in the presence of technology incompatibilities. However, only the inter-domain routing part was considered, and the intra-domain routing part could further be studied. The technology model could be extended to include the cost of technology adaptations/conversions (instead of simply binary values). The routing algorithms can also be extended for finding min-sum disjoint technology-aware paths instead of simply the shortest simple technology-aware path. Practical implementations of our algorithms in the Software-Defined Networking (SDN) platforms would also be of further interest.
- Chapter 3 focused on impairment-aware routing problem in the presence of transmission impairments. In addition to the impairment constraints that were considered, the proposed model could also be incorporated with other variety of unconsidered impairment constraints as well. The proposed model could also be extended with additional network equipment instead of the existing ones. It might also be of interest to quantify the differences of the proposed Figure-of-Impact (FoI) in representing the potential harm of Self-Phase Modulation (SPM) to the actual value computed by high fidelity computation.
- Chapter 4 studied the modeling of spatiotemporal disaster risks and the risk-averse routing problem. Instead of spatiotemporal disasters, it might also be interesting study cascading and correlated disasters as well using the proposed risk profile model. Other possible directions are finding the minimum delay path that satisfies an availability constraint, using a probability density function to represent the risk profile, and extending the grid-based model for use in a three-dimensional Cartesian plane.
- Chapter 5 considered the problem of detecting spatially-close fibers, compute their spatially-close intervals and grouping them accordingly. Examples of possible future work that can be derived from this topic are, finding two paths P_1 and P_2 between two network nodes such that the minimum separation distance of the two paths is maximized, and finding two paths P_1 and P_2 between two network nodes such that the total interval length of P_1 that is spatially close to P_2 is minimized.

REFERENCES

- [1] F. Iqbal and F. Kuipers, “Disjoint paths in networks,” *Wiley Encyclopedia of Electrical and Electronics Engineering*, 2015.
- [2] F. Harary, *Graph theory*. Addison-Wesley, 1969.
- [3] E. F. Moore, “The shortest path through a maze,” in *Proceedings of the International Symposium Switching Theory 1957, Part II*, 1959.
- [4] T. H. Cormen, C. E. Leiserson, R. L. Rivest, and C. Stein, *Introduction to algorithms*. The MIT press, 2001.
- [5] E. W. Dijkstra, “A note on two problems in connexion with graphs,” *Numerische Mathematik*, pp. 269–271, 1959.
- [6] M. L. Fredman and R. E. Tarjan, “Fibonacci heaps and their uses in improved network optimization algorithms,” *Journal of the ACM*, vol. 34, no. 3, pp. 596–615, 1987.
- [7] R. E. Bellman, “On a routing problem,” *Quarterly of Applied Mathematics*, vol. 16, pp. 87–90, 1958.
- [8] L. R. Ford, “Flows in networks,” *RAND Report*, 1956.
- [9] D. B. Johnson, “Efficient algorithms for shortest paths in sparse networks,” *Journal of the ACM*, vol. 24, no. 1, pp. 1–13, 1977.
- [10] J. Edmonds and R. M. Karp, “Theoretical improvements in algorithmic efficiency for network flow problems,” *Journal of the ACM*, vol. 19, no. 2, pp. 248–264, 1972.
- [11] R. Bhandari, “Optimal physical diversity algorithms and survivable networks,” in *IEEE Symposium on Computers and Communications*, 1997.
- [12] D. B. Johnson, “A note on Dijkstra’s shortest path algorithm,” *Journal of the ACM*, vol. 20, no. 3, pp. 385–388, 1973.

-
- [13] T. A. J. Nicholson, "Finding the shortest route between two points in a network," *BCS The Computer Journal*, vol. 9, no. 3, pp. 275–280, 1966.
- [14] R. W. Floyd, "Algorithm 97: shortest path," *Communications of the ACM*, vol. 5, no. 6, p. 345, 1962.
- [15] S. Warshall, "A theorem on boolean matrices," *Journal of the ACM*, vol. 9, no. 1, pp. 11–12, 1962.
- [16] S. E. Dreyfus, "An appraisal of some shortest-path algorithms," *INFORMS Operations Research*, vol. 17, no. 3, pp. 395–412, 1969.
- [17] J. Y. Yen, "Finding the k shortest loopless paths in a network," *INFORMS Management Science*, vol. 17, no. 11, pp. 712–716, 1971.
- [18] L. R. Ford Jr and D. R. Fulkerson, *Network Flow Theory*. Princeton University Press, 1962.
- [19] D. Zhou and S. Subramaniam, "Survivability in optical networks," *IEEE Network*, vol. 14, no. 6, pp. 16–23, 2000.
- [20] S. Ramamurthy, L. Sahasrabudde, and B. Mukherjee, "Survivable WDM mesh networks," *IEEE Journal of Lightwave Technology*, vol. 21, pp. 870–883, 2003.
- [21] D. A. Dunn, W. D. Grover, and M. H. MacGregor, "Comparison of k-shortest paths and maximum flow routing for network facility restoration," *IEEE Journal on Selected Areas in Communications*, vol. 12, no. 1, pp. 88–99, 1994.
- [22] J. W. Suurballe, "Disjoint paths in a network," *Wiley Networks*, vol. 4, no. 2, pp. 125–145, 1974.
- [23] C.-L. Li, S. T. McCormick, and D. Simchi-Levi, "The complexity of finding two disjoint paths with min-max objective function," *Elsevier Discrete Applied Mathematics*, vol. 26, no. 1, pp. 105–115, 1990.
- [24] K. Thulasiraman and M. N. S. Swamy, *Graphs: Theory and Algorithms*. John Wiley & Sons, 1992.
- [25] L. Guo and H. Shen, "On finding min-min disjoint paths," *Springer Algorithmica*, vol. 66, no. 3, pp. 641–653, 2013.

- [26] D. Xu, Y. Chen, Y. Xiong, C. Qiao, and X. He, "On the complexity of and algorithms for finding the shortest path with a disjoint counterpart," *IEEE/ACM Transactions on Networking*, vol. 14, no. 1, pp. 147–158, 2006.
- [27] A. Itai, Y. Perl, and Y. Shiloach, "The complexity of finding maximum disjoint paths with length constraints," *Wiley Networks*, vol. 12, no. 3, pp. 277–286, 1982.
- [28] A. Bley, "On the complexity of vertex-disjoint length-restricted path problems," *Springer Computational Complexity*, vol. 12, no. 3-4, pp. 131–149, 2003.
- [29] A. Beshir and F. A. Kuipers, "Variants of the min-sum link-disjoint paths problem," in *IEEE Symposium on Communications and Vehicular Technology in the Benelux (SCVT'09)*, 2009.
- [30] J. W. Suurballe and R. E. Tarjan, "A quick method for finding shortest pairs of disjoint paths," *Wiley Networks*, vol. 14, no. 2, pp. 325–336, 1984.
- [31] N. Taft-Plotkin, B. Bellur, and R. Ogier, "Quality-of-service routing using maximally disjoint paths," in *IEEE International Workshop on Quality of Service, (IWQoS'99)*, 1999, pp. 119–128.
- [32] C. Doerr and F. Kuipers, "All quiet on the Internet front?" *IEEE Communications Magazine*, vol. 52, no. 10, pp. 46–51, 2014.
- [33] P. K. Agarwal, A. Efrat, S. K. Ganjugunte, D. Hay, S. Sankararaman, and G. Zussman, "The resilience of WDM networks to probabilistic geographical failures," *IEEE/ACM Transactions on Networking*, vol. 21, no. 5, pp. 1525–1538, 2013.
- [34] [Online]. Available: <http://www.evolver.com/blog/downtime-outages-and-failures-understanding-their-true-costs.html>
- [35] C. Doerr, R. Gavrila, F. A. Kuipers, and P. Trimintzios, "Good practices in resilient internet interconnection," *ENISA Report*, 2012.
- [36] J. P. Sterbenz, D. Hutchison, E. K. Çetinkaya, A. Jabbar, J. P. Rohrer, M. Schöller, and P. Smith, "Resilience and survivability in communication networks: Strategies, principles, and survey of disciplines," *Elsevier Computer Networks*, vol. 54, no. 8, pp. 1245–1265, 2010.

- [37] M. K. Jha, "Natural and anthropogenic disasters: An overview," in *Natural and Anthropogenic Disasters: Vulnerability, Preparedness and Mitigation*. Springer, 2010, pp. 1–16.
- [38] S. V. Buldyrev, R. Parshani, G. Paul, H. E. Stanley, and S. Havlin, "Catastrophic cascade of failures in interdependent networks," *Nature*, vol. 464, no. 7291, pp. 1025–1028, 2010.
- [39] S. C. Liew and K. W. Lu, "A framework for characterizing disaster-based network survivability," *IEEE Journal on Selected Areas in Communications*, vol. 12, no. 1, pp. 52–58, 1994.
- [40] D. L. Msongaleli, F. Dikbiyik, M. Zukerman, and B. Mukherjee, "Disaster-aware submarine fiber-optic cable deployment," in *International Conference on Optical Networking Design and Modeling (ONDM'15)*, 2015.
- [41] S. Neumayer, A. Efrat, and E. Modiano, "Geographic max-flow and min-cut under a circular disk failure model," *Elsevier Computer Networks*, vol. 77, pp. 117–127, 2015.
- [42] S. Trajanovski, F. A. Kuipers, A. Ilic, J. Crowcroft, and P. Van Mieghem, "Finding critical regions and region-disjoint paths in a network," *IEEE/ACM Transactions on Networking*, vol. 23, no. 3, pp. 908–921, 2015.
- [43] S. Neumayer, G. Zussman, R. Cohen, and E. Modiano, "Assessing the vulnerability of the fiber infrastructure to disasters," *IEEE/ACM Transactions on Networking*, vol. 19, no. 6, pp. 1610–1623, 2011.
- [44] S. Neumayer and E. Modiano, "Network reliability with geographically correlated failures," in *IEEE Conference on Computer Communications (INFOCOM'10)*, 2010.
- [45] A. Izaddoost and S. S. Heydari, "Enhancing network service survivability in large-scale failure scenarios," *IEEE Journal of Communications and Networks*, vol. 16, no. 5, pp. 534–547, 2014.
- [46] C. Cao, M. Zukerman, W. Wu, J. H. Manton, and B. Moran, "Survivable topology design of submarine networks," *IEEE Journal of Lightwave Technology*, vol. 31, no. 5, pp. 715–730, 2013.

- [47] P. K. Agarwal, A. Efrat, S. K. Ganjugunte, D. Hay, S. Sankararaman, and G. Zussman, "Network vulnerability to single, multiple, and probabilistic physical attacks," in *IEEE Military Communications Conference (MILCOM)*, 2010.
- [48] A. Sen, B. H. Shen, L. Zhou, and B. Hao, "Fault-tolerance in sensor networks: A new evaluation metric," in *IEEE Conference on Computer Communications (INFOCOM'06)*, 2006.
- [49] A. Izaddoost and S. S. Heydari, "Topology-based proactive network protection in large-scale failure scenarios," *Elsevier Procedia Computer Science*, vol. 34, pp. 111–117, 2014.
- [50] H. Saito, "Geometric evaluation of survivability of disaster-affected network with probabilistic failure," in *IEEE Conference on Computer Communications (INFOCOM'14)*, 2014, pp. 1608–1616.
- [51] X. Zhang, X. Wang, X. Jiang, and S. Lu, "Degree of network damage: A measurement for intensity of network damage," in *IEEE European Conference on Networks and Optical Communications (NOC'14)*, 2014.
- [52] [Online]. Available: http://www.nasa.gov/vision/earth/lookingatearth/h2005_katrina.html
- [53] J. P. Sterbenz, E. K. Cetinkaya, M. A. Hameed, A. Jabbar, S. Qian, and J. P. Rohrer, "Evaluation of network resilience, survivability, and disruption tolerance: analysis, topology generation, simulation, and experimentation," *Springer Telecommunication systems*, vol. 52, no. 2, pp. 705–736, 2013.
- [54] B. Mukherjee, M. Habib, and F. Dikbiyik, "Network adaptability from disaster disruptions and cascading failures," *IEEE Communications Magazine*, vol. 52, no. 5, pp. 230–238, 2014.
- [55] A. Berger, C. Kousky, and R. Zeckhauser, "Obstacles to clear thinking about natural disasters: five lessons for policy," in *Risking house and home: disasters, cities, public policy*, J. M. Quigley and L. A. Rosenthal, Eds. Berkeley Public Policy Press, 2008, pp. 73–94.
- [56] H. Saito, "Analysis of geometric disaster evaluation model for physical networks," *IEEE/ACM Transactions on Networking*, vol. 23, no. 6, pp. 1777–1789, 2015.

- [57] —, “Spatial design of physical network robust against earthquakes,” *IEEE Journal of Lightwave Technology*, vol. 33, no. 2, pp. 443–458, 2015.
- [58] R. Tiwari, S. Savas, M. F. Habib, P. Chowdhury, and B. Mukherjee, “Disaster resilience in SDN: A case study,” in *OSA Asia Communications and Photonics Conference, (ACP’15)*, 2015.
- [59] F. Dikbiyik, M. Tornatore, and B. Mukherjee, “Minimizing the risk from disaster failures in optical backbone networks,” *IEEE Journal of Lightwave Technology*, vol. 32, no. 18, pp. 3175–3183, 2014.
- [60] N.-H. Bao, M. F. Habib, M. Tornatore, C. U. Martel, and B. Mukherjee, “Global versus essential post-disaster re-provisioning in telecom mesh networks,” *OSA Journal of Optical Communications and Networking*, vol. 7, no. 5, pp. 392–400, 2015.
- [61] S. Ferdousi, F. Dikbiyik, M. Tornatore, and B. Mukherjee, “Progressive datacenter recovery over optical core networks after a large-scale disaster,” in *International Conference on Design of Reliable Communication Networks (DRCN’16)*, 2016.
- [62] M. T. Gardner, Y. Cheng, R. May, C. Beard, J. Sterbenz, and D. Medhi, “Creating network resilience against disasters using service level agreements,” in *International Conference on Design of Reliable Communication Networks (DRCN’16)*, 2016.
- [63] A. Sivasankaran, M. Razo, M. Tacca, and A. Fumagalli, “Preemption based lightpath restoration,” in *IEEE International Conference on Communications (ICC’12)*, 2012.
- [64] S. Xu, N. Yoshikane, M. Shiraiwa, and T. Tsuritani, “Multi-vendor interconnection-based emergency optical networks design with optimal placement of portable EDFAs in disaster recovery,” in *International Conference on Design of Reliable Communication Networks (DRCN’16)*, 2016.
- [65] [Online]. Available: http://www.geant.org/Networks/Pan-European_network/Pages/GEANT_topology_map.aspx
- [66] J. Q. Hu, “Diverse routing in optical mesh networks,” *IEEE Transactions on Communications*, vol. 51, no. 3, pp. 489–494, 2003.

- [67] J. Berthold, A. A. Saleh, L. Blair, and J. M. Simmons, "Optical networking: past, present, and future," *IEEE Journal of Lightwave Technology*, vol. 26, no. 9, pp. 1104–1118, 2008.
- [68] R. Ramaswami, K. Sivarajan, and G. Sasaki, *Optical networks: a practical perspective*. Morgan Kaufmann, 2009.
- [69] I. Chlamtac, A. Ganz, and G. Karmi, "Lightpath communications: An approach to high bandwidth optical WAN's," *IEEE Transactions on Communications*, vol. 40, no. 7, pp. 1171–1182, 1992.
- [70] F. Iqbal, J. Van Der Ham, and F. Kuipers, "Technology-aware multi-domain multi-layer routing," *Elsevier Computer Communications*, vol. 62, pp. 85–96, 2015.
- [71] [Online]. Available: <http://home.web.cern.ch/about/accelerators/large-hadron-collider>
- [72] [Online]. Available: <http://www.sdss.org/>
- [73] [Online]. Available: <https://www.skatelescope.org/>
- [74] [Online]. Available: <http://www.lsst.org/lsst/>
- [75] [Online]. Available: <http://www.surf.nl/en/about-surf/subsidiaries/surfnet>
- [76] [Online]. Available: <http://www.myren.net.my>
- [77] [Online]. Available: <http://www.glif.is/>
- [78] [Online]. Available: <https://www.surf.nl/en/services-and-products/netherlight/index.html>
- [79] [Online]. Available: <http://cernlight.web.cern.ch/cernlight>
- [80] [Online]. Available: <http://czechlight.cesnet.cz/en/>
- [81] "Architecture for the automatically switched optical network (ASON)," *ITU-T G. 8080/Y. 1304*, 2001.
- [82] A. Farrel, J. P. Vasseur, and J. Ash, "A path computation element (PCE)-based architecture," *RFC 4655*, 2006.

- [83] R. Muñoz, R. Casellas, R. Martínez, and R. Vilalta, "PCE: What is it, how does it work and what are its limitations?" *IEEE Journal of Lightwave Technology*, vol. 32, no. 4, pp. 528–543, 2014.
- [84] G. Roberts, T. Kudoh, I. Monga, J. Sobieski, and J. Vollbrecht, "Network services framework v1.0," Open Grid Forum, 2010. [Online]. Available: <http://www.ogf.org/documents/GFD.173.pdf>
- [85] G. Roberts, T. Kudoh, I. Monga, J. Sobieski, J. MacAuley, and C. Guok, "NSI connection service protocol v2.0," GFD-R-P.212, Open Grid Forum, 2014. [Online]. Available: <http://www.ogf.org/documents/GFD.212.pdf>
- [86] [Online]. Available: <http://www.glif.is/publications/press/20131203.html>
- [87] S. Yang and F. Kuipers, "Energy-aware path selection for scheduled light-paths in IP-over-WDM networks," in *18th IEEE Symposium on Communications and Vehicular Technology in the Benelux (SCVT'11)*, 2011.
- [88] G. Shen and R. S. Tucker, "Energy-minimized design for IP over WDM networks," *IEEE Journal on Selected Areas in Communications*, vol. 27, no. 3, 2009.
- [89] A. L. Chiu and E. H. Modiano, "Traffic grooming algorithms for reducing electronic multiplexing costs in WDM ring networks," *IEEE Journal of Lightwave Technology*, vol. 18, 2000.
- [90] P. Demeester, M. Gryseels, A. Autenrieth, C. Brianza, L. Castagna, G. SIGNORELLI, R. Clemenfe, M. Ravera, A. Jajszczyk, D. Janukowicz, K. Van Doorselaere, and H. Yohnosuke, "Resilience in multilayer networks," *IEEE Communications Magazine*, vol. 37, no. 8, pp. 70–76, 1999.
- [91] F. Iqbal, S. Yang, and F. Kuipers, "Energy considerations in EoS-over-WDM network configuration," in *3rd International Conference on Sustainable Internet and ICT for Sustainability (SustainIT'13)*, 2013.
- [92] A. Hadjiantonis, M. A. Ali, H. Chamas, W. Bjorkman, S. Elby, A. Khalil, G. Ellinas, and N. Ghani, "Evolution to a converged layer 1, 2 in a global-scale, native ethernet over WDM-based optical networking architecture," *IEEE Journal on Selected Areas in Communications*, vol. 25, pp. 1048–1058, 2007.
- [93] F. Kuipers and F. Dijkstra, "Path selection in multi-layer networks," *Elsevier Computer Communications*, vol. 32, no. 1, pp. 78–85, 2009.

- [94] A. Martinez, M. Yannuzzi, V. Lopez, D. Lopez, W. Ramirez, R. Serral-Gracia, X. Masip-Bruin, M. Maciejewski, and J. Altmann, "Network management challenges and trends in multi-layer and multi-vendor settings for carrier-grade networks," *IEEE Communications Surveys and Tutorials*, vol. 16, no. 4, pp. 2207–2230, 2014.
- [95] J. van der Ham, F. Dijkstra, R. Łapacz, and J. Zurawski, "Network markup language base schema version 1," GFD-R-P206, Open Grid Forum, May 2013. [Online]. Available: <http://www.ogf.org/documents/GFD.206.pdf>
- [96] I. Chlamtac, A. Farago, and T. Zhang, "Lightpath (wavelength) routing in large WDM networks," *IEEE Journal on Selected Areas in Communications*, vol. 14, no. 5, pp. 909–913, 1996.
- [97] B. Jabbari and G. Shujia, "On constraints for path computation in multi-layer switched networks," *IEICE Transactions on Communications*, vol. 90, no. 8, pp. 1922–1927, 2007.
- [98] M. Shirazipour and S. Pierre, "Multi-layer/multi-region path computation with adaptation capability constraints," in *IEEE Global Telecommunications Conference (GLOBECOM'10)*, 2010.
- [99] M. L. Lamali, H. Pouyllau, and D. Barth, "Path computation in multi-layer multi-domain networks," in *IFIP/TC6 Networking Conference (NETWORKING'12)*, 2012, pp. 421–433.
- [100] E. Mannie, "Generalized multi-protocol label switching (GMPLS) architecture," *IETF RFC 3945*, 2004.
- [101] D. Papadimitriou, M. Vigoureux, K. Shiimoto, D. Brungard, and J. Le Roux, "Generalized MPLS (GMPLS) protocol extensions for multi-layer and multi-region networks (MLN/MRN)," *IETF RFC 6001*, 2010.
- [102] S. Gong and B. Jabbari, "Optimal and efficient end-to-end path computation in multi-layer networks," in *IEEE International Conference on Communications (ICC'08)*, 2008, pp. 5767–5771.
- [103] F. Dijkstra, B. Andree, K. Koymans, J. van der Ham, P. Grosso, and C. de Laat, "A multi-layer network model based on ITU-T G. 805," *Elsevier Computer Networks*, vol. 52, no. 10, pp. 1927–1937, 2008.

- [104] S. Das, G. Parulkar, and N. McKeown, "Why OpenFlow/SDN can succeed where GMPLS failed," in *38th European Conference and Exhibition on Optical Communications (ECOC'12)*, 2012.
- [105] M. L. Lamali, H. Pouyllau, and D. Barth, "Path computation in multi-layer multi-domain networks: A language theoretic approach," *Elsevier Computer Communications*, vol. 36, no. 5, pp. 589–599, 2013.
- [106] L. Xu, F. Dijkstra, D. Marchal, A. Taal, P. Grosso, and C. De Laat, "A declarative approach to multi-layer path finding based on semantic network descriptions," in *13th International Conference on Optical Networking Design and Modeling (ONDM'09)*, 2009.
- [107] S. Uludag, K. S. Lui, K. Nahrstedt, and G. Brewster, "Analysis of topology aggregation techniques for QoS routing," *ACM Computing Surveys*, vol. 39, no. 3, 2007.
- [108] P. Zhang and W. Zhao, "On the complexity and approximation of the min-sum and min-max disjoint paths problems," in *Combinatorics, Algorithms, Probabilistic and Experimental Methodologies*, 2007, pp. 70–81.
- [109] E. I. Chong, S. Maddila, and S. Morley, "On finding single-source single-destination k shortest paths," *Journal of Computing and Information*, vol. 95, pp. 40–47, 1995.
- [110] P. Van Mieghem and F. Kuipers, "Concepts of exact QoS routing algorithms," *IEEE/ACM Transactions on Networking*, vol. 16, no. 9, pp. 851–864, 2004.
- [111] P. Erdős and A. Rényi, "On random graphs," *Publicationes Mathematicae Debrecen*, vol. 6, pp. 290–297, 1959.
- [112] ———, "On the evolution of random graphs," *Publications of the Mathematical Institute of the Hungarian Academy of Sciences*, vol. 5, pp. 17–61, 1960.
- [113] B. M. Waxman, "Routing of multipoint connections," *IEEE Journal on Selected Areas in Communications*, vol. 6, no. 9, pp. 1617–1622, 1988.
- [114] [Online]. Available: <http://www.geant.net/>

- [115] A. R. Moral, P. Bonenfant, M. Krishnaswamy, and O. In, "The optical internet: architectures and protocols for the global infrastructure of tomorrow," *IEEE/ACM Transactions on Networking*, vol. 39, no. 7, pp. 152–159, 2001.
- [116] P. Van Mieghem, "Paths in the simple random graph and the Waxman graph," *Probability in the Engineering and Informational Sciences*, vol. 15, no. 04, pp. 535–555, 2001.
- [117] C. Pavan, R. M. Morais, J. R. Ferreira Da Rocha, and A. N. Pinto, "Generating realistic optical transport network topologies," *OSA Journal of Optical Communications and Networking*, vol. 2, no. 1-3, pp. 80–90, 2010.
- [118] M. Naldi, "Connectivity of Waxman topology models," *Elsevier Computer Communications*, vol. 29, pp. 24–31, 2005.
- [119] A. P. Bianzino, L. Chiaraviglio, and M. Mellia, "GRiDA: a green distributed algorithm for backbone networks," in *IEEE Online Conference on Green Communications (GreenCom'11)*, 2011.
- [120] F. Iqbal, R. Smets, and F. Kuipers, "A pragmatic approach to impairment awareness in optical networks," in *20th European Conference of Networks and Optical Communications (NOC'15)*, 2015.
- [121] F. Kuipers, A. Beshir, A. Orda, and P. Van Mieghem, "Impairment-aware path selection and regenerator placement in translucent optical networks," in *IEEE International Conference on Network Protocols (ICNP'10)*, 2010.
- [122] S. Azodolmolky, M. Klinkowski, E. Marin, D. Careglio, J. S. Pareta, and I. Tomkos, "A survey on physical layer impairments aware routing and wavelength assignment algorithms in optical networks," *Elsevier Computer Networks*, vol. 53, no. 7, pp. 926–944, 2009.
- [123] B. Ramamurthy, D. Datta, H. Feng, J. P. Heritage, and B. Mukherjee, "Impact of transmission impairments on the teletraffic performance of wavelength-routed optical networks," *IEEE Journal of Lightwave Technology*, vol. 17, no. 10, p. 1713, 1999.
- [124] J. Strand, A. L. Chiu, and R. Tkach, "Issues for routing in the optical layer," *IEEE Communications Magazine*, vol. 39, no. 2, pp. 81–87, 2001.

- [125] P. Soproni, T. Cinkler, and J. Rak, "Methods for physical impairment constrained routing with selected protection in all-optical networks," *Springer Telecommunication Systems*, vol. 56, no. 1, pp. 177–188, 2014.
- [126] A. Beshir, R. Nuijts, R. Malhotra, and F. Kuipers, "Survivable impairment-aware traffic grooming," in *IEEE European Conference of Networks and Optical Communications (NOC'11)*, 2011.
- [127] H. A. Pereira, D. A. R. Chaves, C. J. A. Bastos-Filho, and J. F. Martins-Filho, "OSNR model to consider physical layer impairments in transparent optical networks," *Springer Photonic Network Communications*, vol. 18, no. 2, 2009.
- [128] S. Pachnicke, N. Luck, and P. M. Krummrich, "Online physical-layer impairment-aware routing with quality of transmission constraints in translucent optical networks," in *International Conference on Transparent Optical Networks (ICTON'09)*, 2009.
- [129] G. Markidis, S. Sygletos, A. Tzanakaki, and I. Tomkos, "Impairment aware based routing and wavelength assignment in transparent long haul networks," in *International Conference on Optical Networking Design and Modeling (ONDM'07)*, 2007.
- [130] "Characteristics of a single-mode optical fibre and cable," *ITU-T G. 652*, 2009.
- [131] "Characteristics of non zero dispersion shifted single mode optical fiber cable," *ITU-T G. 655*, 2009.
- [132] "Generic characteristics of optical amplifier devices and subsystems," *ITU-T G. 662*, 2005.
- [133] L. Grüner-Nielsen, M. Wandel, P. Kristensen, C. Jørgensen, L. V. Jørgensen, B. Edvold, B. Pálsdóttir, and D. Jakobsen, "Dispersion-compensating fibers," *IEEE Journal of Lightwave Technology*, vol. 23, no. 11, pp. 3566–3579, 2005.
- [134] "Optical fibre attenuators," *ITU-T L. 31*, 1996.
- [135] N. Zulkifli, S. M. Idrus, A. S. M. Supa'at, and M. A. Farabi, "Network performance improvement of all-optical networks through an algorithmic based

- dispersion management technique,” *Springer Journal of Network and Systems Management*, vol. 20, no. 3, 2012.
- [136] S. P. Singh and N. Singh, “Nonlinear effects in optical fibers: Origin, management and applications,” *EMW Progress In Electromagnetics Research*, vol. 73, pp. 249–275, 2007.
- [137] S. Yang and F. Kuipers, “Impairment-aware routing in translucent spectrum-sliced elastic optical path networks,” in *17th IEEE European Conference on Networks and Optical Communications (NOC’12)*, 2012.
- [138] Z. Wang and J. Crowcroft, “Quality-of-service routing for supporting multimedia applications,” *IEEE Journal on Selected Areas in Communications*, vol. 14, no. 7, pp. 1228–1234, 1996.
- [139] [Online]. Available: <https://www.surf.nl/en/services-and-products/surfinternet/network-topology-surfnet7/index.html>
- [140] H. Zang, J. P. Jue, and B. Mukherjee, “A review of routing and wavelength assignment approaches for wavelength-routed optical wdm networks,” *IEEE Communications Magazine*, vol. 1, no. 1, pp. 47–60, 2000.
- [141] F. Iqbal and F. Kuipers, “Spatiotemporal risk-averse routing,” in *IEEE INFO-COM Workshop on Cross-Layer Cyber-Physical Systems Security (CPSS’16)*, 2016.
- [142] X. Wei, L. Guo, X. Wang, Q. Song, and L. Li, “Availability guarantee in survivable WDM mesh networks: A time perspective,” *Elsevier Information Sciences*, vol. 178, no. 11, pp. 2406–2415, 2008.
- [143] D. A. Schupke, “Guaranteeing service availability in optical network design,” *Proceedings of SPIE - The International Society for Optical Engineering*, vol. 6022 I, 2005.
- [144] R. W. Burpee, S. D. Aberson, J. L. Franklin, S. J. Lord, and R. E. Tuleya, “The impact of Omega dropwindsondes on operational hurricane track forecast models,” *Bulletin of the American Meteorological Society*, vol. 77, no. 5, pp. 925–933, 1996.
- [145] R. M. Allen, “Probabilistic warning times for earthquake ground shaking in the San Francisco Bay Area,” *SSA Seismological Research Letters*, vol. 77, no. 3, pp. 371–376, 2006.

- [146] A. Donnellan, L. Grant Ludwig, J. W. Parker, J. B. Rundle, J. Wang, M. Pierce, G. Blewitt, and S. Hensley, "Potential for a large earthquake near Los Angeles inferred from the 2014 La Habra earthquake," *Earth and Space Science*, vol. 2, pp. 378–385, 2015.
- [147] J. Zheng and H. T. Mouftah, *Optical WDM networks: concepts and design principles*. John Wiley & Sons, 2004.
- [148] F. Iqbal, S. Trajanovski, and F. Kuipers, "Detection of spatially-close fiber segments in optical networks," in *International Conference on Design of Reliable Communication Networks (DRCN'16)*, 2016.
- [149] S. Yang, S. Trajanovski, and F. A. Kuipers, "Availability-based path selection," in *6th International Workshop on Reliable Networks Design and Modeling (RNDM'14)*, 2014.
- [150] J. Zhang, K. Zhu, H. Zang, N. S. Matloff, and B. Mukherjee, "Availability-aware provisioning strategies for differentiated protection services in wavelength-convertible WDM mesh networks," *IEEE/ACM Transactions on Networking*, vol. 15, no. 5, pp. 1177–1190, 2007.
- [151] A. Guttman, "R-trees: a dynamic index structure for spatial searching," in *ACM Special Interest Group Management Data (SIGMOD'84)*, 1984.
- [152] H. Alborzi and H. Samet, "Execution time analysis of a top-down r-tree construction algorithm," *Elsevier Information Processing Letters*, vol. 101, no. 1, pp. 6–12, 2007.
- [153] Q. Ma and P. Steenkiste, "On path selection for traffic with bandwidth guarantees," in *IEEE International Conference on Network Protocols (ICNP'97)*, 1997.
- [154] F. A. Kuipers, "An overview of algorithms for network survivability," *ISRN Communications Networking*, 2012.
- [155] S. Ferdousi, M. Tornatore, M. F. Habib, and B. Mukherjee, "Rapid data evacuation for large-scale disasters in optical cloud networks [invited]," *OSA Journal of Optical Communications and Networking*, vol. 7, no. 12, pp. B163–B172, 2015.

- [156] S. Yang, S. Trajanovski, and F. A. Kuipers, "Availability-based path selection and network vulnerability assessment," *Wiley Networks*, vol. 66, no. 4, pp. 306–319, 2015.
- [157] S. Sahhaf, W. Tavernier, D. Colle, M. Pickavet, and P. Demeester, "Availability analysis of resilient geometric routing on internet topology," in *International Conference on Design of Reliable Communication Networks (DRCN'14)*, 2014.
- [158] M. Tornatore, G. Maier, and A. Pattavina, "Availability design of optical transport networks," *IEEE Journal on Selected Areas in Communications*, vol. 23, no. 8, pp. 1520–1532, 2005.
- [159] A. K. Ziliaskopoulos and H. S. Mahmassani, "Time-dependent, shortest-path algorithm for real-time intelligent vehicle highway system applications," *Transportation Research Record*, 1993.
- [160] [Online]. Available: <http://www.telecomasia.net/content/subsea-cable-breaks-bad-2006-quake>
- [161] [Online]. Available: <http://www.submarinenetworks.com/news/cables-cut-by-taiwan-earthquake-and-typhoon-morakot>
- [162] [Online]. Available: <http://www.modernghana.com/news/414121/1/telcos-co-share-ducts-to-lay-fibre-cables>
- [163] [Online]. Available: <http://www.computing.co.uk/ctg/news/1937275/bt-reveals-hotly-anticipated-pricing-proposals-duct-pole-access>
- [164] H. Zang, C. Ou, and B. Mukherjee, "Path-protection routing and wavelength assignment (RWA) in WDM mesh networks under duct-layer constraints," *IEEE/ACM Transactions on Networking*, vol. 11, no. 2, pp. 248–258, 2003.
- [165] [Online]. Available: <http://www.submarinecablemap.com>
- [166] J. L. Bentley, "Multidimensional binary search trees used for associative searching," *Communications of the ACM*, vol. 18, no. 9, pp. 509–517, 1975.
- [167] S. M. Omohundro, "Five balltree construction algorithms," International Computer Science Institute Berkeley, Tech. Rep., 1989.

- [168] L. Arge, M. De Berg, H. J. Haverkort, and K. Yi, “The priority R-tree: A practically efficient and worst-case optimal R-tree,” in *ACM Special Interest Group Management Data (SIGMOD’04)*, 2004.
- [169] [Online]. Available: <https://github.com/stevesong/afterfibre-kml>
- [170] [Online]. Available: <http://www.opengeospatial.org/>
- [171] [Online]. Available: <http://www.eurofiber.com/network-map>
- [172] [Online]. Available: <http://www.monroecounty.gov/google-map>
- [173] [Online]. Available: <http://projectionwizard.org>
- [174] [Online]. Available: <https://github.com/OSGeo/proj.4/wiki>
- [175] J.-C. Bermond, D. Coudert, G. D’Angelo, and F. Z. Moataz, “Finding disjoint paths in networks with star shared risk link groups,” *Elsevier Theoretical Computer Science*, vol. 579, pp. 74–87, 2015.
- [176] P. Datta and A. K. Somani, “Graph transformation approaches for diverse routing in shared risk resource group (SRRG) failures,” *Elsevier Computer Networks*, vol. 52, no. 12, pp. 2381–2394, 2008.
- [177] E. A. Akkoyunlu, “The enumeration of maximal cliques of large graphs,” *SIAM Journal on Computing*, vol. 2, no. 1, pp. 1–6, 1973.
- [178] R. D. Luce and A. D. Perry, “A method of matrix analysis of group structure,” *Springer Psychometrika*, vol. 14, no. 2, pp. 95–116, 1949.
- [179] M. R. Garey and D. S. Johnson, “Strong NP-completeness results: Motivation, examples, and implications,” *Journal of the ACM*, vol. 25, no. 3, pp. 499–508, 1978.
- [180] C. Bron and J. Kerbosch, “Algorithm 457: finding all cliques of an undirected graph,” *Communications of the ACM*, vol. 16, no. 9, pp. 575–577, 1973.
- [181] E. Tomita, A. Tanaka, and H. Takahashi, “The worst-case time complexity for generating all maximal cliques and computational experiments,” *Elsevier Theoretical Computer Science*, vol. 363, no. 1, pp. 28–42, 2006.

-
- [182] J. W. Moon and L. Moser, "On cliques in graphs," *Springer Israel Journal of Mathematics*, vol. 3, no. 1, pp. 23–28, 1965.
- [183] D. Xu, Y. Xiong, C. Qiao, and G. Li, "Trap avoidance and protection schemes in networks with shared risk link groups," *IEEE Journal of Lightwave Technology*, vol. 21, no. 11, p. 2683, 2003.

ABBREVIATIONS

ASE	Amplifier Spontaneous Emission
ASK	Amplitude-Shift Keying
ASON	Automatically Switched Optical Network
ATM	Asynchronous Transfer Mode
BFS	Breadth-First Search
BIP	Binary Integer Program
DAG	Directed Acyclic Graph
DSCFC	Detection of Spatially-Close Fiber Segments
DSCM	Dispersion Slope Compensating Module
DSL	Digital Subscriber Lines
DVC	Detection of Vulnerable Connections
DWDM	Dense WDM
EoS	Ethernet-over-SONET/SDH
ETARA	Exact Technology-Aware Routing Algorithm
FDDI	Fast Distributed Data Interface
FEC	Forward Error Correction
FoI	Figure-of-Impact
FoM	Figure-of-Metric
FSC	Fiber Switch Capable
FTARA	Feasible Technology-Aware Routing Algorithm
GE	Gigabit Ethernet
GLIF	Global Lambda Integrated Facility
GMPLS	Generalized MPLS
GSCF	Grouping of Spatially-Close Fibers
IETF	Internet Engineering Task Force
ILP	Integer Linear Programming
IP	Internet Protocol
IPSCF	Intervals of a Pair of Spatially-Close Fibers
ISI	Inter-Symbol Interference
ISSCF	Intervals to a Set of Spatially-Close Fibers
ITU	International Telecommunication Union

ITU-T	ITU Telecommunication Standardization Sector
KML	Keyhole Markup Language
<i>k</i> TARA	<i>k</i> Technology-Aware Routing Algorithm
L2SC	Layer 2 Switch Capable
LSC	Lambda Switch Capable
LSP	Label Switched Path
MBR	Minimum Bounding Rectangle
MCE	Maximal Clique Enumeration
MIR	Multi-constrained Impairment-aware Routing
MIRWA	Multi-constrained Impairment-aware Routing and Wavelength Assignment
MPLS	Multi-Protocol Label Switching
MSDP	Min-Sum Disjoint Paths
NAS	Network Architectures and Services
NDSF	Non Dispersion-Shifted Fiber
NML	Network Markup Language
NP	Nondeterministic Polynomial Time
NREN	National Research and Education Network
NRZ	Non-Return-to-Zero
NSA	Network Service Agent
NSF	Network Service Framework
NSI	Network Service Interface
NZDSF	Non-Zero Dispersion-Shifted Fiber
OADM	Optical Add-Drop Multiplexer
OEO	Optical-Electrical-Optical
OGC	Open Geospatial Consortium
OGF	Open Grid Forum
OXC	Optical Cross-Connect
PCE	Path Computation Element
PCEP	PCE Protocol
PDA	Push Down Automaton
PMD	Polarization Mode Dispersion
PoP	Point-of-Presence
PSC	Packet Switch Capable
RAM	Random-Access Memory
ROADM	Reconfigurable OADM
SDH	Synchronous Digital Hierarchy

SDP	Service Demarcation Point
SLA	Service Level Agreement
SONET	Synchronous Optical Network
SPM	Self-Phase Modulation
SPT	Shortest feasible Paths Tree
SR	Selective Routing
SRR	Spatiotemporal Risk-averse Routing
STP	Service Termination Point
STS	Synchronous Transport Signal
TDM	Time Division Multiplex
TF	Transfer Function
TASP	Technology-Aware Shortest Path
VC	Virtual Container
VLAN	Virtual Local Area Network
WDM	Wavelength-Division Multiplexing
XPM	Cross-Phase Modulation

NOTATIONS

A	availability
A_{eff}	effective fiber core area
α	fiber loss coefficient
α^{in}	insertion loss
α^{out}	outgoing loss
α^{pass}	pass-through loss
β	DSCM compensation coefficient
\mathcal{B}	symbol rate
B	set of link blocks
$ B $	number of link blocks
b	a link block in the set B
\mathcal{C}	number of maintained entries
C	set of connections
$ C $	number of connections in the set C
c	a connection in the set C
\mathcal{D}	fiber dispersion coefficient
D	set of domains
$ D $	number of domains in the set D
d	a domain in the set D
E	set of links
$ E $	number of links
e	a link in the set E
ϵ	constant
F	set of grid rectangles
$ F $	number of grid rectangles in the set F
f	a grid rectangle in the set F
FoI	Figure-of-Impact
FoM	Figure-of-Metric
G	network graph
H	(auxiliary) network graph
h	hop count

\mathcal{I}	spatially-close interval
I	pulse intensity
i	temporary variables
k	path identifier
κ	technology probability
\mathcal{L}	total loss
L	set of links
$ L $	number of links in the set L
l	a link in the set L
ℓ	weight
ℓ_d	weight of domain d
ℓ_{uv}	weight of link (u, v)
ℓ_{eff}	effective fiber length
m	midpoint of link segment
N	set of nodes
$ N $	number of nodes in the set N
n	a node in the set N
η_{eff}	fiber effective refractive index coefficient
η_0	fiber linear refractive index coefficient
η_2	fiber non-linear refractive index coefficient
σ	dispersion
δ	connection rate
P	path
p_{in}	initial signal power
p_l	optical launch power
p_{sat}	power saturation limit
$\Pr(r)$	probability of disaster r occurring and damaging its area-of-effect
$\Pr(r^o)$	probability of the occurrences of disaster r
$\Pr(r^i)$	probability of the impact of disaster r
Q	priority queue
R	set of disaster risks
$ R $	number of disaster risks in the set R
r	a disaster risk in the set R
S	set of link segment
$ S $	number of link segment in the set S
s	a link segment in the set S
T	set of time slots

$ T $	number of time slots in the set T
t	a time slot in the set T
(u, v)	a link connecting nodes u and v
V	set of nodes
$ V $	number of nodes in the set V
v	a node in the set V
W	set of wavelengths
$ W $	number of wavelengths in the set W
w	tentative weight
X	technology matrix/vector
x	source domain/node
X_d	technology matrix of a domain $d \in D$
X_{uv}	technology vector of a link $(u, v) \in L$
v	FoI coefficient
Y	tree
y	destination domain/node
Z	set of technologies
$ Z $	number of technologies in the set Z
z	a technology in the set Z
Δ	constraint
$\Delta\phi_{NL}$	chirp
$\Delta\tau_{NL}$	time shift in which signal power is dispersed
$\Delta\tau_{\sigma}$	time shift due to dispersion
λ	a wavelength in the set W
π	tentative predecessor
ϕ	phase shift
ϕ_{NL}	non-linear phase shift

ACKNOWLEDGEMENTS

Alhamdulillah, my four-year experiences in the Netherlands have shaped me to be a better person, both in my daily and academic life. I would like to convey my appreciations to the people who have helped me along my journey.

Firstly, I am deeply thankful to my promotor, Prof. dr. ir. Piet Van Mieghem for giving me the opportunity to conduct my research in the NAS group, and for his support and encouragement. I express my heartfelt gratitude to my daily supervisor (and co-promotor), Dr. ir. Fernando Kuipers for all his assistance, ideas, guidance and understanding throughout my PhD. Having them as my PhD advisors are indeed a blessing. I would also like to thank all committee members for reviewing my thesis and providing valuable comments and suggestions.

It has been a pleasure to work with Dr. Song Yang who helped me kick-start my PhD research, Dr. Ebisa Negeri for his kind motivations, Niels van Adrichem for all our (research) discussions and for translating the Dutch parts of this thesis. I also convey my appreciations to all my other paper collaborators, namely Dr. Stojan Trajanovski, Dr. Rob Smets and Dr. Jeroen van der Ham.

I truly enjoy the pleasant working environment of the NAS group, thanks to: Aleksandar, Annalisa, Bo, Chuan, Cong, Dajie, Ebisa, Edgar, Evangelos, Hale, Huijuan, Javier, Jil, Marcus, Marloes, Niels, Negar, Nico, Norbert, Qiang, Remco, Rob, Rogier, Ruud, Song, Stojan, Wendy, Wynand, Xiangrong, Zhidong, and all the others. Thank you for aiding my research, and for all the memories that we shared in the past four years. I also offer my gratitude to all my Malaysian friends in the Netherlands who made my stay enjoyable and felt like home.

I am especially indebted to my beloved wife, Munirah for accompanying me to the Netherlands, devoting her time for the family, and providing reassurance whenever the weight of the world overwhelms me. Thank you for our dearest children, Aneesa and Ilham. Without you, this journey would be improbable.

Last, but not least, thank you to my parents, Akmar Alauddin and Iqbal Shahrhom for their unconditional love and endless support throughout my life.

*Muhammad Al Farabi bin Muhammad Iqbal
Delft, May 2016*

CURRICULUM VITÆ

Muhammad Al Farabi bin Muhammad Iqbal



Muhammad Al Farabi bin Muhammad Iqbal was born in Ohio, United States on May 1987. He obtained a Bachelor of Electrical Engineering (Telecommunications) with First Class Honours on August 2009, and a Master of Electrical Engineering (Electronics and Telecommunications) with CGPA 3.90/4.00 on March 2011, both from Universiti Teknologi Malaysia, Malaysia. He later became a junior lecturer (since September 2009) in University Teknologi Malaysia. Beginning June 2012, he is funded by the Malaysian Ministry of Higher Education to pursue his PhD in the Network Architectures and Services (NAS) group at Delft University of Technology, The Netherlands under the supervision of Dr. ir. Fernando Kuipers and Prof. dr. ir. Piet Van

Mieghem. His research interests revolve around routing aspects of optical networks (e.g., energy-efficiency, impairments, survivability, technology compatibility, risk-averse, and uncertainty) and the robustness aspects of optical networks (e.g., disaster awareness, network design, and topology distribution). During his PhD, he published a number of peer-reviewed papers and was one of the contributors for eight Research on Networks (RoN) projects under SURFnet (the Dutch National Research and Education Network). He has also provided teaching assistance for several MSc courses, and reviewed a number of international journal and conference papers.

LIST OF PUBLICATIONS

9. **N.L.M. van Adrichem, F. Iqbal and F.A. Kuipers**, *Computing Backup Forwarding Rules in Software-Defined Networks*, arXiv:1605.09350.
8. **F. Iqbal and F.A. Kuipers**, *Spatiotemporal Risk-Averse Routing*, IEEE INFOCOM Workshop on Cross-Layer Cyber-Physical Systems Security (CPSS 2016), San Francisco, United States, April 2016.
7. **F. Iqbal, S. Trajanovski and F.A. Kuipers**, *Detecting Spatially-Close Fiber Segments in Optical Networks*, 12th International Conference on Design of Reliable Communication Networks (DRCN 2016), Paris, France, March 2016.
6. **F. Iqbal, R. Smets and F.A. Kuipers**, *A Pragmatic Approach to Impairment Awareness in Optical Networks*, 20th European Conference of Networks and Optical Communications (NOC 2015), London, United Kingdom, June 2015.
5. **F. Iqbal and F.A. Kuipers**, *Disjoint Paths in Networks*, Wiley Encyclopedia of Electrical and Electronics Engineering, June 2015.
4. **F. Iqbal, J. van der Ham and F.A. Kuipers**, *Technology-Aware Multi-Domain Multi-Layer Routing*, Elsevier Computer Communications, vol 62, pp. 85-96, May 2015.
3. **R. Koning, S. Konstantaras, M. Zivkovic, P. Grosso, F. Iqbal, and F.A. Kuipers**, *Topology Exchange and Path Finding in NSI Environments*, OGF NSI-WG proposal/technical report, February 2015 (also demonstrated at the Supercomputing Conference (SC 2014) exhibition, Dutch booth, New Orleans, United States, November 2014).
2. **F. Iqbal, S. Yang, and F.A. Kuipers**, *Energy Considerations in EoS-over-WDM Network Configuration*, 3rd IFIP Conference on Sustainable Internet and ICT for Sustainability (SustainIT 2013), EINS paper, Palermo, Italy, October 2013.
1. **N. Zulkifli, S.M. Idrus, A.S.M. Supa'at and F. Iqbal**, *Network Performance Improvement of All-Optical Networks Through an Algorithmic Based Dispersion Management Technique*, Springer Journal of Network and Systems Management, vol 20, pp. 401-416, September 2012.

Relations with Thesis

This thesis consists of previously published publications by the author. The following table provides the relations between the aforementioned publications and the chapters of this thesis, where • denotes a major relation and ◦ denotes a minor relation.

Publication	Chapter 1	Chapter 2	Chapter 3	Chapter 4	Chapter 5	Chapter 6
1						
2						
3		◦				
4	◦	•				◦
5	◦					
6	◦		•			◦
7	◦				•	◦
8	◦			•		◦
9	◦					